



# NEAR-SHORE FIELD SURVEY FOR TSUNAMI RISK ASSESSMENT

BARRIO BARRETTO,  
OLONGAPO CITY, PHILIPPINES

JANUARY 2013



*Produced under the project on Enhancing Coastal Hazard Early Warning and Response: Tools and Institutional Strengthening, funded by ESCAP through the Multi-Donor Trust Fund for Tsunami, Disaster and Climate Preparedness in Indian Ocean and Southeast Asia*

# CONTENTS

<b>CHAPTER</b>	<b>PAGE</b>
<b>1. INTRODUCTION</b>	<b>1</b>
1.1 Pilot Site: Barrio Barretto, Olongapo City	2
1.2 Key Activities	3
1.3 Standard Accuracy Data Requirements for Tsunami Risk Assessment	3
1.3.1 Bathymetric DEM	4
1.3.2 Topographic DEM	6
1.3.3 Building Footprints and Properties	7
1.4 Project Timeline and Field Survey Schedule	8
<b>2. BATHYMETRIC SURVEY</b>	<b>10</b>
2.1 Methodology	10
2.1.1 Sonar Survey	10
2.1.2 Tidal Survey	17
2.2 Data and Equipment	21
2.2.1 Data	21
2.2.2 Equipment	22
2.2.3 Tidal Installation and Measurement	24
2.3 Results and Discussion	25
2.3.1 Sonar Survey	25
2.3.2 Tidal Survey	26
2.3.3 Accuracy Assessment	28
2.4 Problems Encountered and Recommendations	31
2.4.1 Sonar Survey	31
<b>3. TOPOGRAPHIC SURVEY</b>	<b>34</b>
3.1 Methodology	34
3.1.1 Calculation of Undulation Value (Geoid Height)	34
3.1.2 Ground Control Point using Static GPS Observation	36
3.1.3 Land Evaluation using Real-Time Kinematic Observation	40
3.1.4 Accuracy Assessment	43
3.2 Data and Equipment	43
3.2.1 Data	44
3.2.2 Equipment	44
3.3 Results and Discussion	45
3.3.1 Undulation Value Calculation (Geoid Height)	45
3.3.2 Ground Control Points using Static GPS Observation	45
3.3.3 Land Elevation using Real-Time Kinematic Observation	46
3.4 Problems Encountered and Recommendations	49
3.4.1 Undulation Value Calculation (Geoid Height)	49
3.4.2 Ground Control Points (GCPs) using GPS Static Observation	50
<b>4. SHORELINE DELINEATION</b>	<b>51</b>
4.1 Methodology	51
4.2 Data and Equipment	52
4.3 Results and Discussion	52
4.4 Problems Encountered and Recommendations	53

# CONTENTS

<b>CHAPTER</b>	<b>PAGE</b>
<b>5. RIVER SURVEY</b>	<b>54</b>
5.1 Methodology	54
5.1.1 Sonar Survey	54
5.1.2 Pole Survey	54
5.1.3 RTK GPS	55
5.2 Data and Equipment	55
5.3 Results and Discussion	56
5.3.1 Pole Survey	56
5.3.2 RTK GPS	57
5.4 Problems Encountered and Recommendations	59
5.4.1 Pole Survey	59
5.4.2 RTK GPS	59
<b>6. EXPOSURE SURVEY</b>	<b>61</b>
6.1 Tsunami Vulnerability and Loss Estimation	61
6.1.1 Selection of Tsunami Fragility Curves for Philippines	61
6.1.2 Methodology	69
6.1.3 Equipment and Personnel	70
6.1.4 Results	71
6.1.5 Problems Encountered and Recommendations	75
6.2 Assessment of People's Ability to Evacuate	79
6.2.1 Methodology	80
6.2.2 Equipment and Personnel	80
6.2.3 Results	81
6.2.4 Problems Encountered and Recommendations	97
<b>REFERENCES</b>	<b>98</b>
<b>ANNEX1: Participant and Contact List</b>	<b>101</b>
<b>ANNEX2: Topographic Survey Data</b>	<b>105</b>

## CHAPTER 1 INTRODUCTION

For countries with inadequate resources for disaster preparedness, as is the case for most countries in the Indian Ocean and Southeast Asian region, identification of areas at high risk to tsunamis is crucial for prioritizing resource allocation. Tsunami risk assessment, which provides an estimate of potential losses in lives and cost of building damage, would reveal communities that would be highly vulnerable to the hazard and, hence, need to be prioritized for enhancing readiness. The assessment, however, entails detailed inundation modeling for a range of scenarios from most important source zones, and requires computational capability and good-quality near-shore bathymetric, topographic, and exposure datasets, which most countries in the region lack.

Investment of scarce resources also favors ventures that are effective, efficient, and have longer-lasting impact. In this regard, development of tsunami early warning systems has taken a multi-hazard approach, and early warning integration into broader disaster risk reduction and development and regional resource sharing are among the sustainability strategies.

The project entitled “*Enhancing coastal hazard early warning and response: tools and institutional strengthening*”, supported by the United Nations Economic and Social Commission for Asia and the Pacific (ESCAP) through the Trust Fund for Tsunami, Disaster and Climate Preparedness, aims to build tsunami risk assessment capacities in Myanmar, Philippines, Sri Lanka, and Thailand, building on UNESCO/IOC efforts in the Indian Ocean region and taking advantage of low-cost methodologies developed at RIMES; and develop a regional data sharing policy for RIMES Member States and collaborating countries, for improving data availability for warning purposes. RIMES shall build tsunami risk assessment capacity through training, demonstration of tool application, and transfer of equipment, software, systems, and training manuals to the countries to facilitate replication/upscaling. These tools are: a) low-cost near-shore bathymetric, topographic, and exposure survey methodologies, and data processing tool to generate high-resolution data required for tsunami risk assessment; and b) computer-based tsunami risk assessment (named INSPIRE) and evacuation mapping (named ESCAPE).

Target groups for this project are:

- a) Technical government agencies involved in the generation of near-shore bathymetric and topographic maps and exposure data in Myanmar: Myanmar National Hydrographic Center and Department of Land Survey; Philippines: National Mapping and Resource Information Authority (NAMRIA); and Sri Lanka: National Aquatic Resources Research and Development Agency (NARA) and the Survey Department
- b) Technical agencies involved in tsunami risk assessment in Myanmar: Department of Meteorology and Hydrology (DMH); Philippines: Philippine Institute for Volcanology and Seismology (PHIVOLCS); Sri Lanka: Coast Conservation Department; and Thailand: Department of Disaster Prevention and Mitigation (DDPM)
- c) Research institutions/ universities involved in risk assessment
- d) Users of risk assessment products in Myanmar: DMH, Relief and Resettlement Department, and General Administration Department; Philippines: PHIVOLCS and National Disaster Risk Reduction and Management Council (NDRRMC); Sri Lanka: Department of Meteorology (DoM) and Disaster Management Center (DMC); and Thailand: Department of Disaster Prevention and Mitigation (DDPM)

- e) Local authorities and other disaster management organizations at the pilot sites, such as the National Red Cross Society, NGOs, and CBOs
- f) Members of the RIMES Council, consisting of National Meteorological and Hydrological Services (NMHSs) and/or technical agencies mandated to generate and provide early warning

This report, as part of the project, presents details of field data collection and demonstration of a low-cost methodology to generate geographic information needed for tsunami inundation modeling, tsunami risk assessment, and evacuation planning for the pilot site in the Philippines.

### 1.1 Pilot Site: Barrio Barretto, Olongapo City

The project inception meeting on 2 October 2012 agreed on Barrio Barretto in Olongapo City (Figure 1.1) as the project’s pilot site, in view of PHIVOLCS’ relevant activities and working network from previous efforts. The size of the site is also appropriate for piloting the topographic, bathymetric, and exposure survey methodology. NAMRIA confirmed the availability of national topographic and bathymetric maps for the area (Table 1.1), which can be used in the analysis. The meeting also requested NAMRIA to assist in generating a building footprint map, required for the risk assessment.

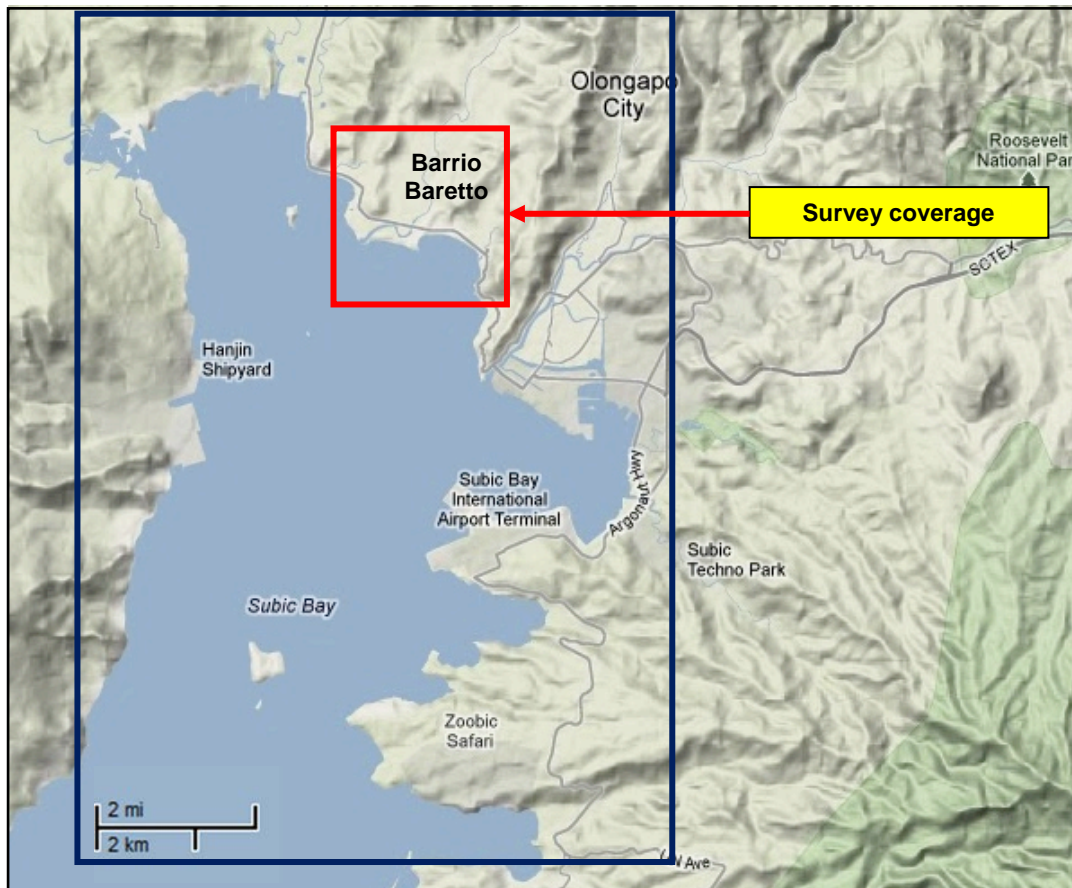


Figure 1.1 Pilot site at Barrio Barretto, Olongapo City, Philippines

Table 1.1 List of data provided by NAMRIA

Data Type	Description
<b>Bathymetric data</b>	
1. Hydrographic chart	Subic Bay scale 1:30,000 Port Olongapo and vicinity scale 1:15,000
2. Tidal benchmarks	Description and elevation of tidal benchmarks at Subic Bay, Zambales
<b>Topographic data</b>	
1. Aerial Photographs	year 1991
2. Spot 5 image	year 2008
3. Benchmarks	
4. Land cover map	Barrio Baretto scale 1: 15,000 Subic Bay scale 1: 60,000
5. Topographic map	Barrio Baretto scale 1: 10,000 Olongapo city scale 1:10,000 and 1:50,000 Bagac scale 1:50,000 San Antonio scale 1:50,000 Mariveles scale 1:50,000 Corregidor Island scale 1: 50,000 Orion scale 1: 50,000 Guagua scale 1: 50,000
6. Slope map	
7. Vector layer	Barrio Baretto

## 1.2 Key Activities

Data collection and demonstration of the survey methodology involved the following key technical and disaster management agencies: PHIVOLCS, NAMRIA, Olongapo City Disaster Risk Reduction and Management Office (OCDRRMO), and Barangay Barretto. The activities were undertaken from 18 January to 1 February 2013, and included:

- 1) Project launch meeting at the OCDRRMO for project introduction and implementation arrangement with local authorities
- 2) Data collection from the city planning and development office, Olongapo City
- 3) Bathymetric survey
- 4) Topographic survey
- 5) Exposure survey

## 1.3 Standard Accuracy Data Requirements for Tsunami Risk Assessment

Standard accuracy data are geographic data that are publicly available for free or for a minimum cost. Higher accuracy data, such as large-scale topographic maps and nautical charts, if available, are preferred. Otherwise, lower accuracy data such as ASTER GDEM for topographic DEM, GEBCO-08 for bathymetric DEM, and Google Earth for building properties estimation may be used. These data sources were selected as baseline for standard accuracy data, since they are available for all parts of the world and have the highest spatial resolution among the freely available data in the Internet. In addition, GEBCO-08, with spatial resolution of 30 seconds, meets standards set by UNESCO Intergovernmental Oceanographic Commission (IOC) for tsunami modeling. Table 1.2 shows the accuracy of each data source.

Table 1.2 Accuracy of data sources

Data type	Spatial resolution	Accuracy	Data source
Topographic DEM	30 m x 30 m	X,Y: 20m / Z: 30 m	ASTER G DEM
Bathymetric DEM	30 sec x 30 sec (900 m x 900 m)	N/S	GEBCO-08
Building location	1 m	X,Y: 5 m	Google Earth
Building properties	N/S	N/S	N/S

*N/S: Not Specified*

### 1.3.1 Bathymetric DEM

Bathymetry can be defined as the seafloor topography relative to a known vertical datum, such as the Mean Sea Level (MSL) for coastal area management, or the Mean Lower Low Water (MLLW) for navigation. Bathymetric maps represent the seafloor depth as a function of geographic coordinates, in the same way the topographic maps represent the elevation of the earth's surface at different geographic points. Usually, seafloor terrain is shown as depth contours (isobaths) and spot depths on bathymetric maps.

A digital elevation model (DEM) is a digital representation of the Earth's surface. Although it can be represented as triangulated irregular networks (TIN), it is more often represented as a raster or grid of squares for ease in model calculations. Land DEMs are typically acquired by remote sensing satellites, but bathymetric DEMs are mostly generated by interpolating ship-mounted depth soundings. Available data sources that can provide standard accuracy bathymetric DEM, without the need for field survey, include interpolated sounding data from bathymetric maps and DEMs that can be downloaded freely from the Internet, such as ETOPO and GEBCO DEMs.

Depending on the scale, accuracy of bathymetric maps or nautical charts varies from high accuracy large-scale maps (1:50,000) to low accuracy small-scale maps (1:200,000). Compared to ETOPO and GEBCO DEMs, most bathymetric maps can provide higher accuracy. However, unlike the two DEMs which can cover almost all areas in the world, bathymetric maps may be not be available, or may have limited extent for the areas of interest. Up until 2009, ETOPO1 DEM (Earth TOPOgraphy 1), developed by NOAA NGDC with 1 arcminute or approximately 2 km spatial resolution, was the most common source of bathymetric DEM. ETOPO1 is the latest version of the Global Relief Models developed by NOAA NGDC in August 2008. It was developed to upgrade the resolution and accuracy of the previous version ETOPO2v, a 2 arcminute global relief model designed to aid in tsunami forecasting, modeling and warning, as well as ocean modeling and earth visualization. It is a one minute grid, integrated from different topographic and bathymetric datasets, such as shoreline, bathymetry, topography, integrated bathymetry-topography, and bedrock all over the world, that are shifted to a common horizontal and vertical datum, the WGS84 and the sea level, respectively (Table 1.3).

Table 1.3 ETOPO1 DEM characteristics

Versions	Ice Surface, Bedrock
Coverage Area	Global: -180° to 180°; -90° to 90°
Posting interval (spatial resolution)	1 arcminute
Geographic coordinates	Geographic latitude and longitude( WGS84)
Vertical Datum	Sea Level
Vertical Units	Meters
Data Format	Multiple: netCDF, g98, binary float, tiff, xyz

*Source: Amante & Eakins, 2009*

In January 2009, the GEBCO-08 Grid (General Bathymetric Chart of the Oceans DEM), with a 30 arcsecond spatial resolution, was released by the British Oceanographic Data Center (BODC). This is generated by quality-controlled ship depth soundings, with interpolation between sounding points guided by satellite-derived gravity data. Although it is currently a development product, it undergoes periodic updates to reduce errors in the dataset. GEBCO's aim is to provide the most authoritative publicly

available bathymetry of the world's oceans. It operates under the joint auspices of IOC and the International Hydrographic Organization (IHO).

The GEBCO-08 was developed to improve the resolution and accuracy of the GEBCO One Minute Grid, released in 2003. As with ETOPO1 bathymetric DEM, the accuracy of the GEBCO-08 DEM is only as good as the quality of the sonar equipment and bathymetric surveys conducted in the respective countries. The bathymetric data are generated from the integration of sounding data, bathymetric contour maps, predicted depth data based on version V16.1 of the Sandwell and Smith gravity anomaly from Geosat and ERS1 satellite altimeter and the Smith and Sandwell global topographic grid, as well as SRTM, GTOPO30 and the Geoscience Laser Altimeter System (GLAS) instrument on the Ice, Cloud and land Elevation Satellite (ICESat) laser altimetry digital elevation model for topographic data. The GEBCO-08 comes with a source identifier (SID) grid that identifies which grid cells in the GEBCO-08 Grid are based on bathymetric soundings or predicted depths. The values in the GEBCO-08 SID Grid are as follows:

- 0 data is interpolated with the help of satellite-derived gravity data
- 1 data has been constrained by bathymetric sounding data during the gridding process
- 2 value is taken from version 2.23 of the International Bathymetric Chart of the Arctic Ocean (IBCAO)
- 3 value for land, in positive value

Table 1.4 shows the characteristics of GEBCO-08 DEM.

Table 1.4 GEBCO-08 DEM characteristics

Coverage	Global
Posting interval (spatial resolution)	30 arcsecond (900 m x 900 m)
Geographic coordinates	Geographic latitude and longitude(WGS84)
Data format	netCDF (signed 16 bits), ASCII
Special DN values	Positive for land body, and negative for sea water body

The NOAA Center for Tsunami Research provides integrated bathymetric and topographic DEMs for United States coastal areas through the NOAA National Geophysical Data Center. For the Indian Ocean and Southeast Asian region, RIMES has started an initiative to generate updated and accurate local bathymetric and topographic DEMs for the region, following IOC standards for tsunami modeling.

In accordance with Yeh (IOC, 2001), the Scientific Committee on Oceanic Research of the IOC (SCOR-IOC) has set some scientific requirements on spatial resolution for tsunami modeling. In addition, it has emphasized the need to refer both the topographic and bathymetric DEMs to the same datum to ensure accurate elevation data along the coast. Table 1.5 shows the tsunami modeling requirements set by these three organizations, for comparison.

Table 1.5 IOC Scientific requirements for tsunami models

Area	IOC	NOAA	RIMES
<b>Horizontal Resolution (m)</b>		<1 to <100	5/3 arcsecond (approx. 50 m)
Continental Shelf < 2.5 m deep	50	N/S	N/S
Continental Shelf 2.5–10 m deep	100	N/S	N/S
Continental Shelf 10-250 m deep	100-500	N/S	N/S
Canyons and Ridges	500	N/S	N/S
Open Ocean	>2000	N/S	N/S
<b>Vertical Resolution (m)</b>	N/S	<1	1

Note: N/S for Not Specified

Sources: IOC (2001); NOAA NGDC (2009)

For this project, tsunami propagation and coastal inundation are modeled using INSPIRE. This tool requires four input DEMs, wherein region 1 covers a very large area (regional) while region 4 covers a small area (interest area only). In order to link the large to the small coverage areas, cell size of each region must be fixed according to the ratio defined in the code; for example, ratio of cell sizes for regions 1 to 4 is 1: 1/8: 1/24: 1/72, respectively with corresponding cell sizes of 120:15:5:5/3 arcseconds. The DEMs should be in the same coordinate system; hence, the geographic coordinate system is used.

To meet modeling requirements, this project covered only near-shore areas of up to 30-50 m depths to ensure that the incoming wave is still in constant wavelength and satisfy deep water wave condition. Output DEM should have a horizontal resolution of 5/3 arcseconds and a vertical resolution and accuracy of 1 m.

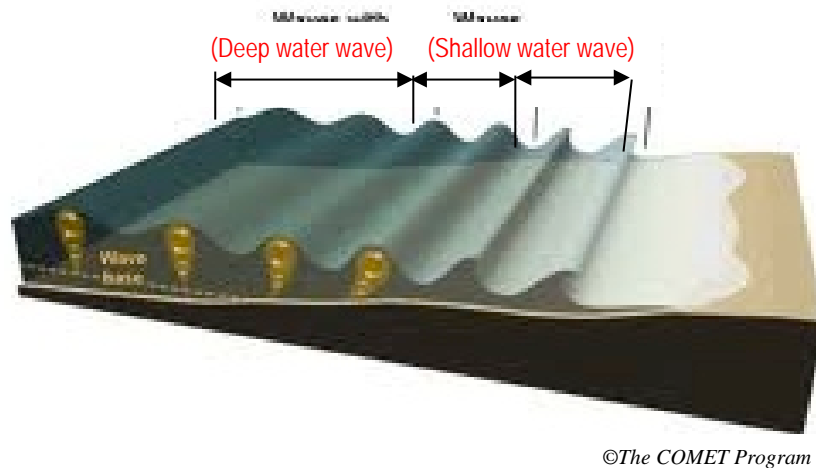


Figure 1.2 Wave shoaling

### 1.3.2 Topographic DEM

There are available data sources that can provide standard accuracy DEM, without the need for field survey, including topographic map (1:50000 scale or larger), ASTER GDEM, and SRTM DTED level 1. Estimated accuracy for these data is better than 20 meters.

Topographic maps are the data provided by local mapping agencies. These can sometimes be represented as high accuracy data, especially for larger scale (1:4000). Large-scale maps, however, are not available everywhere. Normally, these cannot cover the whole extent of the interest area, so that lower accuracy data, such as small-scale maps, ASTER GDEM, or SRTM DTED level 1, can be used to supplement the large-scale map, thus reducing the overall accuracy. Expected accuracies of topographic maps are shown in Table 1.6.

Table 1.6 Topographic map accuracy

Map scale	Data accuracy
1:4,000	1 m contour interval
1:10,000	5 m contour interval
1:50,000	20 m contour interval

The ASTER GDEM covers land surfaces between 83°N and 83°S, and is comprised of 22,600 1°-by-1° tiles. Tiles that contain at least 0.01% land area are included. The ASTER GDEM is in GeoTIFF format, with geographic lat/long coordinates and a 1 arcsecond (approximately 30 m in the Southeast Asian region) grid. It is referenced to the WGS84/EGM96 geoid. Table 1.7 summarizes the basic characteristics of the ASTER GDEM. Pre-production estimated (but not guaranteed) accuracies for this

global product were 20 m at 95 % confidence for vertical data, and 30 m at 95 % confidence for horizontal data.

Table 1.7 ASTER GDEM characteristics

Coverage	North 83° to south 83°
Tile size (download unit)	3601pixel x 3601 pixel (1°-by-1°)
Posting interval (spatial resolution)	1 arcsecond (30 m x 30 m)
Geographic coordinates	Geographic latitude and longitude (WGS84/EGM96 geoid)
Data format	GeoTIFF, signed 16 bits, and 1m/DN
Special DN values	-9999 for void pixels, and 0 for sea water body

SRTM DTED level 1, the Shuttle Radar Topography Mission (SRTM), successfully collected Interferometric Synthetic Aperture Radar (IFSAR) data over 80 percent of the landmass of the Earth between 60 degrees North and 56 degrees South latitudes in February 2000. The mission was co-sponsored by the National Aeronautics and Space Administration (NASA) and National Geospatial-Intelligence Agency (NGA). NASA's Jet Propulsion Laboratory (JPL) performed preliminary processing of SRTM data, and forwarded partially finished data directly to NGA for finishing by NGA's contractors and subsequent monthly deliveries to the NGA Digital Products Data Warehouse (DPDW). All data products delivered by the contractors conform to the NGA SRTM products, and the NGA Digital Terrain Elevation Data (DTED) to the National Center for Earth Resources Observation & Science (EROS) of the U.S. Geological Survey (USGS). The DPDW ingests SRTM data products, checks them for formatting errors, loads the SRTM DTED into the NGA data distribution system, and ships the public domain SRTM DTED to EROS ([http://gcmd.nasa.gov/records/GCMD\\_DMA\\_DTED.html](http://gcmd.nasa.gov/records/GCMD_DMA_DTED.html)). Table 1.8 shows the characteristics of SRTM DTED level 1 data.

Table 1.8 SRTM DTED level 1 characteristics

Coverage	North 60° to south 56°
Tile size (download unit)	3601pixel x 3601 pixel(1°-by-1°)
Posting interval (spatial resolution)	3 arcsecond( 90 m x 90 m)
Geographic coordinates	Geographic latitude and longitude( WGS84/EGM96 geoid)
Data format	GeoTIFF, signed 16 bits, and 1m/DN
Special DN values	-9999 for void pixels, and 0 for sea water body

### 1.3.3 Building Footprints and Properties

Building footprints and properties, such as building location and characteristics, and population distribution maps are required to generate tsunami vulnerability maps. Remote sensing data, including aerial photographs, satellite images, and especially Google Earth, can be used as base data for generating building footprints. Quality of footprints, however, depends on the quality of images.

Image quality is divided into two parts namely, location accuracy and image clarity. Location accuracy requirement is 5 meters or better for standard accuracy data. Horizontal location accuracy for aerial photographs and geo-rectified level 2B satellite images is around half pixel; thus, the 1-meter IKONOS images or higher resolution images can be used for footprints extraction.

Image clarity refers to the quality of buildings that can be identified. Building footprints can be extracted from a high-resolution image as polygon feature. Low-resolution image allows only the extraction of building location as point feature. Initially, Landsat images were used as base image; later, these were replaced by higher resolution images, such as SPOT-5, IKONOS, QuickBird, or Geo-Eye, when available. Google Earth provides data to represent the global world for free. Accuracy of Google Earth images should be the same as the original source, but is not guaranteed.

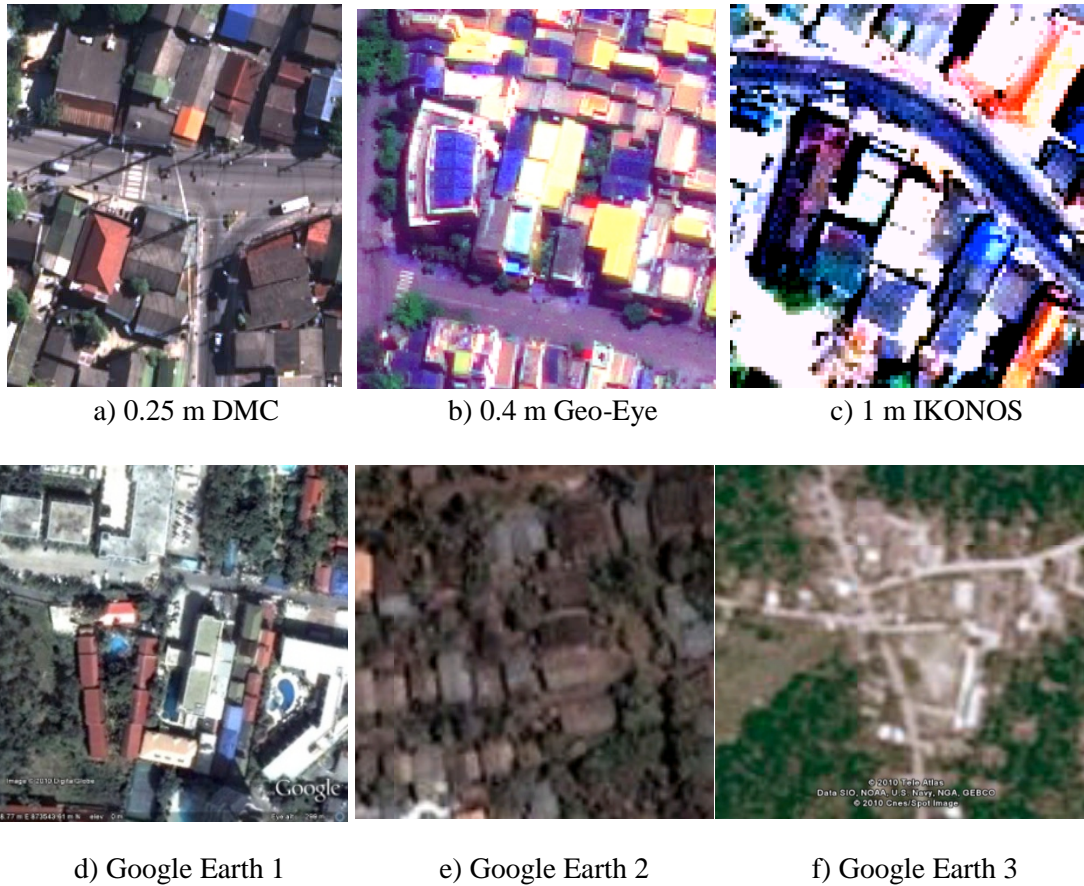


Figure 1.3 Image clarity

### 1.4 Project Timeline and Field Survey Schedule

Table 1.9 provides the updated project schedule. NAMRIA and PHIVOLCS agreed on 21 January 2013 start date for the field surveys. Preparatory works at the pilot site, however, were undertaken earlier. PHIVOLCS coordinated the field activities with the local government, while NAMRIA’s Hydrography Department supported benchmarking, testing, and installation of the temporary tide gauge. A project launch meeting was hosted by Olongapo City DRRM Office on 18 January 2012. Three survey teams for bathymetric, topographic, and exposure surveys were launched simultaneously on 21 January 2013. Table 1.10 presents the survey schedule.

Table 1.9 Updated project schedule

	2012				2013												2014							
	S	O	N	D	J	F	M	A	M	J	J	A	S	O	N	D	J	F	M	A	M	J		
1. Project initiation																								
1.1 Project initiation meeting	M	P	S																					
2. Capacity building in tsunami risk assessment																								
2.1 Training on near-shore field surveys					P	S										M								
2.2 Training on survey data processing, DEM generation										P	S						M							
2.3 Training on tsunami risk assessment, evacuation mapping													P	S			M							
3. Improvement of response capabilities																								
3.1 Evacuation map testing and exercise, manual adaptation														P	S			M						
4. Regional resource sharing policy and mechanism devt																								
4.1 Resource sharing policy and mechanism development																								

Note: M-Myanmar; P-Philippines; S-Sri Lanka



## **CHAPTER 2**

### **BATHYMETRIC SURVEY**

#### **2.1 Methodology**

Bathymetric data acquisition is composed of two parts: (i) sonar and (ii) tidal, both of which can be acquired in parallel. Sonar survey is conducted using a commercial fish finder, following an optimized route design that includes densified surveys in areas with local variation, while tidal data is used to correct raw sonar depth readings. For tidal measurement, a temporary tide gauge is installed near or within the pilot site, and data is recorded periodically by the tide gauge data logger.

A common datum, such as the mean sea level (MSL), will facilitate the merging of both bathymetric and topographic data. This will serve as the vertical reference for both bathymetric and topographic data in the final output. A leveling survey is conducted to transfer the elevation in MSL from a known tidal benchmark to the portable tide gauge, while (i) a GPS observation on a known MSL elevation benchmark, or (ii) a leveling survey on a known GPS benchmark, is conducted to determine the undulation value (geoid height), needed to transform all GPS data to MSL.

##### **2.1.1 Sonar Survey**

###### ***Survey Route Design***

An optimized survey route design was employed without compromising the accuracy requirement for tsunami modeling. The route consists of (i) basic 200m interval lines perpendicular to the shoreline, and (ii) detailed 100m interval in areas with local variation.

The recommended survey route design is composed of three parts:

1. Perpendicular to the shoreline with a 200m interval spacing
2. Parallel to the shoreline up to 1000m offshore:
  - a. 100m interval spacing until 600m offshore
  - b. 200m interval spacing until 1000m offshore
3. Densified survey at 100m interval spacing in areas with local variation

Figure 2.1 shows the extent of the project site in solid yellow line as well as a buffer of 1km in dashed yellow line. The sonar survey covers an approximate area of 25 sq. km. The total distances of the lines perpendicular to the shore (red line), parallel to the shoreline (blue) and local variation (black) are approximately 60km, 60km and 50km, respectively. If a conservative boat speed of 5kph is used, a 6-hour working time per day can generate a total distance of around 30km/day. Increasing the boat speed can generate a longer trip distance per day. The distance going from and back to the boat docking station is estimated at 7km. This is not included in the computed total trip distance per day.

In addition, sonar survey can be run along the centerline of rivers, zigzagging from bank to bank on the way back, or vice versa.

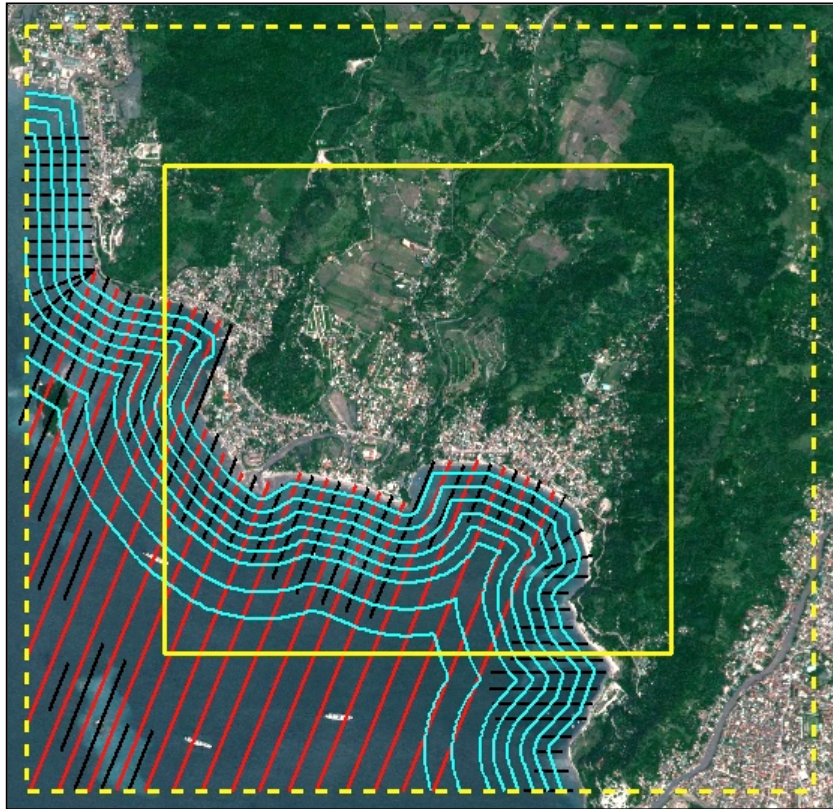


Figure 2.1. Survey route design

### ***Sonar Survey***

A boat survey route plan was created to guide the boat operator during the actual survey. There were two types of surveys conducted, both following the same survey route. The first was conducted from 21-26 January using a Lowrance transom mount fishing sonar, and the second was conducted from 28 January-01 February using an Odom Echotrac MKIII transducer, mounted over the side of the boat.

The sounding data from the fishing sonar was collected from a transducer operating at 200kHz (12° cone angle) at shallow depths and 50kHz (35° cone angle) at deeper depths. Strategic turning points were inputted to the handheld GPS using a freeware called *GPS TrackMaker* (Figure 2.2) to aid the boat operator in navigating the designed route. Skill is necessary to follow a straight line on the sea. Fortunately, the NAMRIA team was very skilled and experienced, in addition to the efficient navigation system they were using (Figures 2.3 and 2.4), so the survey went according to plan.

Since raw sounding data has to be corrected for tide, which is varying over time, it is necessary to synchronize time for all equipment, such as sonar console, portable water level data logger, laptop, and handheld GPS. In Barrio Barretto, all time sources were synchronized with the time at the Subic tidal station, since tidal data from this station will also be used to assess the accuracy of the portable tide gauge and fishing sonar.

To ensure that depth readings are intact, these were transferred to the laptop computer everyday. Draft offset, the distance between the transducer and the water surface, was recorded everyday, especially when the transducer height was adjusted, or when there was a significant change in the weather or boat load, such as personnel and equipment. This information will be used to correct the raw sonar data.

To ensure reliable depth readings and the safety of the surveyors, survey operations were conducted only during calm seawater conditions. Rough seawater condition occurred after 2-3 in the afternoon, so survey operations were conducted before this period.

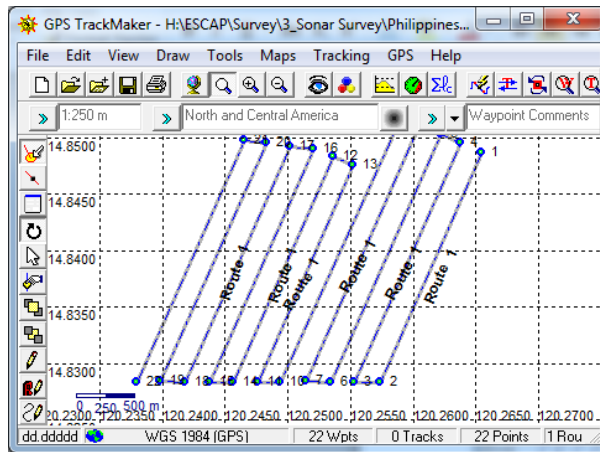


Figure 2.2 Route design in GPS TrackMaker



Figure 2.3 Boat driver

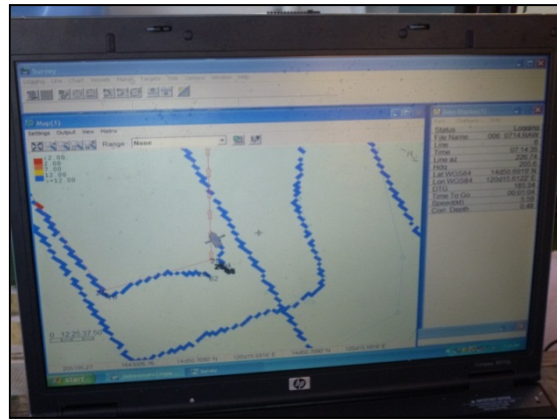


Figure 2.4 Navigation software

Finally, to make a more meaningful assessment of the commercial fishing sonar, another survey using a high-accuracy transducer, such as the Odom Echotrac MKIII (Figure 2.5), mounted over the side of the boat with steel cables attached at each side for support (Figure 2.6), was conducted following the same route. Sounding data from both transducers will be corrected for tide from the same tidal data source, and then compared.

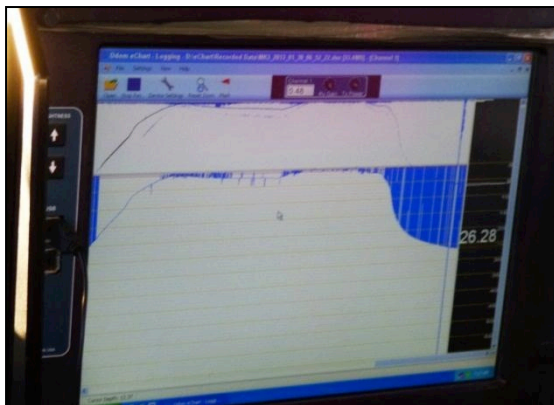


Figure 2.5 Odom Echotrac MKIII console

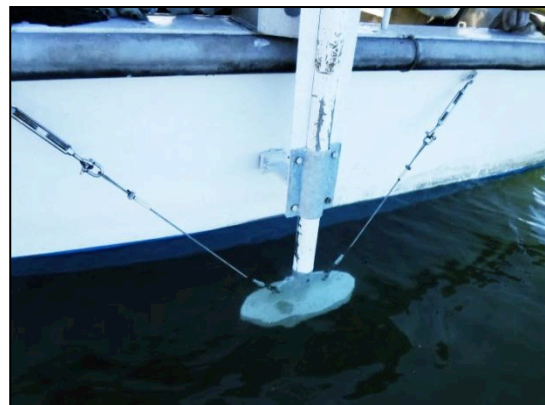


Figure 2.6 Odom Echotrac transducer

## Local Variation

Local variation is characterized by rugged terrain or abrupt changes in elevation in localized areas, such as those occurring along the shores, comprised of rocks and corals, and in the middle of the sea as mounts and depressions, as shown in Figure 2.7. If not well accounted for, these areas will introduce errors in the generated DEM. A local variation index (LVI) can be used to detect rough surfaces or areas where local variation exists (Figure 2.8). This index is defined as the standard deviation of sounding data, in this case 0.5m, over some distance, in this case 200m (Figure 2.9).

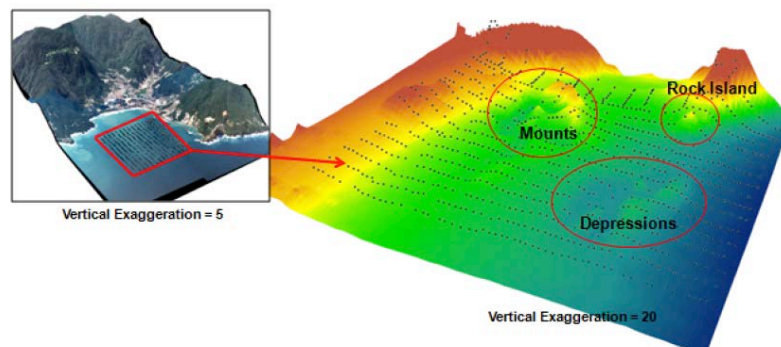


Figure 2.7 Area with local variation

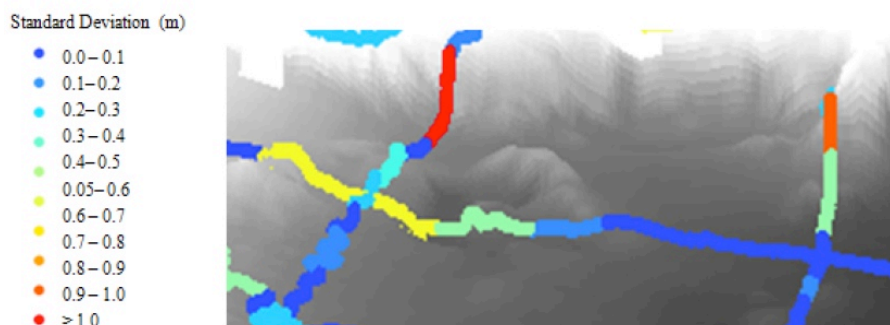


Figure 2.8 Local variation index

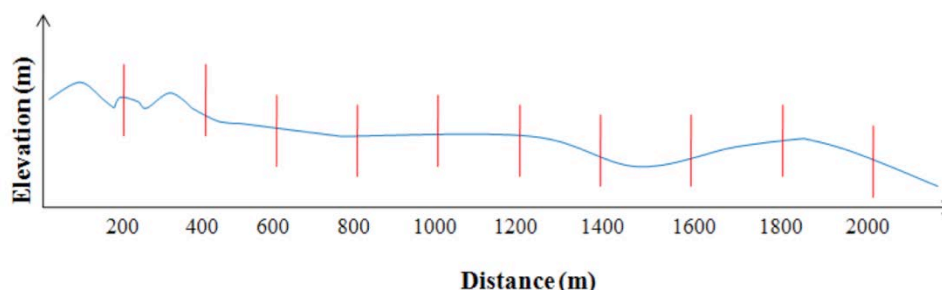
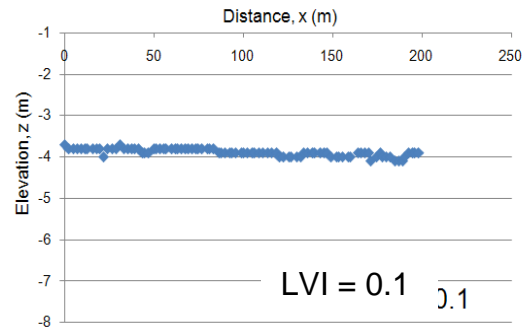
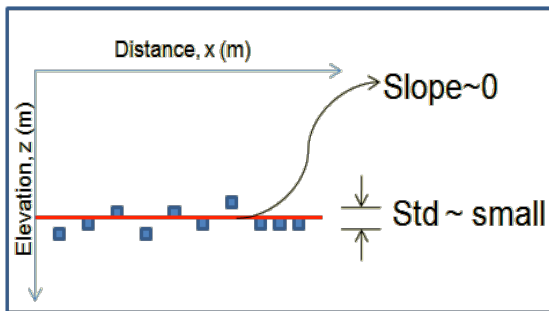


Figure 2.9 Standard deviation computed every 200m interval

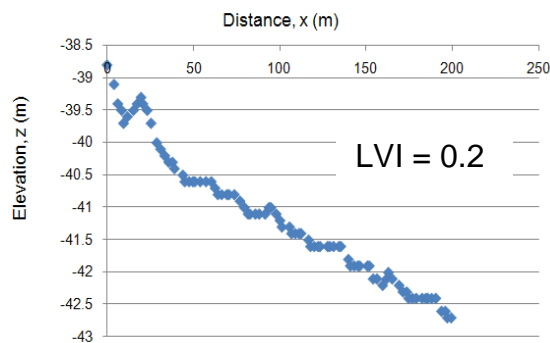
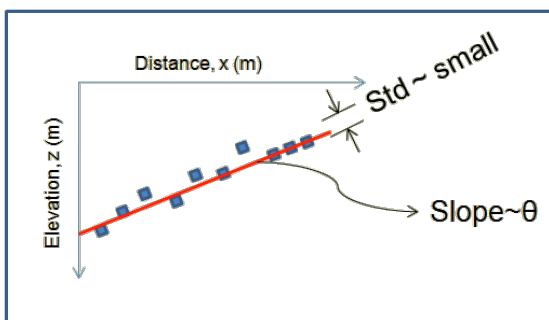
Local variation analysis is important to increase DEM accuracy by increasing survey detail in areas of local variation. Generally, near-shore bathymetry is characterized by smooth terrain. The idea behind the survey route is to create a design with the widest possible interval spacing (e.g. 200m interval) that can still effectively represent the general bathymetry of the sea according to the accuracy requirement for tsunami modeling, which is quite lower than typical hydrographic surveys (50m interval); and then,

densifying survey in areas with variation to effectively represent these variations. As a result, time and cost to survey a large area is significantly reduced.

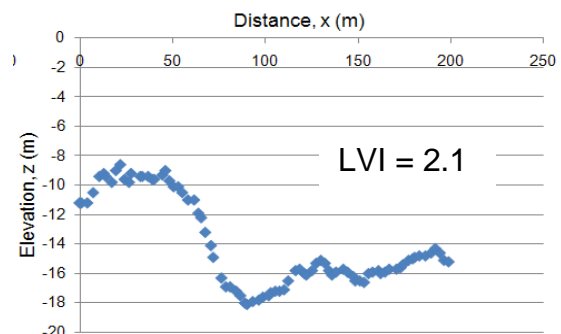
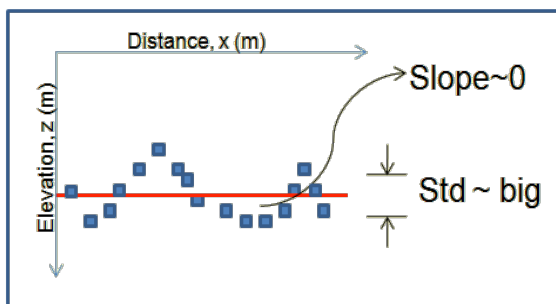
The following figures show the different bathymetric scenarios that can be detected. Mainly, these are categorized into smooth and rough bathymetry. The first two figures show smooth bathymetry in a flat terrain when the slope is approximately zero (Figure 2.10A), and sloping terrain where the slope is of some value  $\theta$  (Figure 2.10B). The LVI or standard deviation of the difference between the actual and modeled point is less than 0.5 m for both cases. The next two figures show local variation in a flat (Figure 2.10C) and sloping (Figure 2.10D) terrain. Also, it can be seen that the LVI for both scenarios are greater than 0.5 m.



(A)



(B)



(C)

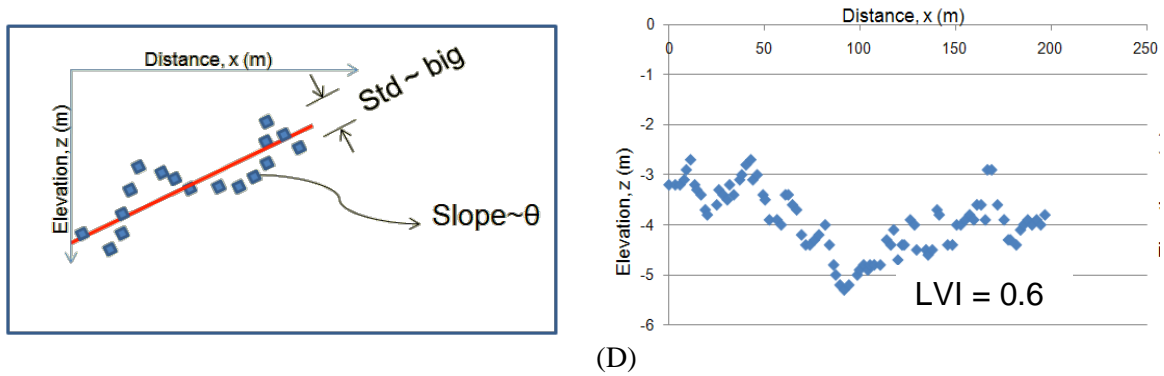


Figure 2.10 Bathymetric scenarios detected by local variation analysis: (A) Smooth and flat, (B) Smooth and sloping, (C) Rough and flat, (D) Rough and sloping

For this project, areas with local variation were initially estimated using the available nautical charts (blue area shown in Figure 2.11), since these were available. After the survey, the sounding data was analyzed for existence of local variation by inputting the raw data to the local variation analysis program, developed for this project. After detecting the hotspot areas, detailed survey was conducted in these localized areas, using the 100m interval spacing to compensate for errors that may be introduced by this condition.

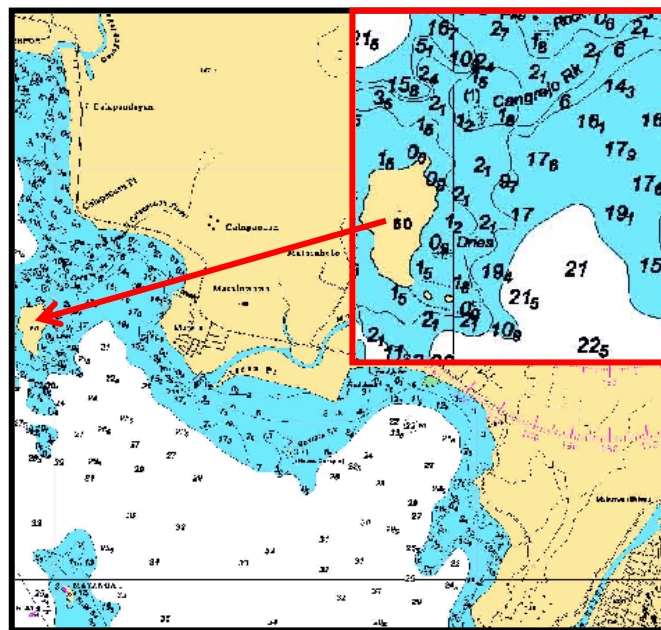


Figure 2.11 Local variation on nautical chart



Figure 2.12 Local variation detected by the commercial fishing sonar

### *Accuracy Assessment*

Initial assessment was conducted on the first day to check the accuracy of the fishing sonar, using a calibrated rope with a 5kg weight at random points, and by bar check method at 2m, 3m and 5m (Figure 2.13), making sure that the rope was vertical and pulled tight during the readings to eliminate inaccuracies introduced by the water current.

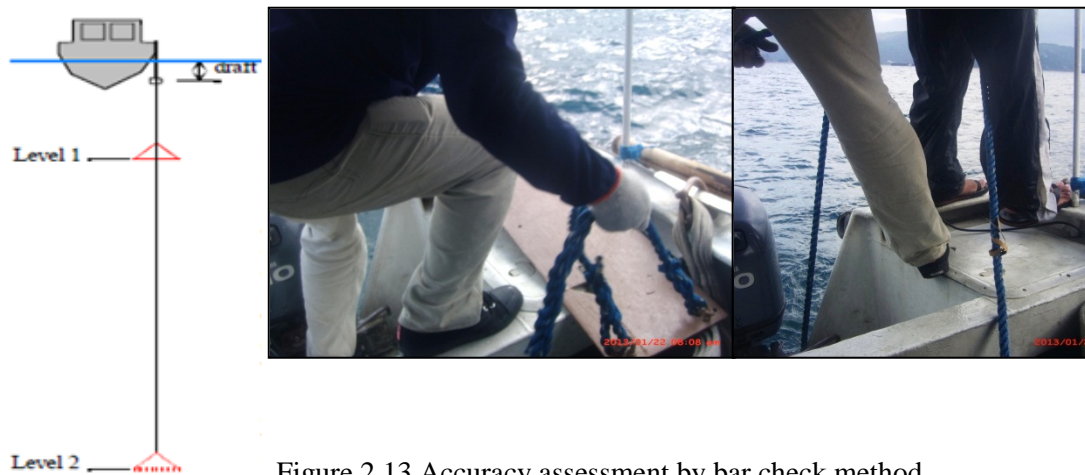


Figure 2.13 Accuracy assessment by bar check method

A secondary assessment of the fishing sonar was done by comparing its data with the data from the higher accuracy sonar, such as the Odom Echotrac MKIII, used by the Hydrographic Division of NAMRIA. Since there were no existing sounding data in the pilot site, another survey following the same survey route was conducted using the Odom transducer. Since it collected data on nearly the same locations as the commercial fishing sonar data, assessment will be more accurate and can cover a wider depth range.

## 2.1.2 Tidal Survey

### *Tide Gauge Installation*

A portable tide gauge (pressure-type sensor with water level recorder) was established on the pier, near Driftwood Beach Resort to collect tidal readings every 10 minutes (Figures 2.14 and 2.15). To ensure that the sensor is submerged in the water for the whole duration of the survey, it was installed below the lowest possible water for that area. Prior to data logging, the instrument was first calibrated at some underwater depth for positive depth values and at atmospheric pressure for zero depth. Depths are then interpolated or extrapolated according to these settings.

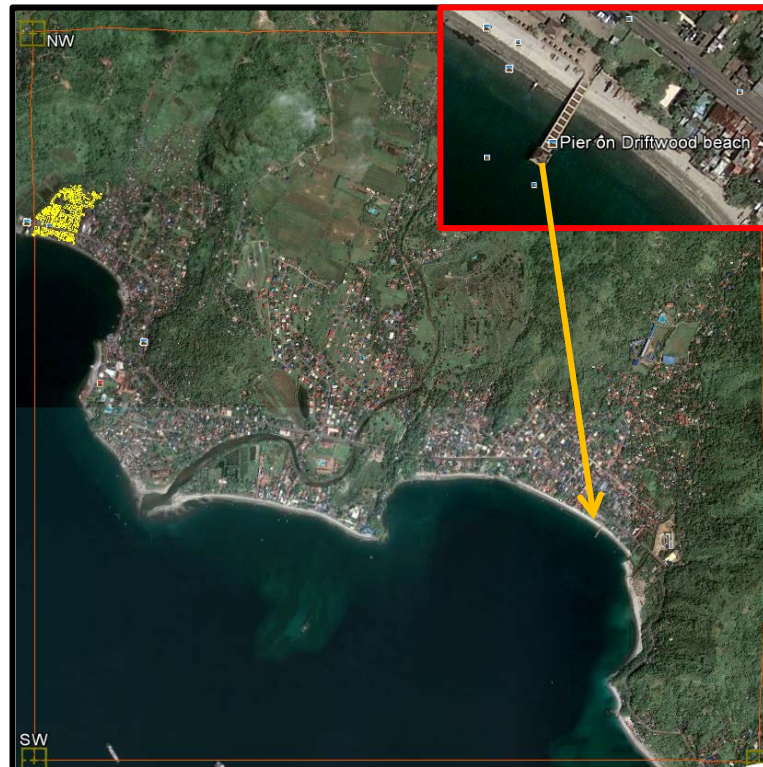


Figure 2.14 Location of portable tide gauge

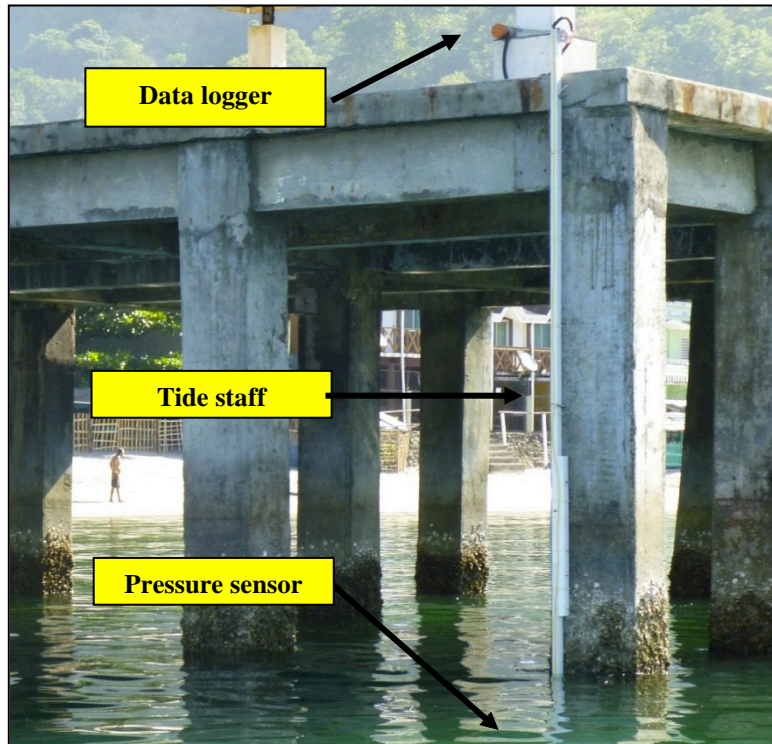
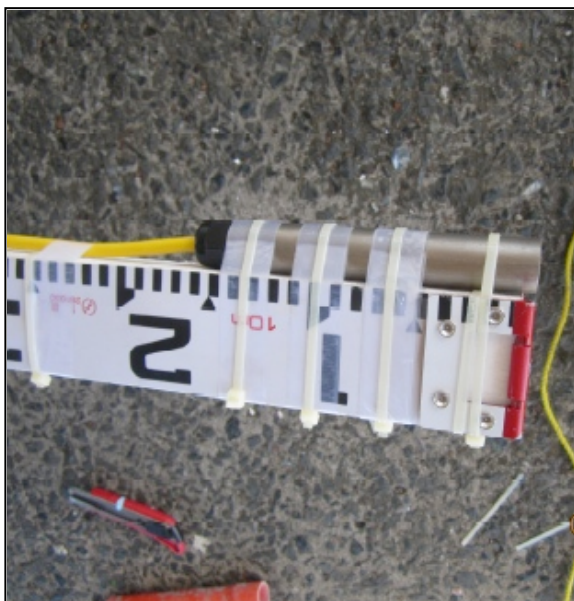


Figure 2.15 Tide gauge setup



Source: NAMRIA, 2013



Source: NAMRIA, 2013

Figure 2.16 PRS sensor attached to zero tide staff

Figure 2.17 Installation of instruments at the pier



Source: NAMRIA, 2013

Figure 2.18 Calibration of tide gauge

### ***Tide Gauge Elevation***

A leveling survey was conducted to transfer the elevation in MSL from a known tide gauge at the Subic Ocean Adventure, located around 10km to the south of the pilot site, to the installed portable tide gauge (Figure 2.19).

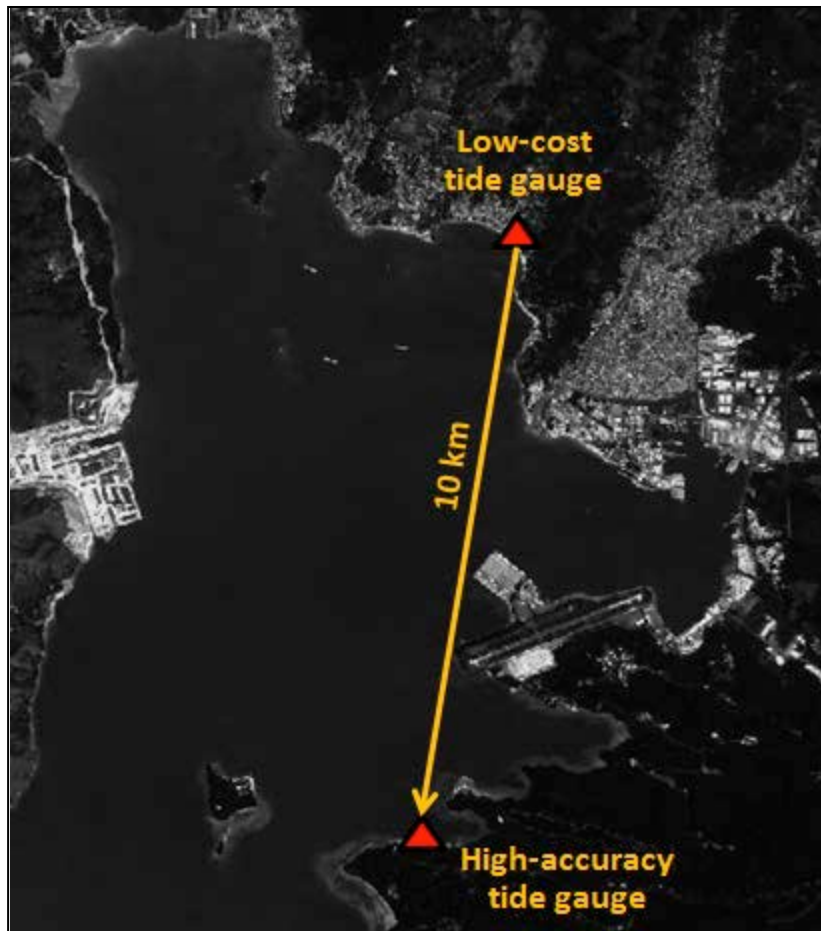


Figure 2.19 Transfer of elevation in MSL from a known benchmark to the pilot site

Prior to leveling survey, a reconnaissance survey was conducted to check the actual location and condition of existing benchmarks (Figure 2.20), as well as to establish benchmarks that will be included in the survey (Figures 2.21 and 2.22).



Source: NAMRIA, 2013

Figure 2.20 Existing benchmark



Source: NAMRIA, 2013

Figure 2.21 Established benchmark



Source: NAMRIA, 2013

Figure 2.22 Establishment of temporary benchmarks

### ***Tidal Measurement***

Tidal measurements every 10 minutes were logged in the portable tide gauge data logger and downloaded to the laptop each day. These data will be used to correct the raw sounding data. In addition, a local staff was hired to measure hourly tidal data against the tide staff installed with the portable tide gauge, as well as to keep the instrument safe for the whole duration of the survey.

### ***Accuracy Assessment***

Tidal measurements from the portable tide gauge in the pilot site will be compared with the hourly measurements made from the tide staff attached to the gauge, as well as to the measurements recorded by the NAMRIA tide gauge the Subic Ocean Adventure to assess the accuracy of the low-cost equipment and tidal variation in both locations. So, it is also important to synchronize the time from both tidal data sources.

## 2.2 Data and Equipment

The following table shows the list of data and equipment used and personnel employed for each activity in the bathymetric survey. The 3 major activities include (i) sonar survey data, (ii) tidal installation and measurement, and (iii) leveling survey. Since most of the equipment used are related to each other, time for all equipment (e.g. commercial fishing sonar, portable tide gauge data logger, handheld GPS, laptop, etc.) should be synchronized.

Table 2.1 List of data and resources used in bathymetric survey

Activity (Duration)	Data Used	Equipment Used	Personnel
1. Sonar survey: Lowrance (21-26 Jan) Odom (25 Jan – 01 Feb)	Nautical chart (1:15,000 & 1:30,000) Topographic map (1:10,000 & 1:50,000) Predicted tide table	Survey vessel (skiff) Fishing sonar Battery (12V 45Ah) Battery charger Laptop SD card Calibrated rope	Boat driver Engine operator Navigator NAMRIA staff (2) RIMES staff (2)
2. Tidal installation (20 Jan) and measurement (21-26 Jan)		Portable tide gauge Tide staff	Tide reader
3. Leveling survey (19, 21-26 Jan)	Tidal benchmark description	Vehicle (van) Leveling scope Tripod Leveling rod Concrete monuments	Driver Level operator Rod man (2) Recorder

### 2.2.1 Data

#### *Nautical chart*

Two nautical charts were used for survey planning to estimate the survey route, extent of shoreline, and location of local variation. The first chart, No. 4213, covers Olongapo port and vicinity at a scale of 1:15,000 while the second chart, No. 4212, covers Subic Bay at a scale of 1:30,000. Both maps are referred to the Mean Lower Low Water (MLLW) vertical datum and to the WGS84 horizontal datum. The MSL is 0.45m above the MLLW.

#### *Vertical benchmark*

Leveling survey was conducted to transfer the MSL elevation of the known tidal benchmark at the Subic tidal station located at the Ocean Park Adventure to the temporary tidal benchmark established on the pier near Driftwood Beach in Barrio Barretto. This temporary tidal benchmark served as the connection point between land and sea survey data.

#### *Tide table*

The predicted tidal readings of the Subic tidal station was used to estimate the low and high tidal hours of the day for river survey as well as the time of zero elevation to delineate the shoreline. The tide table is based on the MLLW and can be converted to MSL using the offset difference of 0.45m determined from 33 months of observation.

#### *Reference data*

The reference sounding data was collected by an Odom Echotrac MKIII echosounder (from the NAMRIA Hydrographic division) using the same survey route design used by the fishing sonar. The reference tidal data was collected by a high accuracy pressure type tide gauge located at the NAMRIA tidal station in Camayan. The corrected sonar data are referred to the WGS84 (horizontal datum) and the MLLW (vertical datum). This will be used to assess the accuracy of the commercial fishing sonar.

## 2.2.2 Equipment

### *Sonar setup on the skiff*

The sonar setup was composed of the display/console, transducer, power supply, handheld GPS for navigation and tracking, and laptop loaded on the skiff, which is owned by the Hydrographic Division of NAMRIA as shown in Figure 2.23.

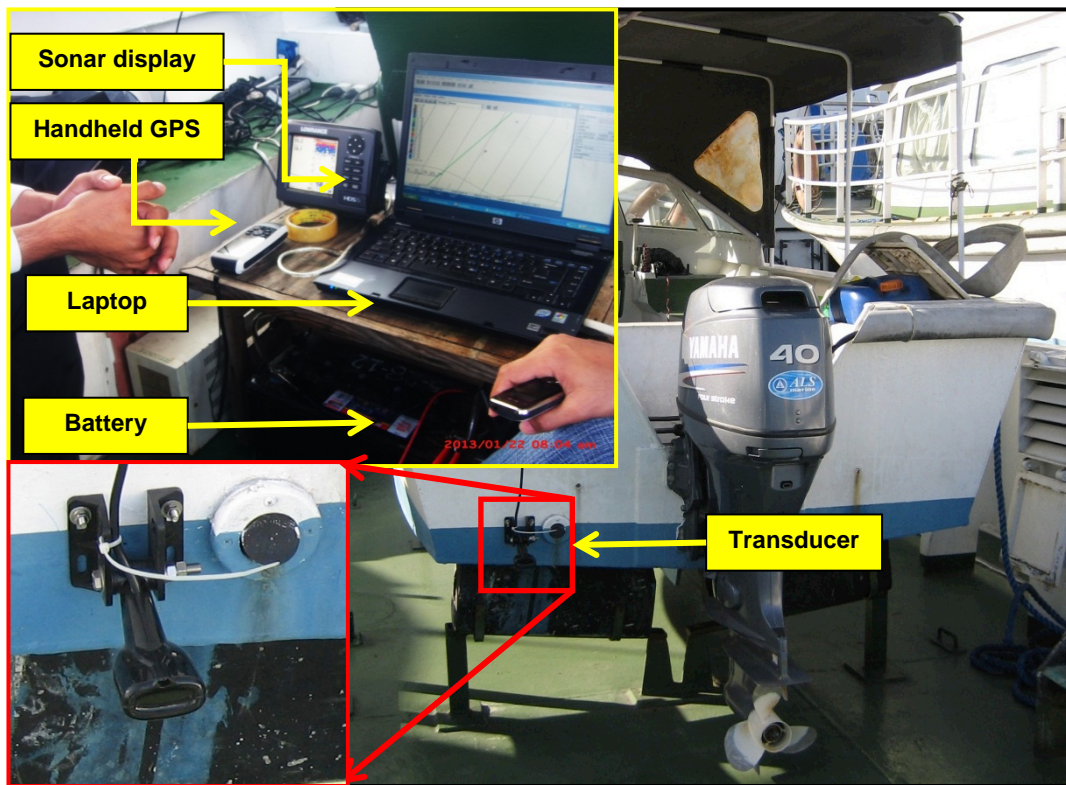


Figure 2.23 Sonar setup on NAMRIA skiff (2013)

### *Fishing sonar*

Bathymetric data were collected using ordinary fishing sonar (refer to Table 2.2 and Figure 2.25), operating at 200kHz (12° cone angle) at shallow depths and 50kHz (35° cone angle) at deeper depths. The transducer (Figure 2.24) was mounted at the transom of the skiff, far enough from the engine to prevent noise interference from the bubbles. It has a built-in internal GPS that can provide horizontal coordinates. An SD card was used to store and transfer data to a laptop computer.

Table 2.2 Fishing sonar characteristics

Brand/Model	Lowrance HDS5 Gen2
Frequency	200kHz/50kHz
Cone Angle	12/35 degrees
Input Power	10-17 VDC
Power Consumption	0.7A at 13 VDC with backlight on, 0.4A with backlight off
Depth Range	0-1524 m.
Display Dimension	480 mm. Width, 480mm. Height,
GPS	Internal, high sensitivity



Figure 2.24 Lowrance transducer



Figure 2.25 Lowrance HDS 5 console

### ***Power source***

A 12V 45Ah battery can be used as a power source to supply energy for a single survey day. To ensure safety of the battery, it is recommended to enclose it in a waterproof container during survey operations.



Figure 2.26 Power supply

### ***Battery charger***

The battery has to be charged everyday to ensure smooth, uninterrupted survey everyday.

### ***Handheld GPS***

In order to keep the vessel on course, a handheld GPS (Figure 2.27) was used to navigate the waters. Strategic points along the survey lines, such as turning points, were inputted to the GPS, using a freeware called *GPS TrackMaker*, prior to the survey and then tracked during the actual survey.

### ***Calibrated rope***

A calibrated rope (Figure 2.28), weighing around 5kg, was used to verify the sounding data.



Figure 2.27 Handheld GPS for tracking



Figure 2.28 Calibrated rope to check sounding data

### ***Laptop computer***

A laptop computer onboard was used to transfer data from the sonar unit, ensuring that survey data is intact after every survey.

### **2.2.3 Tidal Installation and Measurement**

#### ***Portable tide gauge***

A portable tide gauge/ water level logger (Table 2.3 and Figure 2.29) with a pressure-type sensor was established within the pilot site to record tidal readings every minute.

Table 2.3 Water level logger characteristics

Brand/Model	Global Water WL16U
Power supply	Logger: 2 9VDC alkaline batteries Sensor: 10-36 VDC
Output	Sensor: 4-20mA
Operating temperature	Logger: Industrial, -40C to +85C Sensor: 0F to +185F
Sample Modes	Programmable 1sec to 1yr High speed: 10samples/sec Logarithmic sample rate
Storage capacity	81,759 recordings for 2 analog inputs
Communication port	USB Type B



Figure 2.29 Portable tide gauge

#### ***Tide staff***

A tide staff was installed with the portable tide gauge as back up, to assess the accuracy of the tidal readings and to measure the distance of the sensor to the benchmark.

#### ***Leveling survey setup***

Leveling survey was conducted to transfer the elevation from a known tidal benchmark to the portable tide gauge. The leveling survey setup included a leveling scope with tripod, leveling rods, temporary concrete monuments/benchmarks, and a vehicle to transport equipment and personnel.

## 2.3 Results and Discussion

### 2.3.1 Sonar Survey

Sonar survey, using the commercial fishing sonar, was conducted for 6 days, from 21-26 January. Figure 2.30 shows the accomplishment per day, where days 1-6 are represented by the colors red (16km), orange (26km), yellow (27km), green (36km), blue (62km) and pink (16km), respectively.

In general, the bathymetry of the pilot site is characterized by a lot of variation along the shoreline, as well as in the rock islands in the middle of the survey area. Sudden depths or steep slopes can be found within 100m from the shoreline. With regards to sea survey condition, since the area is enclosed in the bay and the survey was conducted in January, which is a good time to survey in the Philippines, the sea condition was smooth in the mornings with very minimal effect to sounding data recordings.

Prior to survey, sounding data from the commercial fishing sonar was first assessed using (i) the calibrated rope with 5kg weight at random points and (ii) bar check at 2m, 3m and 5m. The fishing sonar fared well with a depth difference within 30cm from the rope test (possible sources of error maybe from water current and wave action).

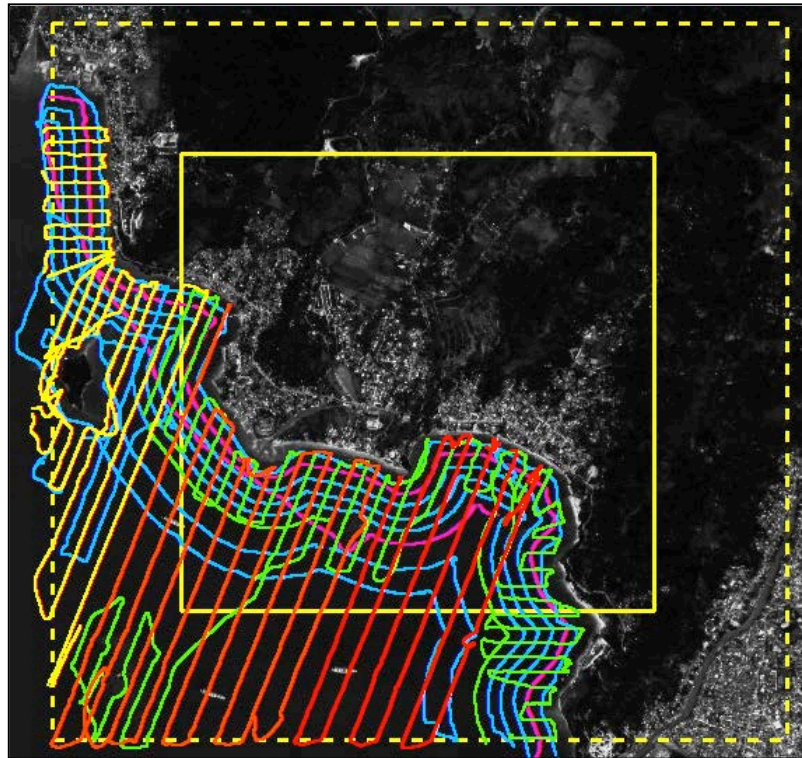


Figure 2.30 Result of sonar survey using the commercial fishing sonar from 21-26 January 2013

For the actual survey, the major lines, which are the lines perpendicular to the shoreline, were completed first followed by the areas with local variation and the shoreline. Since areas nearest to the shore are characterized by shallow depths, these were surveyed during the high tide to make sure that the skiff can navigate safely without damaging the transducer. During the survey, the maximum speed of the skiff is around 8-10 kph. However, much slower speed was used when navigating in areas with local variation to avoid damage to the skiff and equipment. Areas with local variation are located in near-shore areas, Mayanga Island, and the roughest occurring around Snake Island, as shown in Figures 2.31 and 2.32. The trend of bathymetry in this area seemed similar to the trend of exposed rock formation or island topography it is connected to. Small rock islets/extensions can be seen from the main island (Figure 2.31).

Sudden depths of 20m, depressions, and mounts in this area can be detected by the transducer, as shown in Figure 2.32.



Figure 2.31 Topographic condition in Snake Island

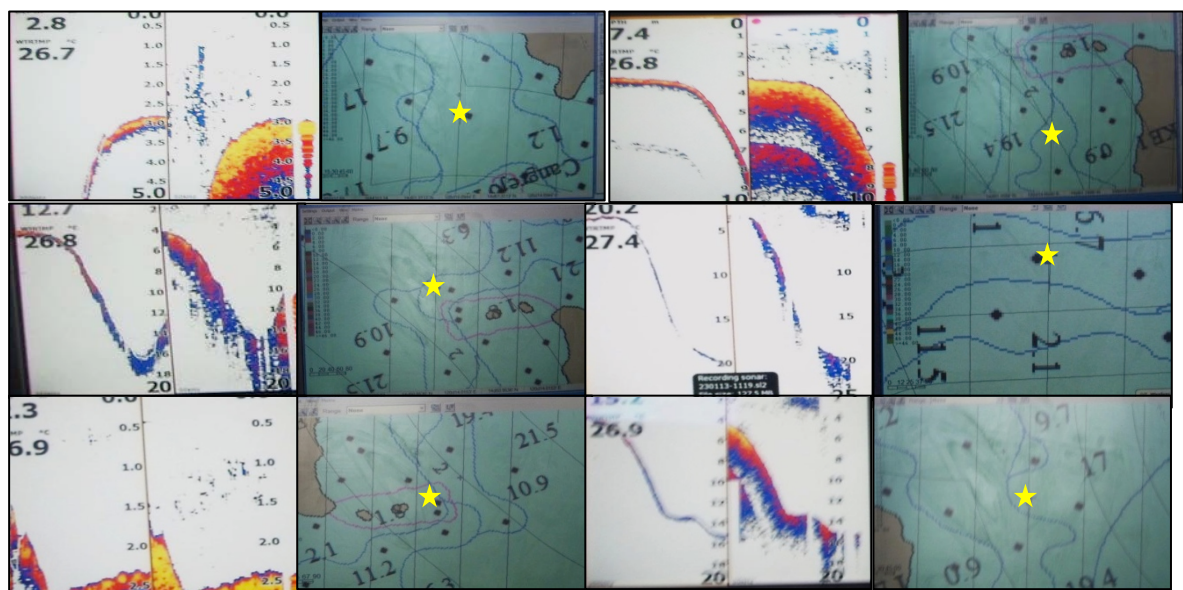


Figure 2.32 Local variations in Snake Island

## 2.3.2 Tidal Survey

### *Tide Gauge Installation*

The portable tide gauge was installed on 20 January, attached to a tide staff on one of the concrete columns of the pier in Driftwood Beach. The distance from the pressure sensor, at zero tide staff, to the floor of the pier (elevation in MSL measured by leveling survey) was determined to refer all tidal data to the MSL datum.

### *Tide Gauge Elevation*

Leveling survey was run from the low-cost tide gauge in the pilot site to the high-accuracy NAMRIA tide gauge in Camayan/Ocean Adventure, Subic for 6 days, from 21-26 January. The following figure shows the accomplishment per day, where days 1-6 are represented by the colors red (2.5km), orange (3.5km), yellow (5km), green (5.5km), blue (5km) and violet (4km), respectively.

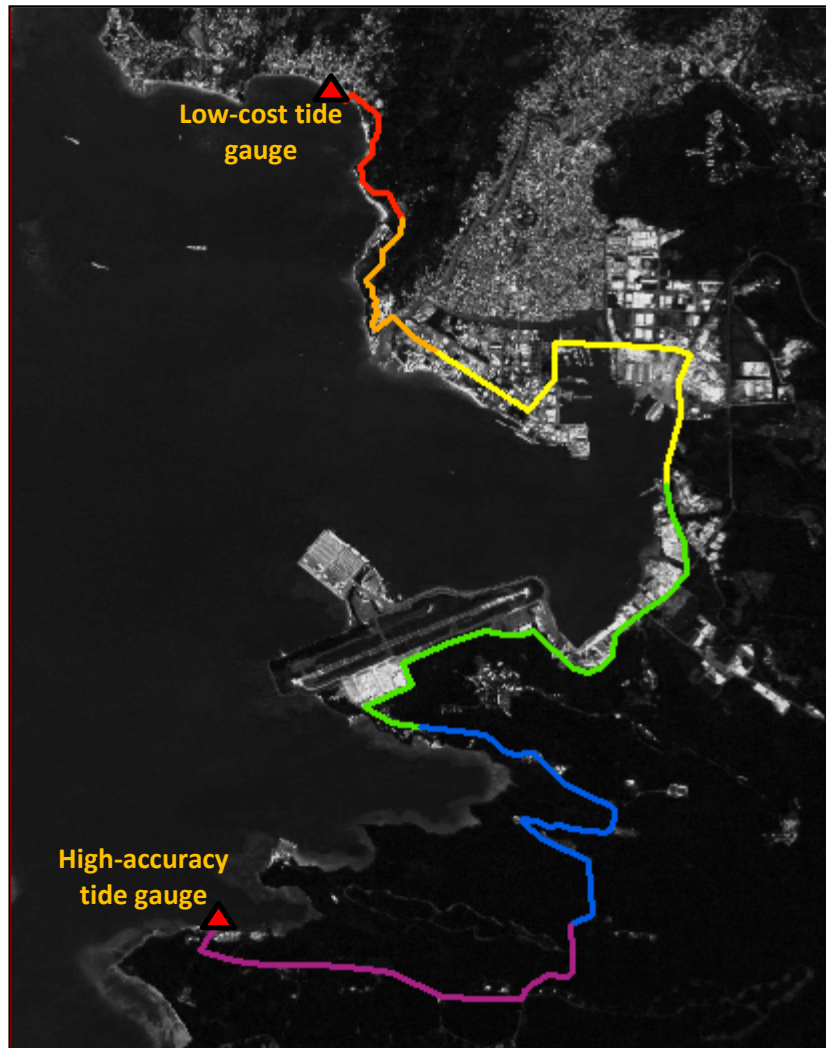


Figure 2.33 Leveling survey carried out from 21-26 January 2013



Source: NAMRIA, 2013

Figure 2.34 Leveling survey along the road network



Source: NAMRIA, 2013

Figure 2.35 Leveling survey near the tide gauge

Results show that the elevation of the low-cost tide gauge is lower than the high-accuracy tide gauge by 0.65m. The elevations of the tide gauges, referred to the MSL datum, are as follows:

Table 2.4 Elevation of tide gauge referred to the MSL datum

Tide gauge	Elevation in m (MSL)
High-accuracy (NAMRIA)	-1.455
Low-cost (RIMES)	-2.10308

### *Tidal Measurement*

Tidal data was recorded for 7 days: every 10 minutes for the first 2 days, and every minute for the next 5 days, as shown in Figure 2.36. Results show that the pilot site is characterized by diurnal tides with a tidal range of 1m.

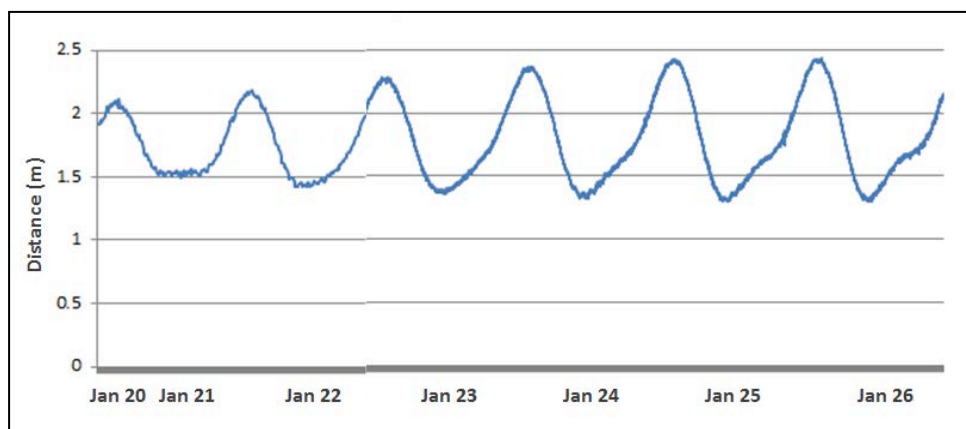


Figure 2.36 Result of tidal measurement carried out from 21-26 January 2013

### **2.3.3 Accuracy Assessment**

#### *Sonar Survey*

Sonar data from the low-cost (Lowrance) transducer were compared to the high-accuracy (Odom) transducer. Before comparison, both datasets were first corrected for draft and tidal offsets. To ensure a meaningful comparison, both datasets were corrected for tide, using the same source (high-accuracy tide gauge from NAMRIA), and referred to the MLLW datum. Forty-five samples were randomly taken along the 3 check lines made, to compare both datasets. Selection of the check lines was done such that most of the terrain conditions (e.g. shallow, deep, smooth, rough) were accounted for (Figure 2.37).

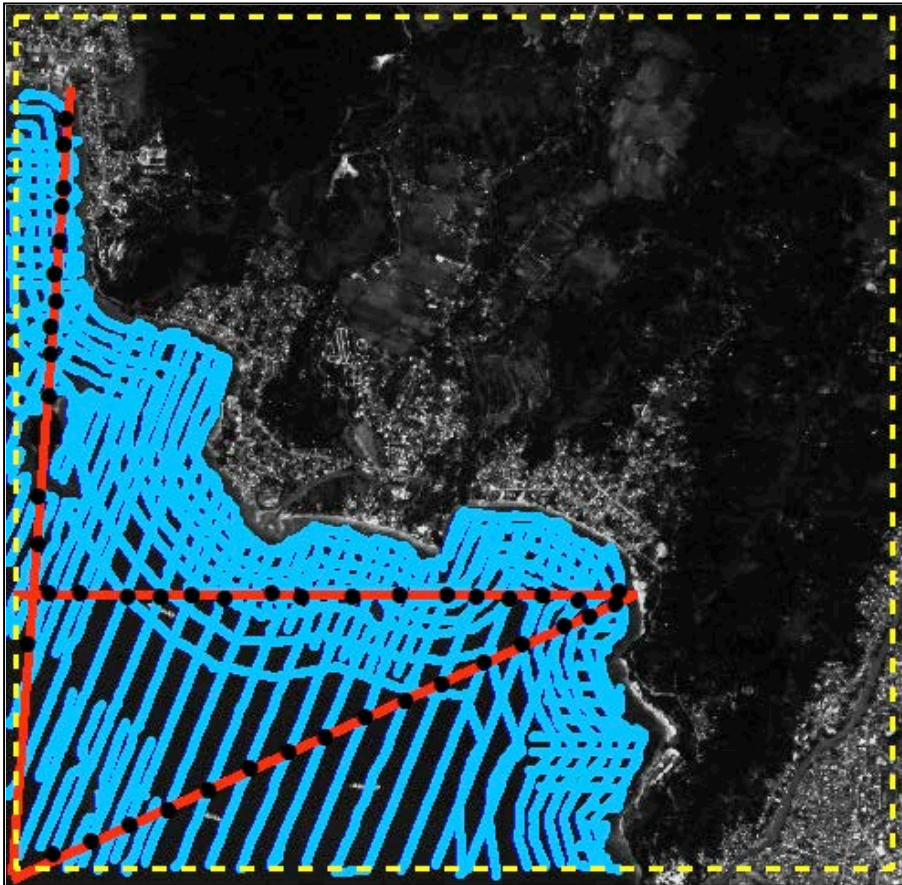


Figure 2.37 Check lines and check points

Among the 45 samples, only 1 data had a large difference (2.45m) between datasets, as shown in Figure 2.38. The rest of the samples have a difference of around 1m or less, which satisfies the vertical accuracy required for tsunami modeling. The large difference may be attributed to the location of the sample, which occurs near Snake Island, an area with a lot of terrain variations.

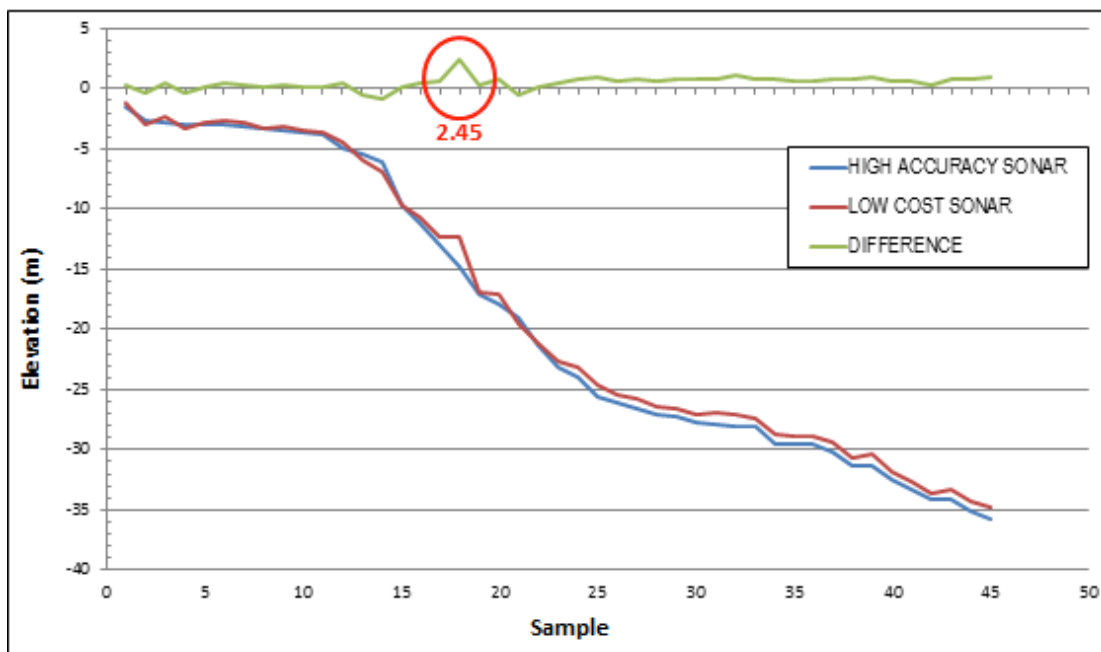


Figure 2.38 Comparison of high-accuracy sonar and low-cost sonar data

## Tidal Survey

Tidal data from the low-cost tide gauge were compared with the tidal data made from (i) manual observation of tide and (ii) high accuracy tide gauge from NAMRIA. The following results show that the performance of the low-cost tide gauge is on par with the high-accuracy tide gauge.

### Low-cost tide gauge vs. tide staff readings

As secondary assessment and back up of the low-cost tide gauge data, hourly manual tide staff readings were also used for comparison (Table 2.5). Results show that the low-cost tide gauge data fared very well, with an average difference of 3cm for the first 2 days and almost negligible difference for the rest of the 4 days.

Table 2.5 Comparison of tide staff readings vs. low-cost tide gauge readings

Time	JANUARY																	
	21			22			23			24			25			26		
	TS	LTG	Diff	TS	LTG	Diff	TS	LTG	Diff	TS	LTG	Diff	TS	LTG	Diff	TS	LTG	Diff
6	1.45	1.53	0.08	1.43	1.46	0.03	1.4	1.41	0.01	1.35	1.37	0.02	1.36	1.36	0	1.34	1.34	0
7	1.48	1.54	0.06	1.46	1.48	0.02	1.43	1.45	0.02	1.42	1.44	0.02	1.4	1.41	0.01	1.4	1.39	-0
8	1.5	1.54	0.04	1.5	1.51	0.01	1.48	1.49	0.01	1.48	1.5	0.02	1.45	1.46	0.01	1.5	1.45	-0.1
9	1.53	1.55	0.02	1.51	1.56	0.05	1.52	1.54	0.02	1.57	1.53	-0	1.56	1.51	-0.1	1.55	1.54	-0
10	1.57	1.58	0.01	1.54	1.59	0.05	1.6	1.59	-0	1.59	1.57	-0	1.58	1.57	-0	1.61	1.6	-0
11	1.6	1.64	0.04	1.64	1.63	-0	1.65	1.64	-0	1.62	1.63	0.01	1.64	1.62	-0	1.65	1.64	-0
12	1.67	1.72	0.05	1.64	1.72	0.08	1.7	1.7	0	1.69	1.68	-0	1.68	1.65	-0	1.67	1.66	-0
13	1.79	1.83	0.04	1.8	1.83	0.03	1.75	1.78	0.03	1.85	1.74	-0.1	1.7	1.69	-0	1.7	1.69	-0
14	1.93	1.94	0.01	1.9	1.92	0.02	1.81	1.89	0.08	1.96	1.82	-0.1	1.82	1.74	-0.1	1.72	1.72	0
15	2.03	2.04	0.01	2.01	2.02	0.01	2.1	2.01	-0.1	2.08	1.93	-0.2	1.89	1.83	-0.1	1.78	1.78	0
16	2.09	2.12	0.03	2.11	2.14	0.03	2.22	2.12	-0.1	2.15	2.06	-0.1	2	1.96	-0	1.89	1.87	-0
17	2.14	2.16	0.02	2.21	2.22	0.01	2.25	2.23	-0	2.2	2.2	0	2.1	2.09	-0	2	1.99	-0
18	2.14	2.16	0.02	2.25	2.27	0.02	2.31	2.33	0.02	2.32	2.32	0	2.3	2.21	-0.1			
<b>Ave Diff</b>			0.03			0.03			-0			-0			-0			-0
<b>Total Ave Diff</b>	<b>-0.003095</b>																	

Notes: TS- tide staff reading; LTG- low-cost tide gauge reading; All data referred to the zero tide staff of the low-cost tide gauge

### Low-cost tide gauge vs. high-accuracy tide gauge

From the tidal analysis conducted by NAMRIA, results show that the accuracy and precision of the low-cost tide gauge with respect to the high-accuracy tide gauge is very good. Figure 2.39 shows the actual tidal data/water level data measured from the both sensors. These data have not yet been referred to any datum. A systematic error of around 40cm can be seen, separating the two datasets. This is due to the elevation of the low-cost tide gauge being lower than the high-accuracy tide gauge, as determined from the results of the leveling survey, assuming that both locations have the same tidal (MSL) conditions.

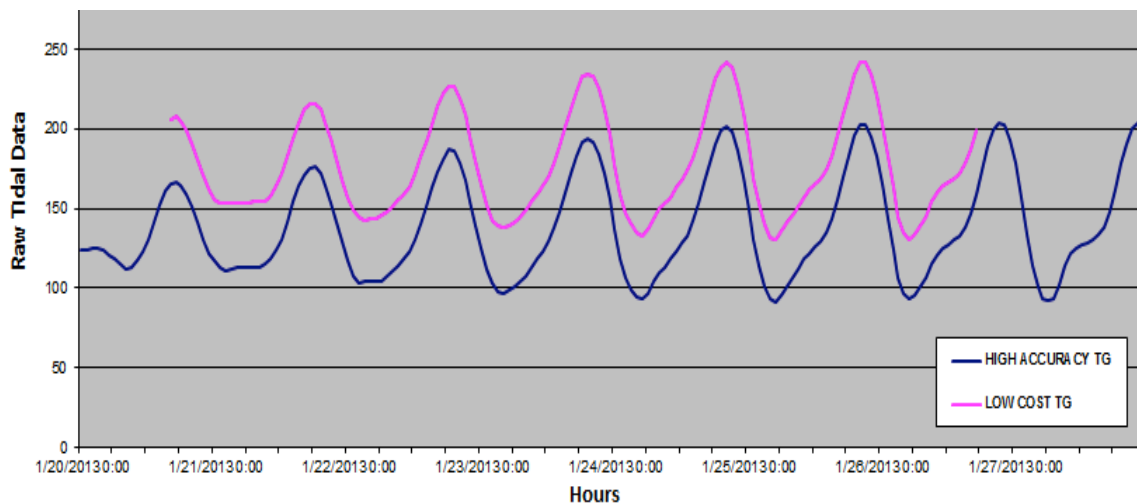


Figure 2.39 Comparison of raw tidal data from both tide gauges

Figure 2.40 shows that tidal data from both gauges fit very well, when the systematic difference was removed. However, after referring both tide gauges to the MSL datum, a systematic difference in elevation of around 0.25m can still be seen, as shown in Figure 2.41. A number of factors may have contributed to this result, including changes in environment, observation error, etc.

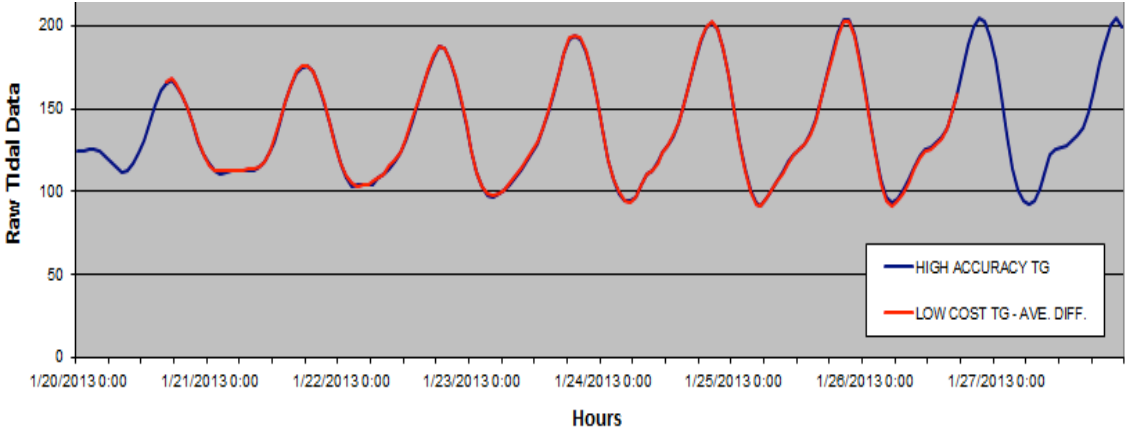


Figure 2.40 Comparison of raw tidal data from both tide gauges when the systematic difference was removed

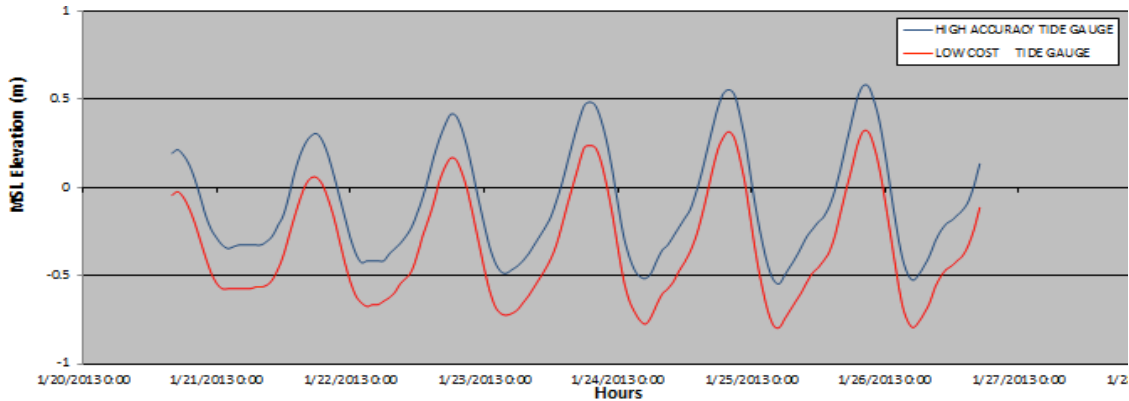


Figure 2.41 Comparison of tidal data referred to the MSL datum

**2.4 Problems Encountered and Recommendations**

**2.4.1 Sonar Survey**

The two major issues encountered during the survey are time and obstruction. Although the survey was accomplished according to the planned duration, it could have been maximized. Survey time was limited by a number of factors. First, the maximum boat speed that the skiff can go is only around 10kph, which is half the speed of an ordinary fishing boat. So, it takes the same time to transfer from one line to the next, which could have been sped up if the boat can run faster. Second, navigating through areas with local variation (Figure 2.42) and obstruction (Figure 2.43), e.g. fishing line, is very critical, so speed is decreased to avoid unnecessary damage to the boat and equipment.

The other major issue is the presence of obstruction, e.g. structures (Figure 2.44), buoys, and large vessel (Figure 2.45) along the survey line, which has to be avoided. The survey vessel has to circumvent around these obstructions and, as a result, moved away from the planned survey route. The restricted area for

swimmers (Figure 2.46) limited access to bathymetric data in this area, an obstruction that cannot be helped.

In reality, these are always present, in one form or another in varying degrees. Although issues of concern, these did not significantly hamper survey operations. However, it is best to be always prepared; know the possible limitations before the survey, so adjustments could be made.



Figure 2.42 Areas with local variation



Figure 2.43 Fishing line



Figure 2.44 Unfinished concrete structure



Figure 2.45 Large vessel



Figure 2.46 Restricted area for swimming

## CHAPTER 3 TOPOGRAPHIC SURVEY

### 3.1 Methodology

For the field survey in the Philippines, two types of GPS survey were conducted to collect topographic data. The first activity uses RTK GPS survey to collect data along every accessible road, avoiding areas within 500m from the mountain to avoid large errors from multipath. The second activity uses fast static GPS observation to collect the position of ground control points (8) and check points (5) that will be used in aerial photogrammetry. These two surveys can be conducted parallel to each other. In addition, WGS-84 and EGM-96 or EGM 2008 can be used as reference during the survey. GPS occupation on a level benchmark can determine the undulation value or the geoid height of an area that can be used to transfer topographic data, based on the ellipsoid to the MSL datum.

#### 3.1.1 Calculation of Undulation Value (Geoid Height)

In this project, the local MSL datum will be used as the vertical reference for all elevations. However, GPS coordinates are normally based on WGS-84 and, in some cases, heights will be transformed to MSL based on the global geoid models called "EGM96" or "EGM2008". Therefore, the undulation value or geoid height must be determined. The equation to calculate the undulation value between local MSL and WGS-84 ellipsoidal height is depicted in Figure 3.1.

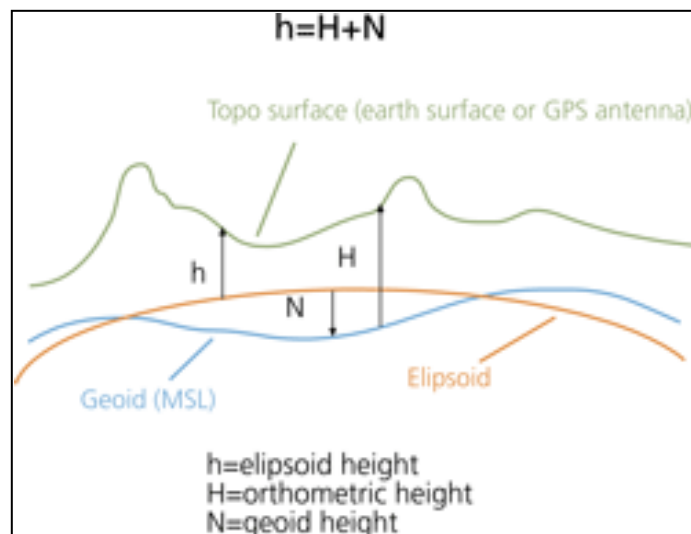


Figure 3.1 Relationship between ellipsoidal height, MSL and undulation value (geoid height)

During survey, some elevation benchmarks will be selected to determine the undulation value of an area. Each elevation in local MSL will be updated and checked, and then subtracted from the ellipsoidal height that will be derived from static GPS observation of the same point (connected to two or more known points with a baseline less than 15 km).

For the survey project in Barrio Barretto, the elevation benchmark with the designation number "BM ZA-17A" was selected to evaluate this value. This point was also used as a GCP (GCP5) for aerial photo rectification. A multi-carrier GNSS receiver (rover station) was setup on the benchmark to evaluate the 3D coordinates of the point as shown in Figure 3.2. Then, two more receivers were setup as base stations on horizontal benchmarks (known points), "ZBS-3200" and "ZBS-3197", as shown in Figures 3.3 and 3.4. Raw observations from all receivers were collected for 30 minutes, using the same starting time, and then downloaded. The resulting coordinates for the rover station were obtained after static post-processing of the downloaded data.



Figure 3.2 GPS setup on a known elevation benchmark (BM ZA-17A)



Figure 3.3 GPS setup on a known horizontal benchmark (ZBS-3200)



Figure 3.4 GPS setup on a known horizontal benchmark (ZBS-3197)

### **3.1.2 Ground Control Point using Static GPS Observation**

#### ***Ground Control Point Survey Design***

GCPs are needed to rectify aerial photographs. As a requirement, GCPs should be located at each corner of a photogrammetry block, as well as one GCP for every 3 images along a photo strip. Each point should be covered by as many images as possible.

To rectify the aerial photos in the pilot site, 10 GCPs and 5 checkpoints were selected, as shown respectively in Figures 3.5 and 3.6, where the rectangles correspond to aerial photo extents. However, it is not sure if GCP 8 is a restricted area, so another option, GCP 8/2, was selected in case GCP 8 cannot be accessed.

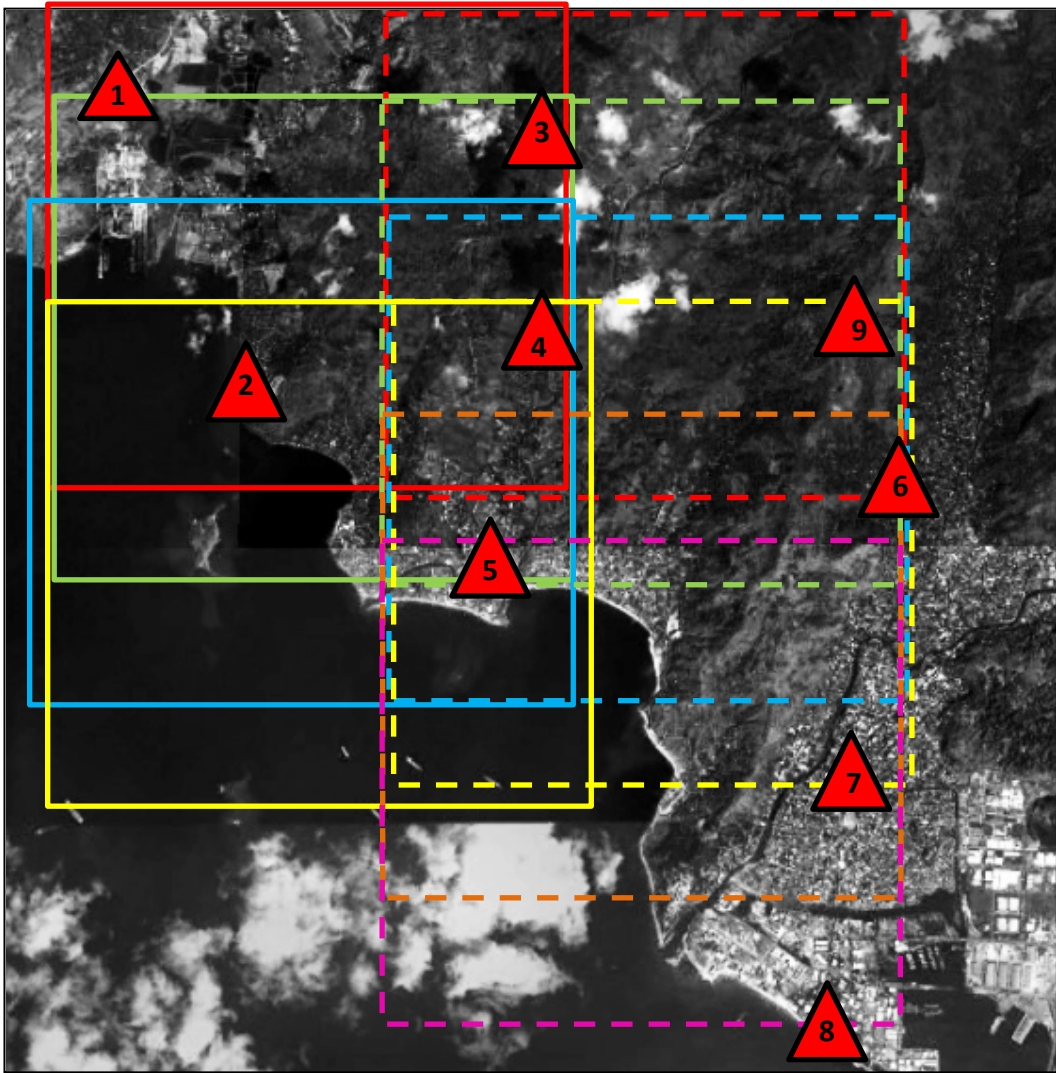


Figure 3.5 GCPs for aerial photogrammetry

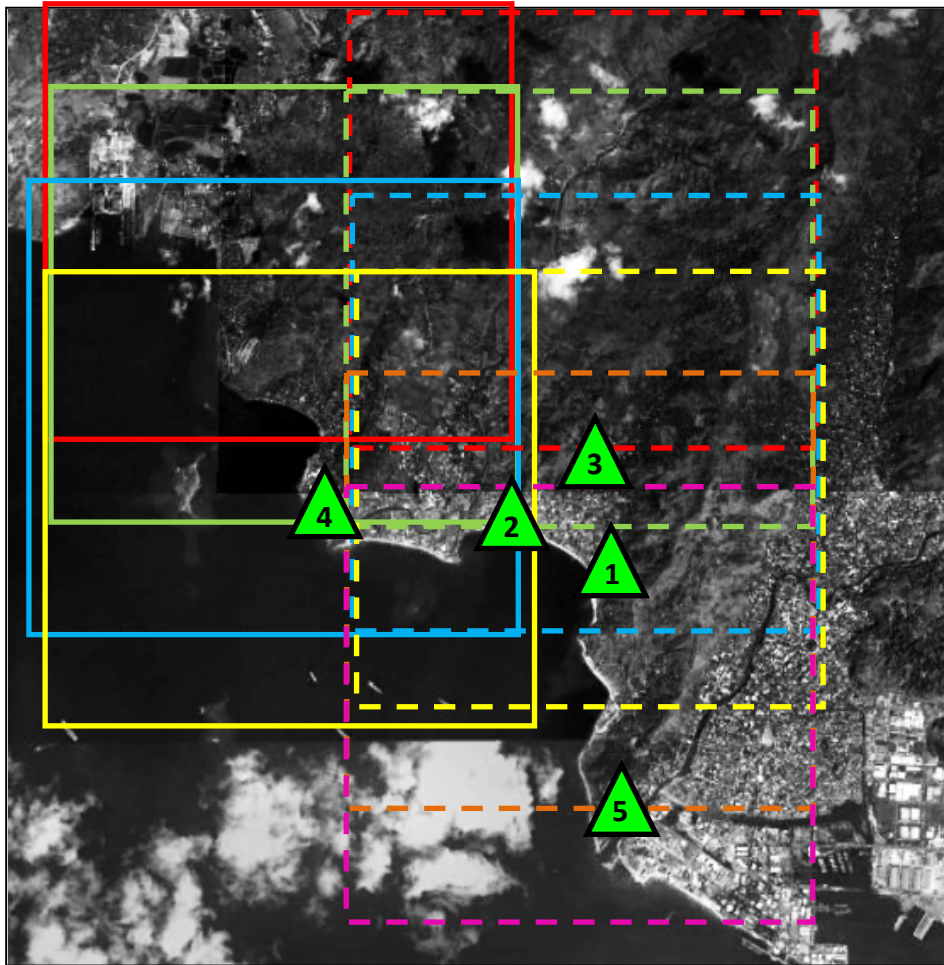


Figure 3.6 Checkpoints for aerial photogrammetry

### *Static GPS Observation*

Table 3.1 shows the list of coordinates of the GCPs and checkpoints in the pilot site. Static GPS survey was conducted on each point, using GCP5 as the base station for all GCPs and checkpoints, including RTK survey. Thus, all GCP and checkpoint coordinates were calculated based on the GCP5. In this project, two teams were deployed to survey all points, one to the left and another to the right side of GCP5 (base station).

Table 3.1 Location of GCPs and checkpoints for aerial photogrammetry

Name	Longitude	Latitude
GCP1	120°13'29.51"E	14°53'27.16"N
GCP2	120°14'5.36"E	14°52'2.06"N
GCP3	120°15'27.46"E	14°53'7.86"N
GCP4	120°15'18.78"E	14°52'7.26"N
GCP5	120°15'16.2"E	14°51'6.53"N
GCP6	120°17'9.74"E	14°51'25.3"N
GCP7	120°16'56.42"E	14°50'16.19"N
GCP8	120°16'48.93"E	14°48'58.33"N
GCP8/2	120°16'52.14"E	14°48'59.96"N
GCP9	120°16'57.08"E	14°52'12.03"N
CHK1	120°16'5.85"E	14°50'49.41"N
CHK2	120°15'43.83"E	14°51'4.54"N
CHK3	120°16'2.2"E	14°51'9.58"N
CHK4	120°14'34.84"E	14°51'7.52"N
CHK5	120°16'12.19"E	4°49'35.31"N

Figure 3.7 shows the GPS static survey condition above GCP1. After setting up all instruments, the height of the GPS antenna above the GCP was measured, using a measurement tape.



Figure 3.7 GPS static survey condition above GCP1

### 3.1.3 Land Evaluation using Real-Time Kinematic Observation

#### *Real-Time Kinematic Observation*

For this project, topographic elevation, gathered along the road network using RTK-GPS, should be finally referred to the local MSL. However, GPS normally calculates a point's position based on WGS-84, or sometimes transforms the height into MSL using a global geoid model. In this case, the undulation value determined from GCP5 was used to transform the ellipsoidal height into local MSL by subtracting the ellipsoidal height with the undulation value.

To survey the road network in the area, a technique called Real-Time Kinematic (RTK) was employed by setting up a base station at GCP5 and broadcasting the correction data using radio to the rover, as shown in Figure 3.8. The correction data was used with the raw observations to calculate the double difference, to gain better accuracy of positioning. There are, however, some limitations, such as (i) the range that the rover can work with, which is normally not more than 3-5 km, and (ii) obstruction like buildings and mountains.



Figure 3.8 RTK GPS base station set up at GCP5 and broadcasting correction data through radio

As with static GPS survey, two teams were deployed to each side of GCP5 to conduct the RTK-GPS survey. This survey was completed in 2 days. On the first day, 2 vans were used to survey most of the major road network. The rover was attached to the van, and the height of the GPS antenna to the ground was measured using a measuring tape, as illustrated in Figure 3.9.

Since there were limitations due to obstructions found along the road network, on the second day, the base station was moved from GCP5 to CHK2, which was closer to the minor road network that was planned for that day. To survey minor road network, the teams were still divided into 2, but the vehicle of one team was changed to the tricycle to easily access narrow roads, as shown in Figure 3.10.



Figure 3.9 GPS receiver attached to the van;  
height from antenna to ground was measured using a measuring tape



Figure 3.10 GPS receiver attached to the tricycle for narrow road network

### ***GPS Data Post-processing***

Solutions allowed for the RTK road network survey are *fixed* and *float* solutions, which can provide sub-meter height accuracy. After completing the road network survey, data were downloaded into the computer for data filtering.

Since vertical accuracy must be better than 1 meter, outliers greater than 1 meter were filtered out from the solution. The methodology to detect the outlier is described below:

**STEP 1:** Calculate the vertical difference and horizontal distance between the point  $P(N, E, h)_t$  and  $P(N, E, h)_{t-1}$ , where N and E are the horizontal components and V is the vertical component, as shown in equation (1) and (2) below.

$$Vdiff_t = \sqrt{(P(h)_t - P(h)_{t-1})^2} \quad (1)$$

$$Hdist_t = \sqrt{((P(N)_t - P(N)_{t-1})^2 + (P(E)_t - P(E)_{t-1})^2)} \quad (2)$$

**STEP 2:** Detect the Start Period of outlier by defining two constants called Hcon and Vcon, which will be used to qualify the RTK solution:

```
Begin
    if ((Vdifft > Vcon)&&(Hdistt > Hcon))
        return 1;
    else
        return 0;
    end;
End
where
    Hcon = 10 and Vcon = 0.5
```

the start period of outlier will begin at time "t"

**STEP 3:** Detect the End Period of outlier using the same constants, using a simpler methodology defined by:

```
Begin
    if ((Vdifft > Vcon))
        return 1;
    else
        return 0;
    end;
End
where
    Vcon = 0.5
```

the end period of outlier will be at time "t"

An example of a detected outlier is shown in Figure 3.11. Hdiff values are the outputs from STEP 2, and Vdiff values are the outputs from STEP 3. Hdiff, Vdiff and "h" values were used as indicators to detect outliers, such that, all "h" values that fall within either Hdiff or Vdiff, that are flagged 1, will be identified as outliers, caused by loss of lock or cycle slip. However, the proposed filtering method is just used to separate data affected by biases. Further steps in DEM generation should be done carefully, especially when dealing with dataset and outliers.

P/t	E	N	h	Hdiff	Vdiff	Start Outlier	End Outlier	Outlier
6562	206229.164	1643556.008	59.706	3.077	0.035	0	0	
6563	206229.794	1643559.294	59.475	3.346	0.231	0	0	
6564	206230.571	1643562.332	59.384	3.136	0.091	0	0	
6565	206231.178	1643565.447	59.91	3.174	0.526	0	1	1
6566	206231.489	1643568.491	59.864	3.060	0.046	0	0	1
6567	206257.444	1643667.975	-13.84	102.814	73.704	1	1	1
6568	206258.295	1643672.033	81.818	4.146	95.658	0	1	1
6569	206283.702	1643697.637	124.76	36.070	42.938	1	1	1
6570	206282.518	1643701.383	111.57	3.929	13.191	0	1	1
6571	206276.71	1643717.529	62.03	17.159	49.535	1	1	1
6572	206276.825	1643720.736	58.091	3.209	3.939	0	1	1
6573	206277.788	1643723.459	58.3	2.888	0.209	0	0	1
6574	206272.235	1643789.175	58.906	65.950	0.606	1	1	1
6575	206272.05	1643791.784	59.438	2.616	0.532	0	1	1
6576	206271.789	1643794.554	59.45	2.782	0.012	0	0	1
6577	206274.433	1643795.552	53.47	2.826	5.980	0	1	1
6578	206274.137	1643798.441	53.451	2.904	0.019	0	0	1
6579	206273.858	1643801.324	53.445	2.896	0.006	0	0	1
6580	206271.074	1643805.765	58.75	5.241	5.305	0	1	1
6581	206270.786	1643808.711	58.752	2.960	0.002	0	0	
6582	206270.484	1643811.649	58.668	2.953	0.084	0	0	
6583	206270.147	1643814.537	58.637	2.908	0.031	0	0	
6584	206269.823	1643817.195	58.635	2.678	0.002	0	0	

Figure 3.11 Outliers detected from the road network survey, carried out on 24 January 2013

### 3.1.4 Accuracy Assessment

Two types of assessment were done to check the reliability of RTK-GPS survey. First, is to check the accuracy of RTK-GPS points with static observation at the same point. This was done by conducting static observation on CHK1-5 and running the RTK-GPS on the same points. Another procedure was to check the precision of RTK-GPS survey. This was done by running an RTK-GPS survey on the same route, on different days. Then, randomly selected points along this route were taken to check the variation of elevation above ellipsoidal height.

### 3.2 Data and Equipment

Table 3.2 shows a list of the data and equipment used, and personnel employed for topographic survey. The 3 major activities include (i) pre-survey preparation and undulation value calculation, (ii) RTK GPS survey along the road network, and (iii) fast static GPS observation on GCPs and checkpoints.

Table 3.2. List of data and resources used in topographic survey

Activity (Duration)	Data Used	Equipment Used	Personnel
1. Instrument preparation, RTK survey testing and undulation value calculation (22 Jan)	GPS benchmark description Level benchmark description	Vehicle (van, tricycle)  <b>Base Station:</b> Multi frequency GNSS receiver with internal memory GNSS Antenna Battery GNSS Controller Tripod	Local security Operator (instrument, data logging and navigation) Driver NAMRIA staff (3) RIMES staff (1)
2. Fast static GPS survey on GCPs and checkpoints (23 Jan)	Location of GCPs and checkpoints derived from aerial photographs	Tribatch Measuring tape Mobile Phones  <b>Rover Station:</b>	
3. RTK GPS along road network (24-25 Jan)	Road network map	Multi frequency GNSS receiver with internal memory GNSS Antenna Battery GNSS Controller Single magnetic mount for GPS Mobile Phone Measuring tape	

### 3.2.1 Data

#### *Benchmark Description*

GPS benchmark descriptions were used in planning the survey. Leveling benchmarks were occupied by static GPS observation to get the offset difference between the datums used by each network.

#### *Aerial Photographs*

Selection of GCPs and checkpoints in the pilot site was based on aerial photographs. The image parameters are as follows:

Table 3.3 Aerial photograph parameters

Altitude scale	1:15,000
Camera	RC8 UAg 291
Focal length	152.53 cm
Date	11/26/91 (strip 11) 11/28/91 (strip 12)

### 3.2.2 Equipment

#### *GPS*

Three Kronos 200 (Horizon brand) GPS units were used: 1 base and 2 rovers for the duration of the survey where correction data was broadcasted through radio. Software that can be used to process the GPS data are the Kronos Processor and Topcon (evaluation copy).



vertical RMS is in between 0.3 to 2.4 centimeters where both results agree with the accuracy requirement in this project.

Table 3.5 GPS observation residuals for all GCPs and CHKs

Name	dN (m)	dE (m)	dHt (m)	Horz RMS (m)	Vert RMS (m)
BASE-GCP1	4300.136	-3223.83	0.025	0.006	0.021
BASE-GCP2	1724.7	-2152.09	0.961	0.003	0.006
BASE-GCP3	3722.835	318.923	9.003	0.013	0.024
BASE-GCP4	1867.147	44.093	2.867	0.003	0.005
BASE-GCP6	583.907	3355.192	49.661	0.013	0.021
BASE-GCP7	-1540.12	2962.3	-0.814	0.007	0.015
BASE-GCP8	-3884.19	2833.966	-3.381	0.012	0.016
BASE-CHK1	-513.099	1439.679	0.418	0.001	0.003
BASE-CHK2	-54.867	785.725	0.737	0.002	0.004
BASE-CHK3	104.947	1344.069	-0.021	0.005	0.01
BASE-CHK4	64.53	-1300.56	-0.097	0.004	0.006
BASE-CHK5	-2811.95	1654.649	1.365	0.008	0.013

Note that there is no residual result for GCP5 since it was set as the base station for all GCPs and checkpoints.

The summary of coordinates for all GCPs and CHKs in Appendix 2.4 is shown in the table below.

Table 3.6 Coordinates of all GCPs and CHKs

Name	DMSLat	DMSLon	h
GCP1	14°53'26.11150"N	120°13'29.50733"E	51.982
GCP2	14°52'02.32234"N	120°14'05.37048"E	51.243
GCP3	14°53'07.33555"N	120°15'28.03136"E	59.788
GCP4	14°52'06.96004"N	120°15'18.83691"E	52.826
GCP5	14°51'06.21142"N	120°15'17.36192"E	49.684
GCP6	14°51'25.20140"N	120°17'09.59310"E	100.254
GCP7	14°50'16.09694"N	120°16'56.44288"E	49.745
GCP8/2	14°48'59.83146"N	120°16'52.14127"E	48.123
CHK1	14°50'49.51606"N	120°16'05.51735"E	50.285
CHK2	14°51'04.42586"N	120°15'43.64391"E	50.469
CHK3	14°51'09.62472"N	120°16'02.32050"E	49.805
CHK4	14°51'08.30980"N	120°14'33.85879"E	49.72
CHK5	14°49'34.72099"N	120°16'12.70254"E	51.887

### 3.3.3 Land Elevation using Real-Time Kinematic Observation

The road network survey was carried out on 24-25 January 2013. The total number of datasets, number of detected outliers, and percentage of detected outliers between 24 and 25 January are summarized in Table 3.7.

Table 3.7 Total number of data and outliers during the road network survey from 24 to 25 January 2013

Date	Total Number of Data	Number of Detected Outliers	Percentage of Detected Outliers
24/01/2013	9801	583	5.95
25/01/2013	5180	777	15

From the table, it can be seen that the result of the road network survey on 24 January 2013 is significantly better than the next day. This may be because the road network for the second day was more complex, and especially since the survey was conducted using a tricycle.

Figures 3.13 and 3.14 show the results of the road network survey from 24-25 January 2013. Surveys were duplicated to check the accuracy between the two days, as shown in Figure 3.15.



Figure 3.13 Result of road network survey carried out on 24 January 2013

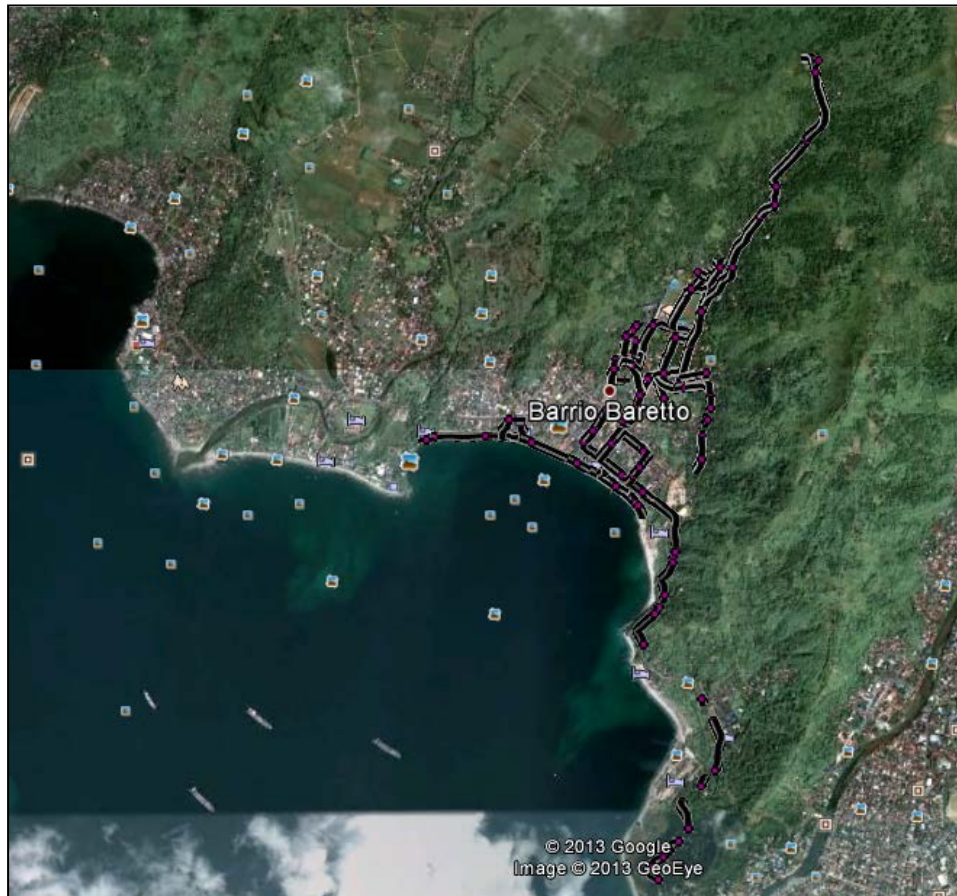


Figure 3.14 Result of road network survey carried out on 25 January 2013

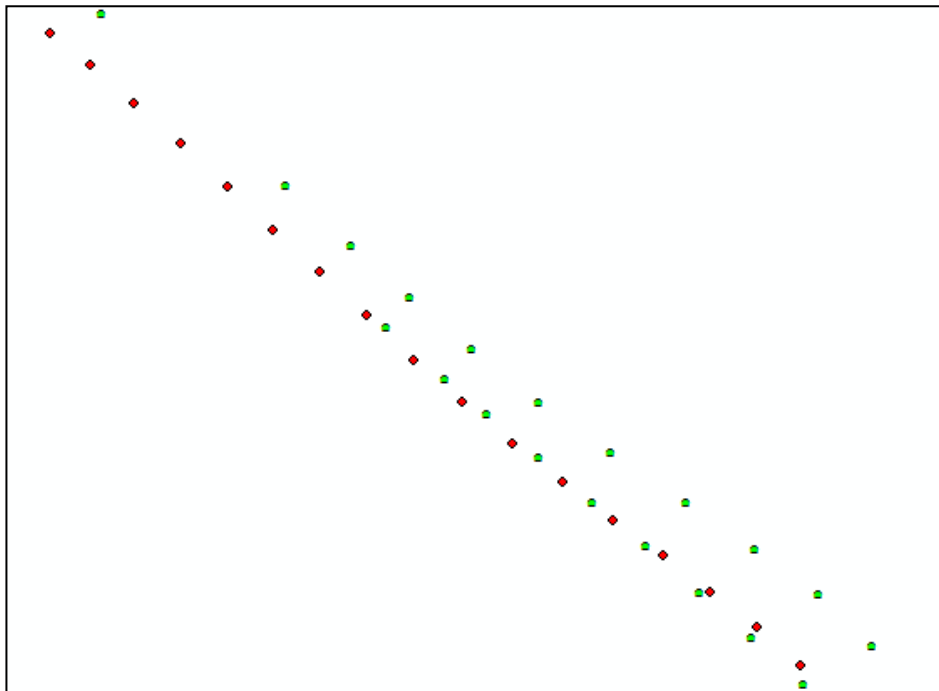


Figure 3.15 Comparison of road network data between two consecutive days

Ten locations were randomly selected to check the variation of elevation above ellipsoidal height, as shown in Table 3.8. From the table it can be clearly seen that the accuracy of the results from the road network agree well with the requirement for tsunami modelling.

Table 3.8 Selected checkpoints and ellipsoidal height difference

Point Number	Point Name	h (m)	Difference (m)
1	Rtk24_9111	49.482	0.075
	Rtk25_1779	49.407	
2	Rtk24_9146	49.249	0.009
	Rtk25_1740	49.24	
3	Rtk24_6688	52.476	0.07
	Rtk25_3342	52.536	
4	Rtk24_6625	55.794	0.011
	Rtk25_4303	55.783	
5	Rtk24_6696	52.37	0.006
	Rtk25_3369	52.364	
6	Rtk24_6625	55.794	0.011
	Rtk25_4303	55.783	
7	Rtk24_6498	51.074	0.133
	Rtk25_1957	50.941	
8	Rtk24_9667	67.468	0.008
	Rtk25_2039	67.476	
9	Rtk24_6572	58.091	0.04
	Rtk25_4462	58.131	
10	Rtk24_9496	50.372	0.131
	Rtk25_1629	50.241	
Mean			0.049
Mode			0.011
STD			0.051
Max			0.133

### 3.4 Problems Encountered and Recommendations

#### 3.4.1 Undulation Value Calculation (Geoid Height)

During the setting up of the reference station at the selected elevation benchmark, an unexpected event occurred. In the morning, the area around the benchmark seemed to be good for setting up the base station, as shown in Figure 3.16, but in the afternoon a food stall was positioned nearby the elevation benchmark, as shown in Figure 3.17. It is difficult to anticipate such events prior to actual survey; thus, it is important to always be prepared, such as good diplomatic skills when negotiating with local people in the area.



Figure 3.16 Base station set up on the elevation benchmark on the morning of 22 January 2013



Figure 3.17 Food stall set up nearby the elevation benchmark in the afternoon of 22 January 2013

### 3.4.2 Ground Control Points using GPS Static Observation

Some benchmarks are located in restricted areas or in areas that are very difficult to access, such as GCP8 and GCP9, where there was no letter of permission provided. It is difficult to check the actual condition when selecting GCPs and CHKs from aerial photographs or satellite image, thus a reconnaissance survey of all the GCPs and CHKs should be conducted prior to actual survey.

Moreover, there was a problem regarding receiver malfunction. Raw observation data was not logged in the receiver for all the GCPs and CHKs in the morning session. As a result, a new receiver was used and a resurvey of the points was conducted in the afternoon. In this case, the condition of the receiver should be checked prior to each survey, as well as raw observation logged in the receiver, which should be downloaded and checked when transferring from one GCP to another.

## CHAPTER 4

# SHORELINE DELINEATION

### 4.1 Methodology

Shoreline or zero elevation line is delineated to define the connection between land and sea. For high slope or cliff areas, shoreline can be determined from existing maps or rectified aerial images. However, higher accuracy is required for low slope areas such as the beach. A walking GPS survey can be conducted to estimate shoreline in this area. This is done by carrying the GPS antenna on a pole, and walking along the water edge during the time when the predicted tide is at zero elevation.

Estimating zero elevation is critical, especially when the bathymetry of the area is very shallow: a slight difference in elevation may mean a big difference (e.g. greater than 50m) in horizontal position. Using the predicted tide to determine the time when the zero elevation occurs can help approximate the exact location of this line.

In Barrio Barretto, the predicted tide data from the tide table was used to set the appropriate time of survey. Since these data are referred to the MLLW, taking the tide at 0.46m MLLW will give the corresponding zero elevation in MSL. On 25 January, this condition is predicted to occur from 14:30-15:30. So, after initializing the instrument, a walking RTK-GPS survey took place at this period to delineate the zero elevation line, using CHK1 as the base station, as shown in Figures 4.1 and 4.2.



Figure 4.1 Base station set up at CHK1



Figure 4.2 Surveyor walking along the beach to survey the shoreline

## 4.2 Data and Equipment

The following table shows the list of data and equipment used, and personnel employed for the shoreline survey.

Table 4.1 List of data and resources used in shoreline survey

Activity (Duration)	Data Used	Equipment Used	Personnel
RTK-GPS survey (25 Jan)	Predicted tide table GPS benchmark description	<b>Base Station:</b> Multi frequency GNSS receiver with internal memory GNSS Antenna Battery GNSS Controller Tripod Tribatch Measuring tape Mobile Phones  <b>Rover Station:</b> Multi frequency GNSS receiver with internal memory GNSS Antenna Battery GNSS Controller Mobile Phone Measuring tape	Staff to carry the 1.GPS antenna 2.GPS controller

## 4.3 Results and Discussion

The shoreline, adjusted to zero elevation MSL in Barrio Barretto, was surveyed on 25 January, from 14:30 to 15:30. The methodology of filtering outliers is similar to the one used in the road network survey, but the Vcon, which is a user-defined constant to set the vertical accuracy, was reduced from 50 centimeters for road network survey to 5 centimeters for shoreline survey. The summary of total number of data and filtered out data is shown in Table 4.2, and the result, after survey, is shown in Figure 4.3.

Table 4.2 Total number of data, number of detected outliers and its percentage

Date	Total Number of Data	Number of Detected Outliers	Percentage of Detected Outliers
25/01/2013	393	55	14

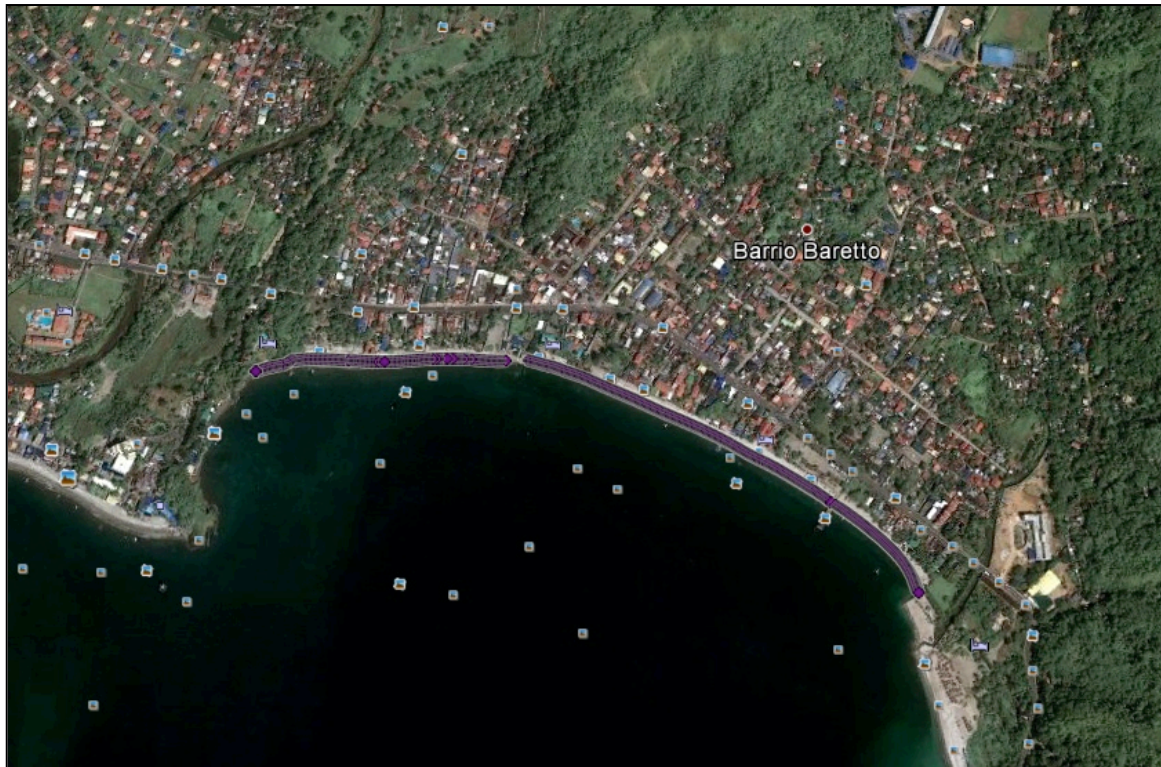


Figure 4.3 Result of shoreline survey carried out on 25 January 2013

#### 4.4 Problems Encountered and Recommendations

In some cases, there are concrete/ breakwater structures (Figure 4.4) that prevent continuous survey of the shoreline. In this case, the gap, if negligible, can be estimated after post-processing of the surveyed data.



Figure 4.4 Breakwater structure

## CHAPTER 5 RIVER SURVEY

### 5.1 Methodology

River survey can be conducted differently, depending on the water level and terrain condition of the river. Three types of surveys can be conducted: sonar, pole, and walking RTK-GPS surveys. Survey can be done along the banks and the centerline if the river is wide or sloping, or only along the centerline if the river is narrow or the terrain is flat.

#### 5.1.1 Sonar survey

When water level is high enough to safely use a motorboat, a sonar survey can be conducted along the centerline of the river, zigzagging along the banks.

In Barrio Barretto, water levels in the 3 rivers (Matatin, Maquinaya, and Kalaklan) were not high enough to conduct sonar survey. Thus, pole survey and RTK-GPS survey were conducted instead, depending on the water level condition at the time of survey.

#### 5.1.2 Pole survey

When water level is not high enough for sonar survey and not low enough for a walking RTK-GPS survey, a pole survey can be conducted. This is done by using a calibrated pole to measure instantaneous depth readings aboard a boat, small enough to travel during the low tide, as shown in Figure 5.1. Since it is not possible to estimate the actual terrain condition of the river below the water, the most conservative recommendation would be to take 3 measurements: (i) left bank, (ii) center, and (iii) right bank of each cross-section of the river, for every 100m interval distance. Prior to actual survey, a survey route, defining strategic points of measurements, is planned and inputted to the handheld GPS as waypoints using the *GPS TrackMaker* for convenient tracking during the actual survey. As in the case with sonar survey, depth readings from the pole survey will be corrected for tide. Hence, it is important to synchronize the time that the depth readings are taken with the time used by the portable tide gauge.



Figure 5.1 Pole survey at Kalaklan River

Since water level condition for this case is critical, it is also important to consider the best time to survey, whether during the high or low tide period. Otherwise, neither pole survey nor RTK-GPS can be conducted until enough water comes in, or runs out. Without prior knowledge about the general terrain condition of the river, deciding the best time will depend mostly on local people's recommendation (e.g. fisherman, boat driver, etc.) and, if there is still uncertainty, on trial and error. A reconnaissance survey to check the terrain of the river should be done prior to actual survey to ensure smooth survey operations.

### 5.1.3 RTK GPS

When water level in the river is not high enough to conduct sonar or pole survey, a walking RTK-GPS can be conducted similar to the shoreline survey, as shown in Figure 5.2. If the river is flat, surveying along the centerline is enough. Otherwise, there may be a need to survey along the banks of the river if the river is sloping from bank to bank, or along the centerline and banks of the river if the river is sloping to the center.



Figure 5.2 RTK GPS survey of Matain River

## 5.2 Data and Equipment

The following table shows the list of data and equipment used, and personnel employed for each activity in river survey. The 2 major activities include (i) pole survey and (ii) walking RTK-GPS survey.

Table 5.1 List of data and resources used in river survey

Activity (Duration)	Data Used	Equipment Used	Personnel
1. Pole survey (25-26 Jan)	Predicted tide table	Boat Calibrated pole Handheld GPS	Boat driver Navigator Recorder Pole measurement
2. RTK-GPS survey (25 Jan)	Predicted tide table GPS benchmark description	<b>Base Station:</b> Multi frequency GNSS receiver with internal memory GNSS Antenna Battery GNSS Controller Tripod Tribatch Measuring tape	Staff to carry the 1.GPS antenna 2.Controller

Activity (Duration)	Data Used	Equipment Used	Personnel
		Mobile Phones	
		<b>Rover Station:</b> Multi frequency GNSS receiver with internal memory GNSS Antenna Battery GNSS Controller Mobile Phone Measuring tape	

## 5.3 Results and Discussion

### 5.3.1 Pole Survey

Pole survey was conducted in 2 rivers: (i) the lower part of Matain River, from the shoreline to the bridge, on 25 January, and (ii) from the shoreline of Kalaklan River to the area where dredging of lahar deposits occurred (Figure 5.5), on 25-26 January. In Matain River, the survey was conducted during the high tide period, since the boat cannot navigate during low tide. On the contrary, in Kalaklan River, it was conducted during the low tide period, since the pole is not long enough to measure the deeper parts of the river. For each cross-section of the river, measurements were taken from the center and both banks of the river, as seen in Figure 5.3.

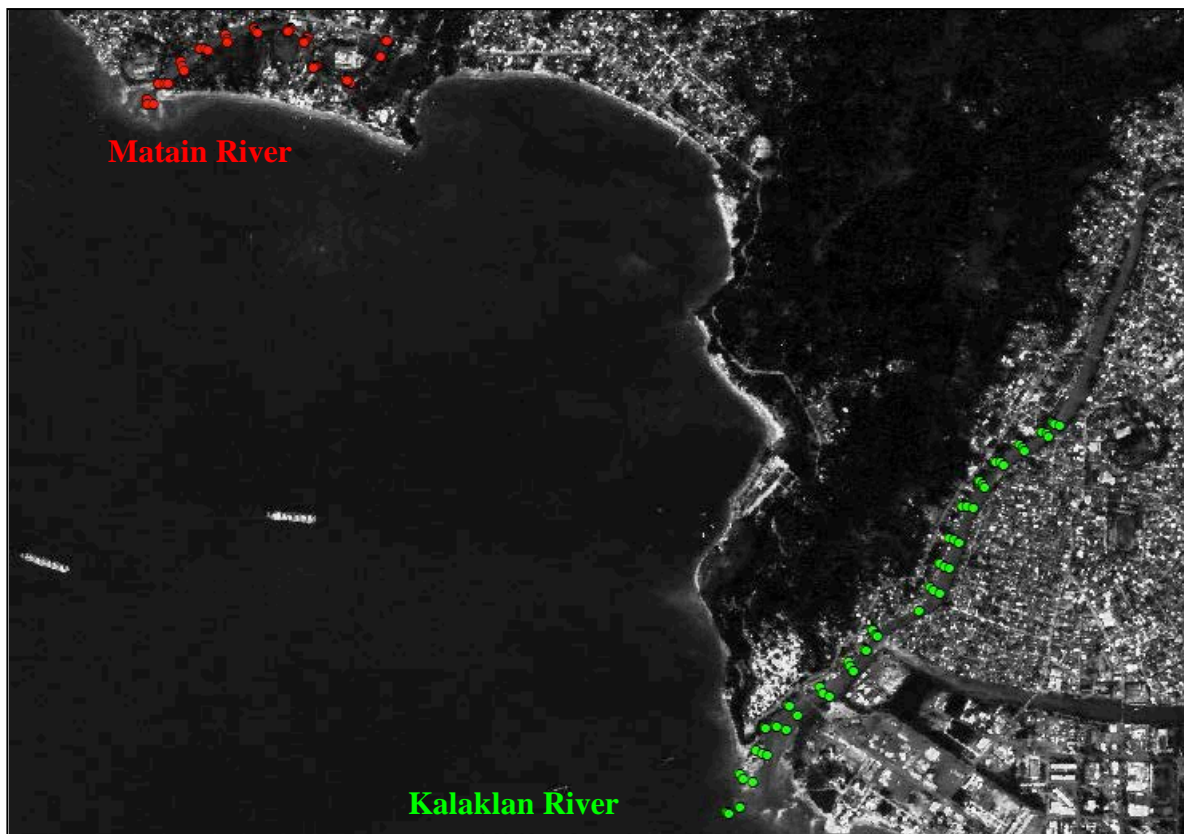


Figure 5.3 Pole survey in Matain and Kalaklan Rivers, carried out on 25-26 January 2013

The rivers are characterized by medium density population, as shown in Figure 5.4. According to the local guide, even though Matain River is usually dry, heavy flooding occurs after rainfall events. This has been one of the major concerns in the area. In Kalaklan River, lahar deposits have continuously accumulated, decreasing the river's carrying capacity. Dredging of lahar deposits is done as a countermeasure (Figure 5.5). Continuous lahar accumulation is still expected due to the large volume of deposits in the upland areas. The river bottom slopes from bank to bank, maybe due to lahar being deposited more on one side of the river. Hence, acquiring more accurate river bathymetric data is important for estimating potential loss and damage from inundation.



Figure 5.4 Medium dense population in Kalaklan River



Figure 5.5 Dredging of lahar deposits

### 5.3.2 RTK GPS

A walking RTK-GPS survey was conducted on 25 January in 2 rivers: (i) the upper half of Matain River, from the bridge towards inland, and (ii) from the shoreline of Maquinaya River to the area with too much tree density. Since the terrain of the rivers is flat across the banks, survey was run only along the centerline of the river. Figure 5.6 shows that the upper half of Matain River has ran out of water.



Figure 5.6 Very low water flow in Matain River

Methodologies in conducting a walking RTK-GPS survey and filtering outliers are the same as with the road network survey. The summary of total data and the number of outliers detected are shown in Table 5.2; result of the RTK survey at Maquinaya River is shown in Figure 5.7.

Table 5.2 Total data, number of outliers, and percentage of detected outliers from RTK survey at Maquinaya River

Date	Total Number of Data	Number of Detected Outliers	Percentage of Detected Outliers
25/01/2013	585	90	15.38

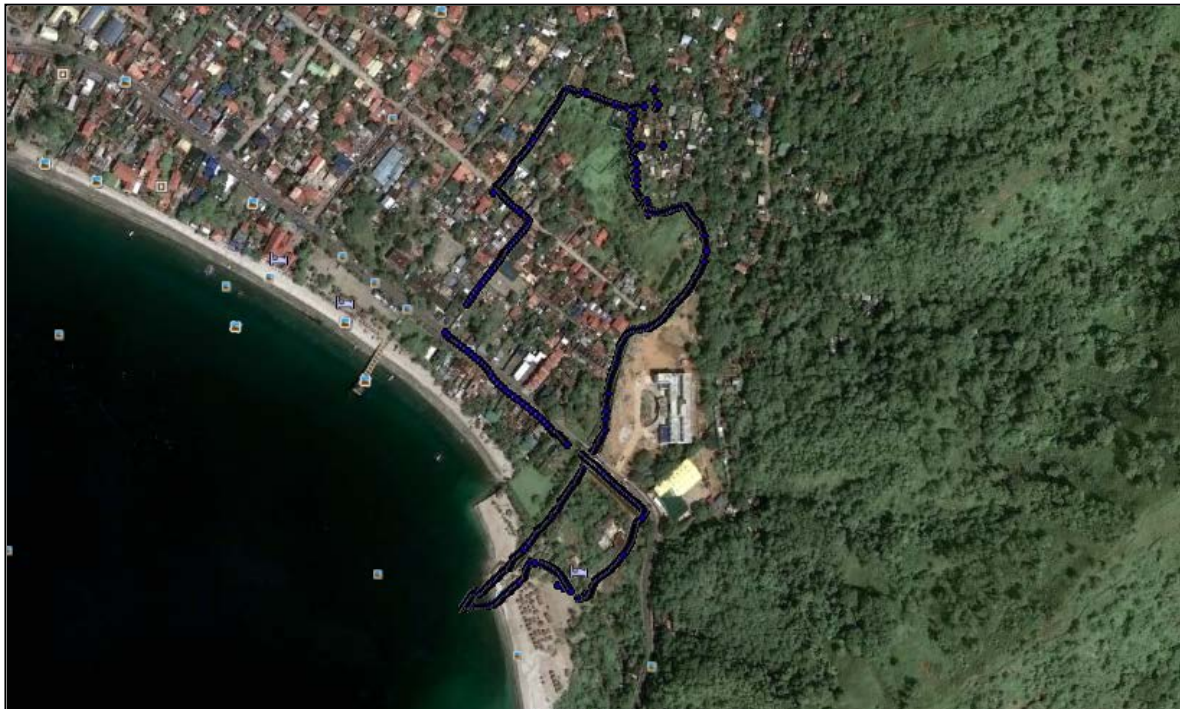


Figure 5.7 Result of RTK survey at Maquinaya River, carried out on 25 January 2013

## 5.4 Problems Encountered and Recommendations

### 5.4.1 Pole Survey

When conducting a pole survey, it is important to consider the time when the high and low tide occurs to ensure uninterrupted survey. If water is too low, the boat cannot be used. Traversing along the river on foot, however, might be dangerous because of the strong current. On the first day of the Kalaklan River survey, the survey started from the middle of the river towards the upland area, so the survey went smoothly. However, when the second half of the survey (from the middle of the river towards the mouth) was about to start, the tide started to come in fast. It was then difficult to measure the depths since the pole was not long enough to measure the bottom of the river. Hence, survey for this area was postponed to the next day, making sure that the survey is conducted during low tide, especially since Kalaklan River is much deeper than the Matain and Maquinaya rivers, which have a very low water flow during this period.

Although most of the lower half of the Kalaklan River was surveyed the next day during low tide hours, some areas were not measured because the water level is still higher than the pole length. So, it is also important to consider the pole length for measuring deeper parts of the river. Another option would be to use a calibrated rope with weight, similar to the one used in accuracy assessment of the sounding data. The rope should be held tight and vertical when taking a reading. Care should be taken when taking measurements because the water current might be strong enough to influence the readings.

Another factor to consider is the safety of the personnel taking the readings. In some places, water quality is not good, especially in high-density population areas. It is therefore recommended to take precautions when conducting the survey, such as wearing gloves when taking the readings to avoid contact with river water.

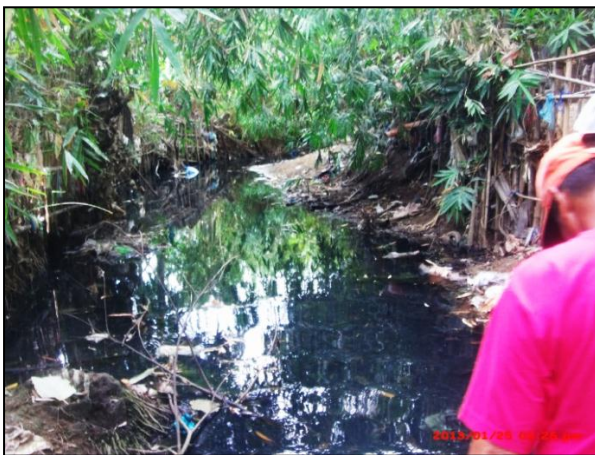


Figure 5.8 Maquinaya River condition



Figure 5.9 Matain River condition

### 5.4.2 RTK GPS

A walking RTK-GPS survey was conducted on rivers, which have very low water flow during low tide. Although it is possible to walk on several centimeters deep of water, the current, however, is strong enough, particularly at the river mouth. Care should be taken when surveying these areas to avoid any untoward accidents. In Kalaklan River, the water current is very strong at the river mouth, so extra care was taken when crossing this area.



Figure 5.10 Strong current at the river mouth

As with the pole survey, extra precaution is necessary to avoid unexpected accidents during survey. To avoid contact with river water and stepping on dangerous debris, it is recommended to wear safety boots when conducting the survey.

## **CHAPTER 6**

### **EXPOSURE SURVEY**

Within this project, assessment of tsunami risk is presented in the context of (i) tsunami vulnerability and loss, and (ii) people's ability to evacuate. Tsunami exposure and lifeline information were, hence, collected to address the spatial and temporal component of the population and property at risk. Concept for the analysis, methodology for exposure data collection, and list of collected data are presented in the following sections.

#### **6.1 Tsunami Vulnerability and Loss Estimation**

In the coastal zone exposed to tsunami inundation, buildings and infrastructure are not uniformly at risk within the flood zone. The probability of damage is related to both vulnerability (structural capacity to resist) and wave energy. In other words, damage level to buildings depends on building type and on inundation depth. The vulnerability criteria used to classify buildings are defined as "intrinsic factors" that influence its vulnerability, such as type of construction material, height, and number of floors. For this project, vulnerability function concept is used to express probable loss or impact to the element at risk for a particular hazard level, ranked in order of severity.

An online tool named "INSPIRE" (Srivihok et al, 2012) has been developed at RIMES for tsunami inundation simulation and tsunami loss estimation. INSPIRE is composed of two main components: (i) tsunami hazard evaluation module, and (ii) tsunami loss estimation module. For tsunami hazard evaluation, the TUNAMI model (IUGG/IOC TIME Project, 1997) was customized and integrated into the system for tsunami propagation and inundation simulation. The user can arbitrarily specify earthquake parameters for generating initial sea-floor deformation, and input local near-shore topographic and bathymetric data, or use default data (GEBCO08\_30sec) for the simulation. Under the current project, near-shore topographic and bathymetric data, obtained from field survey, will be inputted for the analysis. Tsunami losses can be estimated by correlating the most critical tsunami parameter with the location and properties of exposed elements, through the vulnerability function. By this approach, building classification is considered to reflect more realistic building response capability to the tsunami impact and probability of building damage.

Loss and damage estimation will provide information to local authorities on buildings that need to be reinforced or even relocated because of their vulnerability to tsunami damage. This information, thus, is useful for formulating planning regulations, directing building programs, and issue of construction license. Social vulnerability, quantitatively evaluated in terms of probability to survive based on spatial and temporal population distribution, could be of interest to disaster managers and emergency planners. The analysis could provide information on buildings that house large numbers of people who may likely be trapped, population density change over time, and buildings that do not offer opportunity for vertical evacuation.

##### **6.1.1 Selection of Tsunami Fragility Curves for the Philippines**

In general, tsunami fragility curves, also referred to as experience curves, are developed from recorded damages of past tsunami events. The curve expresses the ratio of damaged buildings to all buildings, at a particular level of tsunami hazard. Tsunami fragility curves for building are technically expressed by the cumulative probability of damage occurrence, as standardized normal distribution or log normal distribution functions of the hydrodynamic features of tsunami, e.g. inundation depth, current velocity, and hydrodynamic force:

$$P(x) = \Phi \left[ \frac{x - \mu}{\sigma} \right] \quad (6.1)$$

$$P'(x) = \Phi \left[ \frac{\ln x - \mu'}{\sigma'} \right] \quad (6.2)$$

where  $x$  is the hydrodynamic feature,  $\Phi$  is the standard normal distribution/ lognormal distribution function,  $\mu$  and  $\sigma$  are the mean and standard deviation of  $x$ , and  $\mu'$  and  $\sigma'$  are the mean and standard deviation of  $\ln x$ , respectively. Each fragility curve was developed using a specific method, dataset of the tsunami event and location, and structural type (material, low/high rise) and damage level. Fragility curves should be properly selected for estimating tsunami loss for different types of exposures.

As there is limited tsunami fragility curves specifically developed for the Philippines, fragility curves developed from damage data in Thailand and Sri Lanka after the 2004 tsunami disaster are adopted for estimating tsunami loss in the Philippines, with the assumption of building characteristic similarity. Fragility curves for two main building typologies are proposed for this project.

### ***Engineered reinforced concrete building***

Foytong and Ruangrassamee (2007) used damage data from field surveys in Thailand after the 2004 tsunami event to determine fragility curves and evaluate the effect of the number of storeys for engineered reinforced concrete (RC) buildings. In Thailand, RC buildings generally feature small columns. The number of column ties typically provided is small (e.g. 6mm diameter ties at 150-200 mm spacing for 150x150 mm<sup>2</sup> or 200x200 mm<sup>2</sup> columns). In-filled, un-reinforced masonry panels, generally 100 mm thick, are extensively used as nonstructural elements, with a small number of dowel bars connecting the panels and the boundary RC frames. The ultimate compressive strength of concrete in buildings is normally on the order of 18 MPa, or lower. The specified yield strength of reinforcing bars is usually 240 MPa for plain bars and 300 MPa for deform ones. Bricks and mortar are usually used as nonstructural elements (Ruangrassamee et al, 2006). The capacity of buildings and the construction quality are reflected in the number of storeys. Buildings taller than one storey are usually constructed with better quality and higher capacity than one-storey buildings. Hence, reinforced concrete building data are grouped in two types: ***one-storey buildings*** and ***buildings taller than one storey***. Damage levels are defined in terms of the overall damage of buildings, and classified into four damage levels:

- ***Damage level 0 (No damage)***  
There is no damage in a building, as shown in Figure 6.1.
- ***Damage level 1 (Damage in secondary members only)***  
There is damage only in non-structural components, i.e., walls and/or roofs. At this damage level, there are cracks on wall or wall punching, or tiles are wiped out, but there is no damage in a beam or a column, as shown in Figure 6.2.
- ***Damage level 2 (Damage in primary members)***  
There is damage in structural components, i.e., a column, a beam, or foundation. At this damage level, there are cracks on a beam or a column, but the building is still repairable, as shown in Figure 6.3.
- ***Damage level 3 (Collapse)***  
A building cannot sustain its gravitational load and it is irreparable. At this damage level, a structure may fail at a major joint or absolutely collapse, as shown in Figure 6.4.



Figure 6.1 Damage Level 0 (No damage) for engineered RC building



(a) Cracks on a wall



(b) Wall punching

Figure 6.2 Damage Level 1 (Damage in secondary members only) for engineered RC building



(a) Foundation failure



(b) Bending failure of column

Figure 6.3 Damage Level 2 (Damage in primary members) for engineered RC building



(a) Joint failure

(b) Absolute destruction

Figure 6.4 Damage Level 3 (Collapse) for engineered RC building

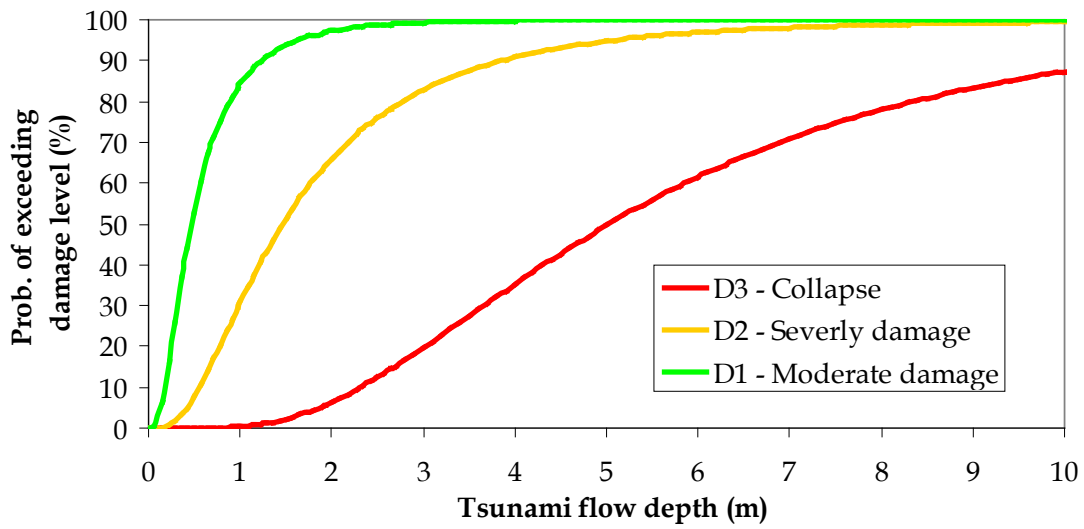


Figure 6.5 Fragility curve for RC building – 1 storey

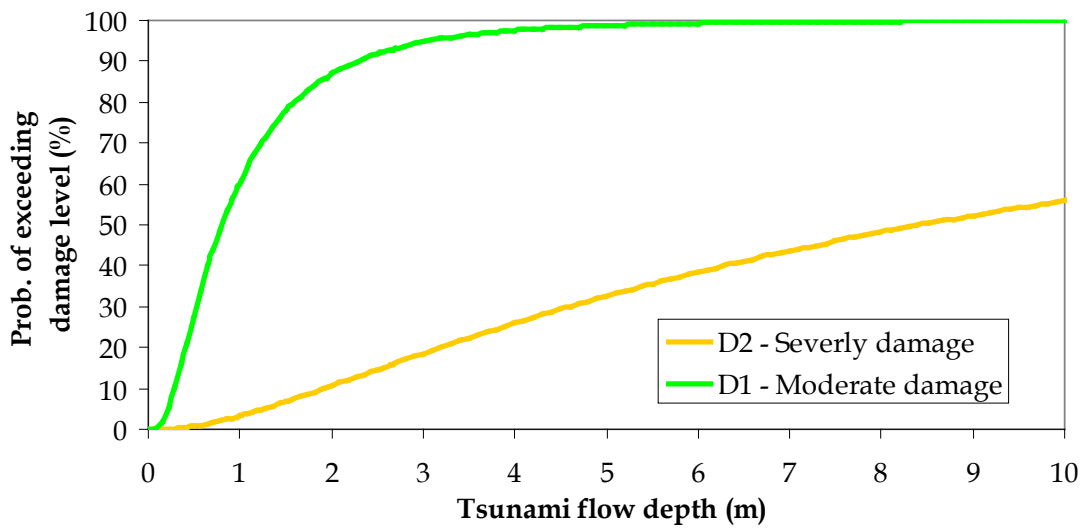


Figure 6.6 Fragility curve for RC building – taller than 1 storey

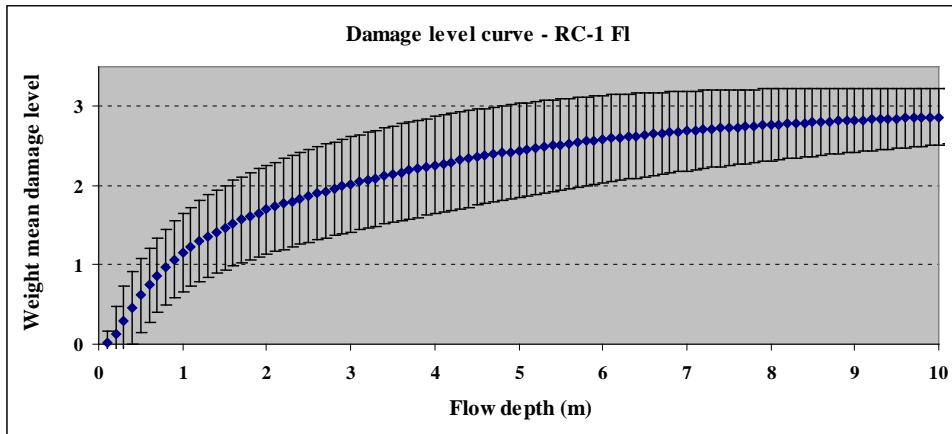
Since the fragility curve can present the ratio of damaged buildings to all buildings, a zoning map can be generated based on the application of the fragility curve, to present comparatively high/medium/low ratio of damaged building zone, e.g. percentage of building damage for each *purok*. In addition, by modifying fragility curves, damage level can be estimated for an individual building, if the tsunami inundation depth is known at the building location. Concept of weight mean damage level, firstly proposed by Valencia et al (2011), is adopted for this project, as presented by the Equation (6.3):

$$\bar{D}_i = \frac{(1 \times nD1_i) + (2 \times nD2_i) + (3 \times nD3_i) + \dots + (k \times nDk_i)}{nD1_i + nD2_i + nD3_i + \dots + nDk_i} \quad (6.3)$$

where  $\bar{D}_i$  is the weight mean damage level,  $nD1_i$  is the total number of buildings with Damage level 1 for the flow depth with interval “i” and  $nD2_i$  the total number of buildings with Damage level 2 for the flow depth with interval “i”; and  $k$  is the maximum damage level, etc. Uncertainty can be expressed by the standard deviation ( $\sigma_{D_i}^2$ ) as presented in Equation (6.4):

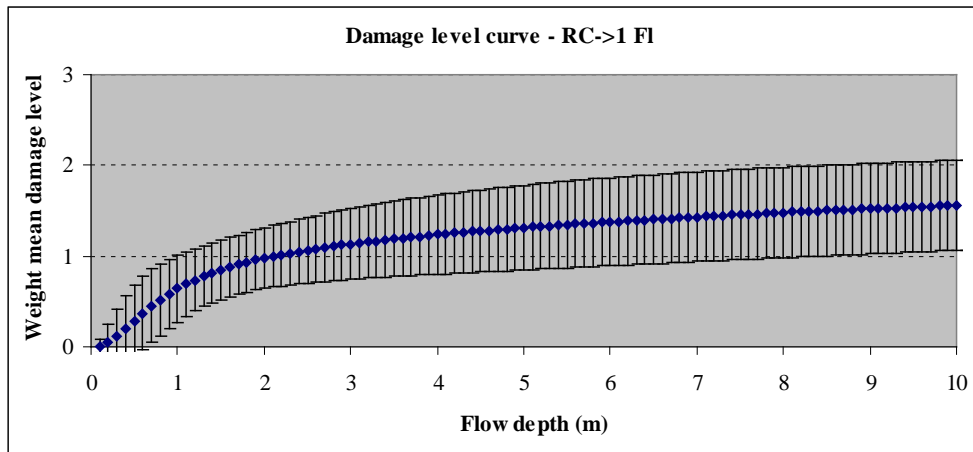
$$\sigma_{D_i}^2 = \frac{nD1_i \times (1 - \bar{D}_i)^2 + nD2_i \times (2 - \bar{D}_i)^2 + nD3_i \times (3 - \bar{D}_i)^2 + \dots + nDk_i \times (k - \bar{D}_i)^2}{nD1_i + nD2_i + nD3_i + \dots + nDk_i} \quad (6.4)$$

Weight mean damage level presents the average damage level for a particular building type when subjected to a particular range of tsunami inundation depth. However, uncertainty of damage range is also included. Damage level curves with uncertainty range developed for reinforce concrete building for one storey and taller than one storey buildings are plotted in Figures 6.7 and 6.8.



Flow depth (m)	Mean damage level
0	0
0 to 0.8	1
0.8 to 2.9	2
> 2.9	3

Figure 6.7 Damage curve for RC building – 1 storey



Flow depth (m)	Mean damage level
0	0
0 to 2.1	1
> 2.1	2

Figure 6.8 Damage curve for RC building taller than 1 storey

### ***Non-solid building***

Garcin et al (2008) used damage data from field survey and bibliographic data for the case of the 2004 tsunami in Sri Lanka to develop a damage scale and damage functions that are appropriate for buildings. The buildings were categorized according to their construction type and material. Non-solid building is defined as building made from light material, e.g. wood, metal sheet, light brick and poor quality cement blocks. Scale of damage was classified into 4 levels:

- ***Damage level 0 (No damage to superficial damage)***  
No structural damage to superficial damage, e.g. cracking, destruction of windows, doors, furnishing tiles and roofs, as shown in Figure 6.9. This damage level can be repaired and the structure is habitable.
- ***Damage level 1 (Moderate damage)***  
Collapse of wall panels, without damage to the integrity of the building, and/or moderate scouring on the foundation, as shown in Figure 6.10. The structure is uninhabitable, but can be rehabilitated.
- ***Damage level 2 (Severe damage)***  
Destruction of several load-bearing walls and significant scouring on the foundation, as shown in Figure 6.11. The structure cannot be rehabilitated.
- ***Damage level 3 (Collapse)***  
Total destruction of the building, as shown in Figure 6.12.

As with RC buildings, damage curve and uncertainty range have been developed for non-solid buildings, as shown in Figure 6.14.



Figure 6.9 Damage Level 0 (No damage to superficial damage) for non-solid building



Figure 6.10 Damage Level 1 (Moderate damage) for non-solid building



Figure 6.11 Damage Level 2 (Severe damage) for non-solid building



Figure 6.12 Damage Level 3 (Collapse) for non-solid building

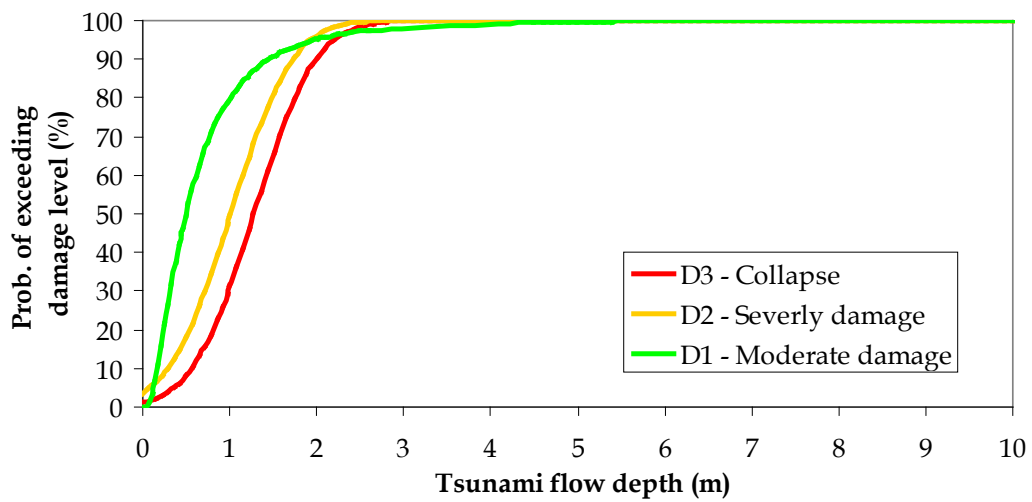
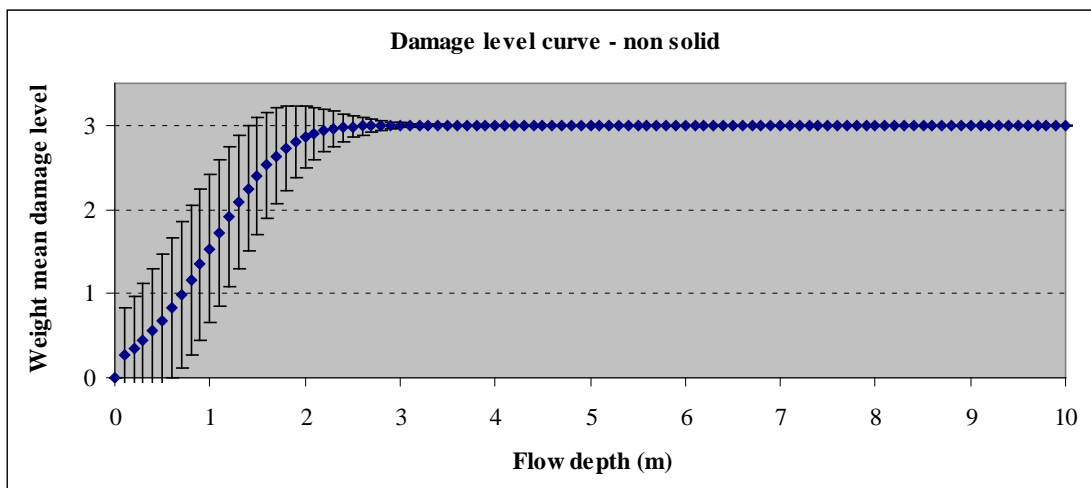


Figure 6.13 Fragility curve for non-solid buildings



Flow depth (m)	Mean damage level
0	0
0 to 0.7	1
0.7 to 1.2	2
> 1.2 m	3

Figure 6.14 Damage curve for non-solid buildings

## 6.1.2 Methodology

Vulnerability and loss estimation uses building inventory as main dataset. The inventory provides information about location and properties of each building, e.g. building construction type, building usage, and number of residents. Building footprint can be captured from high-resolution satellite images or aerial photographs, while building properties are mainly collected from field survey and combined with existing data from national and local government agencies. Google Earth provides free access to satellite images. The most updated image should be selected as base for digitization. For Barrio Barretto, the most recent image from Google Earth is in October 2009.

Under the current project, cameras with GPS receiver, mounted on the survey vehicle, were used to record building image along the survey route. While traveling through road network in the area, building images, with geographical coordinates, were captured. Building construction type and usage will be visually post-processed from the VDO images. Classification of building type in the area would be based on the selected fragility curves, as presented in Section 6.1.1.

Buildings located far from the road networks could not be captured by VDO camera. However, building construction type can be estimated from interpretation of roof shapes from satellite image, while building usage can be estimated from neighboring buildings and land use type, where the building under consideration is located. The estimation technique assists in completing the database gathered during field surveys, which are hardly satisfactory because of limitations in time, as well as in economic and human resources. The local government is encouraged to continually update and improve the dataset in a systematic way.

Population distribution data was collected from the local government office, e.g. statistics and census data. Number of resort and hotel rooms should be also collected for tourist areas, for estimating the number of tourists, especially during the high season. Table 6.1 shows the list of data collected for the vulnerability and loss estimation for Barrio Barretto.

Table 6.1 List of data collected for tsunami vulnerability and loss estimation

Data Type	Data Source	Analysis Details
1. Building footprint	Digitizing from Google Earth	<ul style="list-style-type: none"> <li>○ Roof shape</li> <li>○ Building location</li> </ul>
2. Building construction type	<ul style="list-style-type: none"> <li>○ Field survey (to be analyzed from VDO and linked to building footprint)</li> <li>○ Roof shape interpretation</li> </ul>	<ul style="list-style-type: none"> <li>○ <i>Type A</i>: One-storey engineered reinforced concrete buildings</li> <li>○ <i>Type B</i>: Engineered reinforced concrete buildings taller than one storey</li> <li>○ <i>Type C</i>: Non-solid building made from light material</li> </ul>
3. Building usage	<ul style="list-style-type: none"> <li>○ Field survey (to be analyzed from VDO, and linked to building footprint)</li> <li>○ Land use map interpretation</li> <li>○ Estimate from neighboring buildings</li> </ul>	<ul style="list-style-type: none"> <li>○ Residential</li> <li>○ Commercial</li> <li>○ Industrial</li> <li>○ Agriculture</li> <li>○ Religion</li> <li>○ Government</li> <li>○ Education</li> <li>○ Medical</li> <li>○ Tourist</li> </ul>
4. Population distribution	<ul style="list-style-type: none"> <li>○ Census data from Olongapo City Planning and Development Office (to be linked to building footprint)</li> <li>○ Resident interview at critical buildings</li> </ul>	<ul style="list-style-type: none"> <li>○ Estimated population distribution in each household/function building</li> </ul>
5. Tourist distribution	<ul style="list-style-type: none"> <li>○ Number of hotel rooms from Olongapo Tourism Office</li> <li>○ Google Earth and Google map for hotel location and number of rooms, assumed to have 2 pax/room (if hotel website is available) (to be linked to building footprint)</li> </ul>	<ul style="list-style-type: none"> <li>○ Estimated tourist number distribution in each resort/ hotel building</li> </ul>

### 6.1.3 Equipment and Personnel

#### *VDO Camera with GPS Receiver*

Two VDO cameras with GPS receiver were mounted on the survey vehicle for recording building image at the right and left sides of the road (Figure 6.15). Cameras should be properly mounted at an angle of about 20 degrees from horizontal, in order to capture all building storeys. Traveling speed through the road network in the area was limited to about 30 km/h.



Figure 6.15 VDO camera with GPS receiver mounted on the survey vehicle

#### *Handheld GPS and Computer Laptop*

Handheld GPS was connected to a computer laptop, Internet air card, and Google Earth for navigating the survey route and recording the survey track each day (Figure 6.16).



Figure 6.16 Handheld GPS connecting to laptop for navigation and travel route record

Table 6.2 summarizes the equipment used and personnel employed for the exposure survey.

Table 6.2 Equipment and personnel for the exposure survey

Activity (Duration)	Equipment Used	Personnel
1. VDO camera shooting (21-23 Jan)	Survey Vehicle VDO camera Handheld GPS Computer laptop Internet air card	Driver Local guide Recorder

#### 6.1.4 Results

Figures 6.17 until 6.23 and Table 6.3 present representative data gathered/ generated from the survey.



Figure 6.17 Building footprint (location and roof shape) digitized from Google Earth



Figure 6.18 Example of building classification by construction type in Barrio Barretto



**Education (EDU)**



**Residential (RES)**



**Industrial (IND)**



**Government (GOV)**



**Commercial (COM)**



**Religion (REL)**



**Medical (MED)**



**Tourist (TOUR)**

Figure 6.19 Example of building classification by building usage in Barrio Barretto





Figure 6.22 Household (point) with number of residents and land parcel (polygon) map from Olongapo City Planning and Development Office

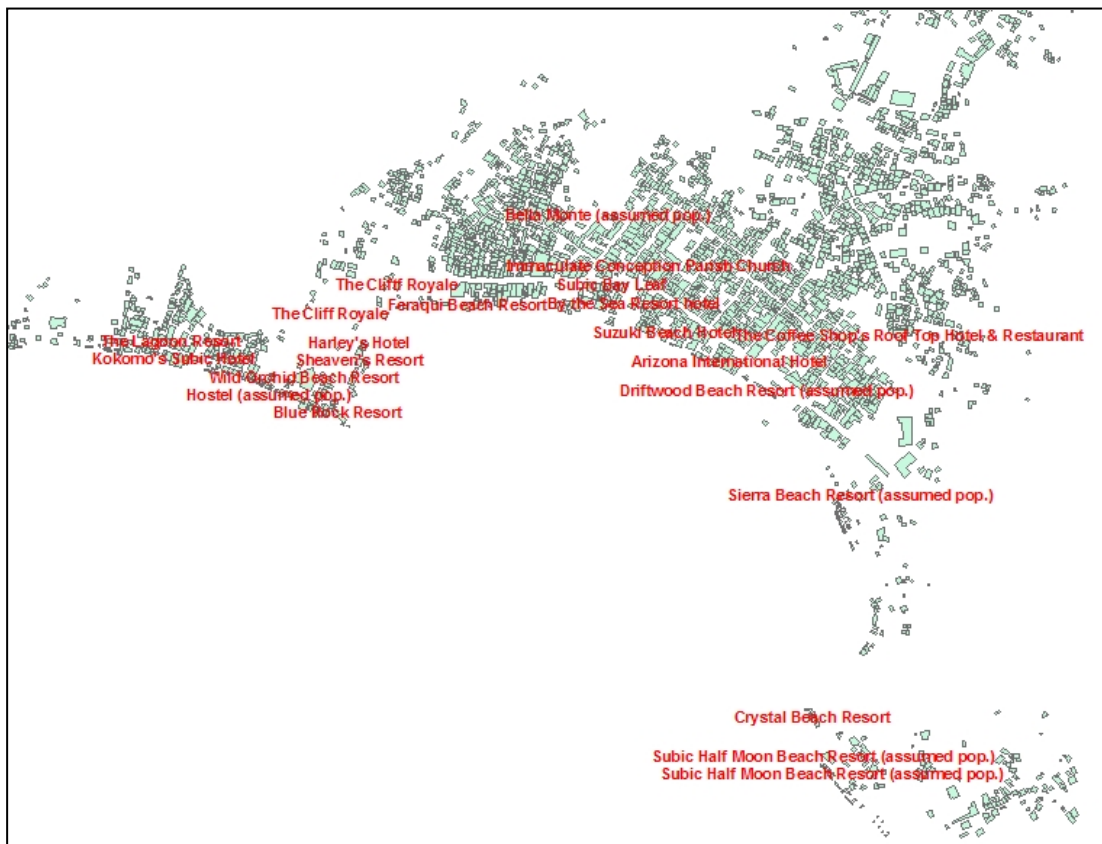


Figure 6.23 Hotel location and number of guests registered in the GIS database

Table 6.3 Total number of hotels, rooms and estimated tourists in GIS database

Hotels/Resorts	No. of Room	Estimated Tourist No. (2pax/room)	Remarks
<b>Source: City Tourism Office</b>			
<b>Barretto</b>			
Blue Rock Resort	41	82	
Columban College Hotel	15	30	
Harley's Hotel	18	36	
Johan's Resort	23	46	
Kokomo's Subic Hotel	14	28	
Seascape Inn	10	20	
Sheaven's Resort	44	88	
Treasure Island Resort	14	28	
Wild Orchid Beach Resort	84	168	
<b>Baloy Area</b>			
Arizona International Hotel	28	56	
By the Sea Resort hotel	35	70	
Geisha Lodge Massage Parlor (Geisha House)	5	10	
Playa Papagayo Resort	19	38	
Subic Bay Leaf	12	24	
Subic Grand Seas Resort	22	44	
Suzuki Beach Hotel	29	58	
The Coffee Shop's Roof Top Hotel & Restaurant	18	36	
<b>Source: Google earth/Google map</b>			
<b>Barretto</b>			
Alemarac Beach Resort	-	-	
Anbon Hotel (assumed tourist no.)	-	-	
Barts Resort Hotel (assumed tourist no.)	-	-	
Bella Monte	-	-	
Crystal Beach Resort	-	-	
Driftwood Beach Resort	-	-	
Dryden hotel	-	-	
Emu Tavern	-	-	
Feraqui Beach Resort	-	-	
Guerrero's Beach House	-	-	
Ghyan's on the beach	-	-	
Krrel's Family Resort	-	-	
LA Sea Side Resort	-	-	
Midori Apartelle	-	-	
Palm Beach Resort	-	-	
Sierra Beach Resort	-	-	
Subic Half Moon Beach Resort	-	-	
The Cliff Royale	16	76	<a href="http://thecliffroyale.com/index.php">http://thecliffroyale.com/index.php</a>
The Sand Castle	-	-	
<b>Baloy Area</b>			
Abarro's Resort	-	-	
Baloy Duplex House	-	-	
Gateway Bar and Hotel	-	-	
GS Apartelle	-	-	
Hostel	-	-	
Palm Coast Inn	-	-	
The Lagoon Resort	-	-	
Up the Alley Apartments	-	-	
VIP Holiday Apartment	-	-	

Note: (-) : data is not available

### 6.1.5 Problems Encountered and Recommendations

#### *Building Footprint*

The total number of buildings in Barrio Barretto, digitized from Google Earth, for the area located eastern side of Matain River is 3, 232 buildings. However, the number of households from data collected from Olongapo City Planning and Development Office shows 3,924 households (i.e. 3,791 households plus 133 households with makeshift walls or roofs), as presented in Table 6.4. The number of buildings digitized from Google Earth might be underestimated due to unclear roof shape; also, several households may be housed under the same roof (e.g. row house, apartment), which is difficult to correctly interpret from the top view. In addition, latest update of Google Earth satellite image was in October 2009, but the household data was updated in 2011. Recently constructed buildings may not have been included in the building footprint digitized from Google Earth.

Table 6.4 Number of households in Barrio Barretto from the City Planning & Development Office

purok	number of households	households living in makeshift house*	
		Magnitude*	Proportion**
<b>Barreto</b>	<b>3924</b>	<b>133</b>	<b>3.39</b>
Purok 1	283	15	5.3
Purok 2	176	6	3.41
Purok 3	265	9	3.4
Purok 4	498	29	5.82
Purok 5	481	31	6.44
Purok 6	226	2	0.88
Purok 7	441	6	1.36
Purok 8	210	2	0.95
Purok 9	122	0	0
Purok 10	129	0	0
Purok 11	337	6	1.78
Purok 12	317	5	1.58
Purok 13	241	6	2.49
Purok 14	198	16	8.08

\*Households with makeshift walls or roof  
\*\*Number of households with makeshift walls or roof over total number of households  
Source: CBMS Census 2011

### ***Linking the Number of Residents to the Building Footprint***

Building locations extracted from Google Earth and represented in tsunami hazard maps, generated from simulation, are referred to the World Geodetic System. The household location map that is linked to the census database collected from the City Planning and Development Office, however, is based on the local geodetic datum. Parameters to convert to World Geodetic System are not available. Figure 6.24 shows the mismatch between the household location map and building locations from Google Earth. For this reason, average household size from demography data (4 person /household) is uniformly distributed to all buildings in this area. By this method, the estimated population in Barangay Barretto is 12,928 people, whereas the population registered in the census data is 14,284 people. The population is, therefore, underestimated by about 10%.

The City Planning and Development Office is encouraged to collect the original geographical coordinate system from agencies that generated the dataset so that the dataset can be diversely applied, especially for natural hazard management using Geographical Information System.

### ***Land Use Map***

As land use map can be used as well to identify building use type for buildings that cannot be captured by VDO camera, detailed and large-scale land use map should be also collected from local authorities.



Figure 6.24 Mismatch between household location from the City Planning and Development Office and building location from Google Earth

### *Hotel Database*

Hotel list collected from the city tourism office was linked to the building footprint by using hotel location presented in Google Map and Google Earth. Hotel address assists in guiding the hotel location on the maps. Some hotels are missing from the list, but appear on Google Map and Google Earth. If the hotel website is available, room number/guest number can be indicated.

Hotel database should be checked in both Google Map and Google Earth, since some hotels are indicated in either one of them. Figure 6.25 and 6.26 present the hotel database in Google Map and Google Earth, respectively. A number of small motels/ guest houses in the area were noted during the field survey. These did not appear in both tourism office database and online sources, e.g. Google Earth and Google Map. The city tourism office could update its hotel database, as well as record the geographical location (latitude and longitude) of the hotel, for generating precise hotel location map and estimating the tourist population in the city.

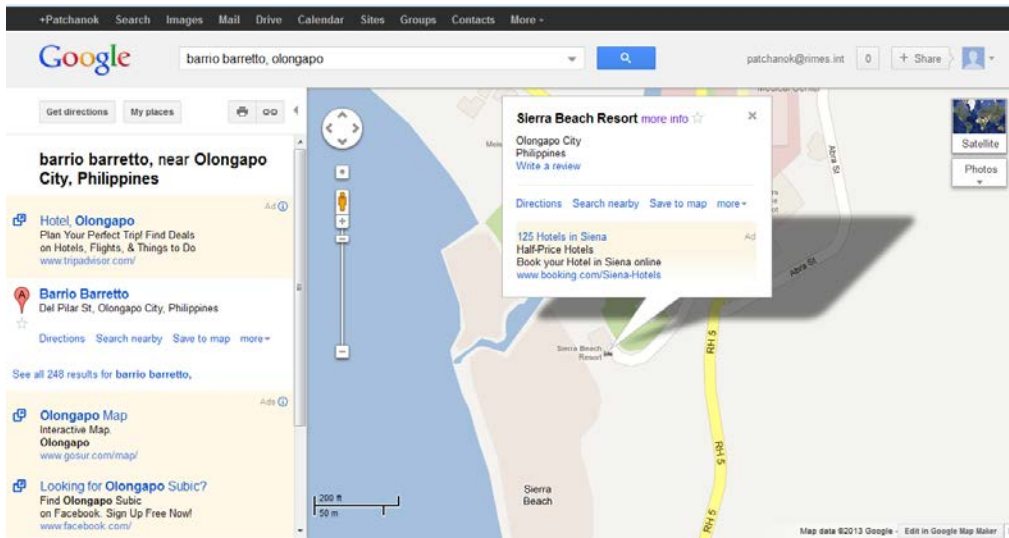


Figure 6.24 Hotel database from Google Map

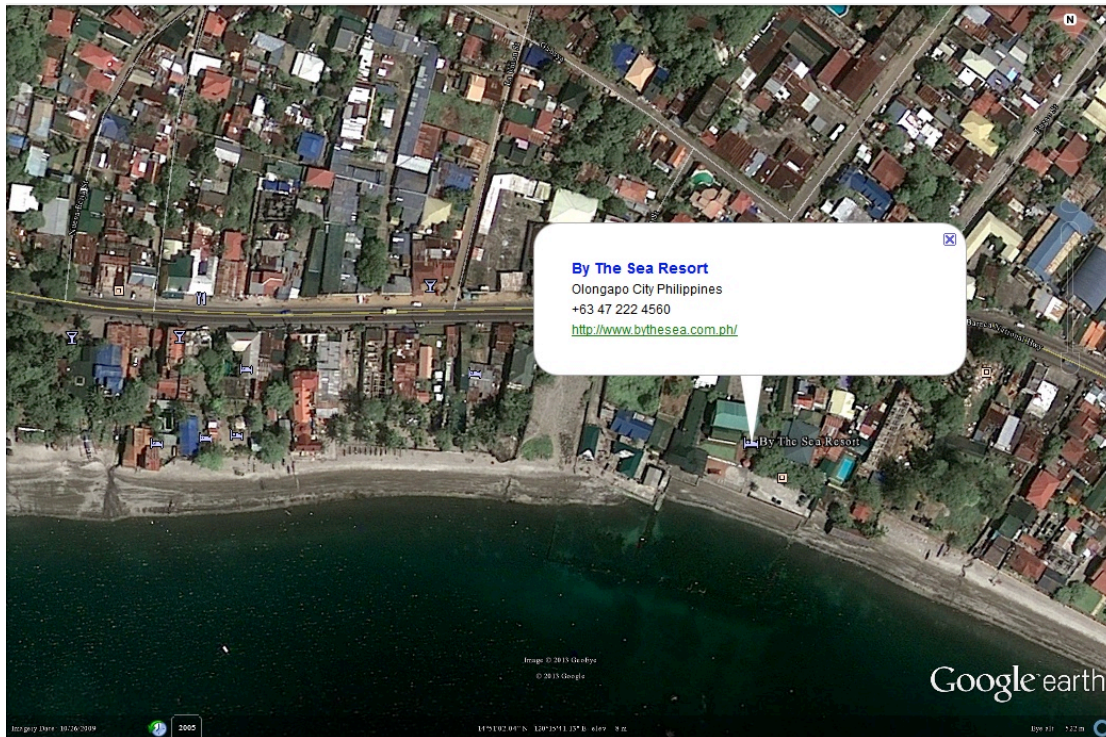


Figure 6.25 Hotel database from Google Earth

## 6.2 Assessment of People's Ability to Evacuate

Assessment of people's ability to evacuate is important for evacuation planning. An evacuation plan should be based on a hazard assessment by analyzing possible scenarios of hazards that could affect the target area, including procedures for safe transfer from the affected area into safe places. Hazard assessment requires knowledge of probable tsunami source, probability of occurrence, and tsunami characteristics at different places along the coast. In cases where past data are limited, numerical model of tsunami inundation can provide estimates of tsunami inundation profile and minimum time of tsunami arrival. This project shall apply INSPIRE's tsunami hazard assessment module for the assessment of tsunami hazard.

To assess people's ability to evacuate, the following questions have to be answered to support decision to evacuate in case of a tsunami event:

- a) ***Where are the safe places for evacuation?*** In general, temporary gathering areas or shelters should be located outside tsunami affected areas at ground elevation higher than 15 m from the mean sea level. Public locations with adequate capacity can be selected as the gathering/assembly points. This evacuation process is called horizontal evacuation (horizontally evacuate away from inundated area). However, in areas that are too far from horizontal evacuation places, people may not have enough time to reach safe places before tsunami strikes. Vertical evacuation, which is the process of moving people to higher floor of buildings, may be considered instead. Public facilities, multi-storey buildings, available reserve space for temporary evacuation, and good quality construction buildings can be identified as vertical evacuation sites. Areas identified as shelters must be manageable, in terms of health, sanitation, and necessary facilities; adequate infrastructure should also be in place (DDPM, 2005).
- b) ***Where are the potential evacuation routes?*** To define the best evacuation route from a given point, the safe and fastest path from that point to the safe places has to be searched. The fastest path is not always the shortest path, but the concept of accessibility is calculated on a "***cost surface***" of the area. The cost surface consists of a regular two-dimension grid, where each cell represents the time required to cross the cell. Physical condition of the area influences travel cost, e.g. a flat road allows faster travel speed (lower cost) than one with dense vegetation. For this reason, calculation of distance between two points considers not only the geometric distance, but also the cost to move along a particular path. Cost Weight Distance (CWD), therefore, replaces geometric distance. Once the cost of all cells is defined, CWD between two given points can be calculated for the best or fastest path. Instead of defining the CWD surface as the distance between starting point and each cell in the cost surface domain, it is possible to define it as the distance between each cell and the safe areas, which can be more than one. The path with the lowest accumulated cost from each cell to the safe place gives the fastest route to the closest evacuation point. The escape route from every point within the domain can then be computed (ADPC, 2007).
- c) ***Are shelter capacities enough to accommodate evacuees?*** By CWD method, it is possible to define the area in each safe place. Disaster managers can understand if the safe place is big enough to accommodate evacuees from a subdivision and estimate the supplies needed during an event.
- d) ***Are people in the risk area able to reach the safe place within the given time?*** Since the safe place can be designated to each subdivision and cost grid is known for the entire area, required evacuation time from any point in the area can be calculated. Disaster managers can assess whether people have enough time to reach the safe place before the tsunami strikes.

## 6.2.1 Methodology

ESCAPE (<http://escape.rimes.int>), a tool developed at RIMES, is used in this project to support evacuation planning. The system provides information on the fastest evacuation path and direction toward the shelters. Evacuation basins partition the threatened area into several zones, which can be accommodated by the designated safe places/shelters. Capacity of shelters can be evaluated if the number of people in the risk areas is identified. Evacuation speed and capability consider several factors, including topographic condition, land cover, location of critical facilities, and population density, age and gender.

A spatial information system shall be developed for Barrio Barretto from the dataset collected from local government agencies and field survey (Table 6.5) to support planning and development of counter-measures to ensure effective and safe evacuation of people from threatened locations, before the tsunami strikes.

Table 6.5 List of data collected for tsunami evacuation planning

Data Type	Data Source	Analysis Details
1. Land use/ Land cover	<ul style="list-style-type: none"> <li>○ NAMRIA land cover map 2010 Barrio Baretto scale 1:15,000</li> </ul>	<ul style="list-style-type: none"> <li>○ Open forest, broadleaved</li> <li>○ Built-up area</li> <li>○ Cultivated, annual crop</li> <li>○ Cultivated, perennial crop</li> <li>○ Natural, barren land</li> <li>○ Wooden land, shrubs</li> <li>○ Wooden land, weeded grassland</li> </ul>
2. Topographic slope	<ul style="list-style-type: none"> <li>○ NAMRIA topographic slope Barrio Baretto scale 1:15,000</li> <li>○ To be derived from field survey data by topographic survey team</li> </ul>	<ul style="list-style-type: none"> <li>○ 0-8% slope, level to undulating</li> <li>○ 8-18% slope, undulating to rolling</li> <li>○ 18-30% slope, rolling to hilly</li> <li>○ 30-50% slope, hilly to mountainous</li> </ul>
3. Road network	<ul style="list-style-type: none"> <li>○ Field survey</li> <li>○ NAMRIA road network map Scale 1:50,000</li> <li>○ Google Earth</li> </ul>	<ul style="list-style-type: none"> <li>○ Highway</li> <li>○ Local road</li> <li>○ Walkway to safe areas</li> </ul>
4. Potential safe areas for horizontal evacuation	<ul style="list-style-type: none"> <li>○ Field survey by exposure survey team</li> </ul>	<ul style="list-style-type: none"> <li>○ Coordinates</li> <li>○ Occupancy/ Capacity</li> </ul>
5. Potential safe areas for vertical evacuation	<ul style="list-style-type: none"> <li>○ Field survey by exposure survey team</li> </ul>	<ul style="list-style-type: none"> <li>○ Coordinates</li> <li>○ Capacity</li> </ul>
6. Critical facilities	<ul style="list-style-type: none"> <li>○ Field survey by exposure survey team</li> </ul>	<ul style="list-style-type: none"> <li>○ Coordinates</li> <li>○ Occupancy/ Capacity</li> </ul>
7. Population density, age and gender	<ul style="list-style-type: none"> <li>○ Census data from Olongapo City Planning and Development Office</li> </ul>	<ul style="list-style-type: none"> <li>○ Total population</li> <li>○ Age/gender ratio</li> </ul>
8. Administration boundary for planning and disaster management	<ul style="list-style-type: none"> <li>○ GIS layers from Olongapo City Planning and Development Office</li> </ul>	<ul style="list-style-type: none"> <li>○ Barangay boundary</li> <li>○ Purok boundary</li> <li>○ Land parcels</li> </ul>

## 6.2.2 Equipment and Personnel

Table 6.6 summarizes the equipment used and personnel employed for the survey.

Table 6.6 Equipment and personnel for the field survey

Activity (Duration)	Data Used	Equipment Used	Personnel
Recording of critical facility data (21-23 Jan)	Local map (captured from Google Earth)	Survey Vehicle Digital camera Handheld GPS	Driver Local guide Recorder

### *Handheld GPS and digital camera*

Handheld GPS and digital camera (Figure 6.26) were used to record geographical location and photos of potential safe places and critical facilities.



Figure 6.26 Handheld GPS and camera for recording location and photos of potential safe places and critical facilities

### **6.2.3 Results**

Figures 6.27 until 6.30 and Table 6.7 present data gathered/ generated from the survey.

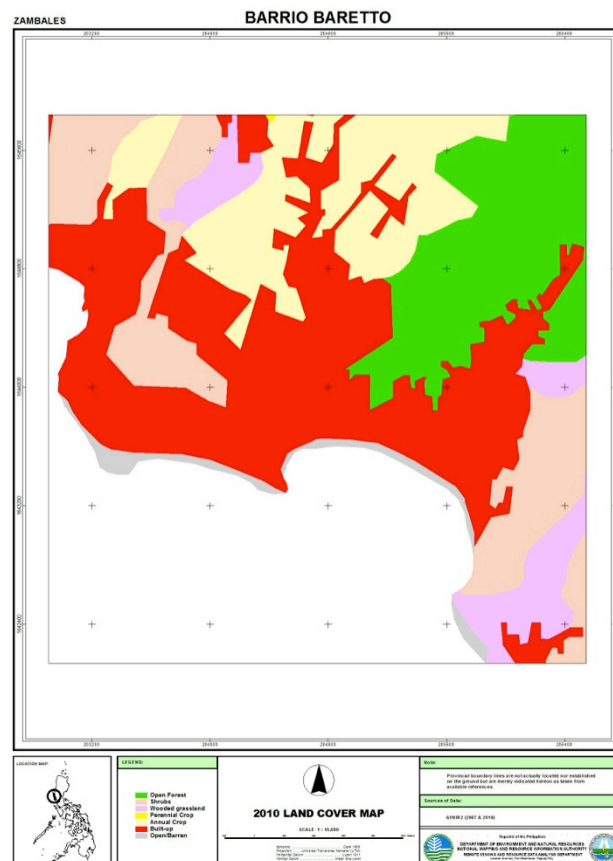


Figure 6.27 Land cover map

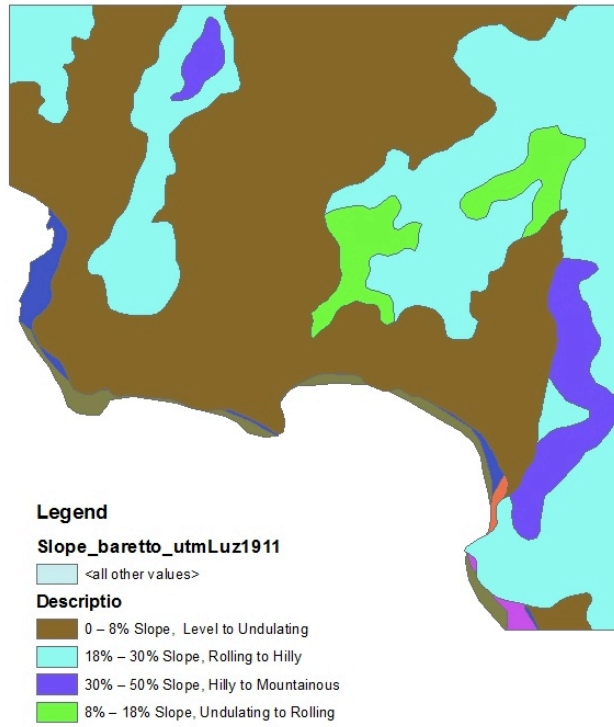








Figure 6.28 Topographic slope map










Figure 6.29 Barangay boundary and land parcel map



Table 6.7 List of critical facilities from the field survey



Facility Type	Coordinates		Description	Photo
	Longitude (E)	Latitude (N)		
<b>School/ College</b>				
1. Barretto I Elementary School	120.26385	14.85191	Students: 1,800 Teachers: 43 Security: 3 (1 person/8hr)  <i>Tsunami prone</i>	
2. Barretto II Elementary School	120.27038	14.85630	Students: N/A Teachers: N/A Security: N/A (Cannot interview during survey)  <i>Shelter capacity: 200 pax (non-school time)</i>	
3. Barretto National High School	120.27065	14.85692	Students: 1,250 Teachers: 41  <i>Shelter capacity: 800 pax (non-school time) 300 pax (temporary retention on open space)</i>	
4. Wesleyan Ecumenical School	120.26523	14.85183	Students: 236 Teachers: 12 Security: 3 (1 person/8hr)  <i>Shelter capacity: 200 pax (non-school time)</i>	





Facility Type	Coordinates		Description	Photo
	Longitude (E)	Latitude (N)		
5. Columban College	120.26804	14.85575	<p>(7:00-18:00)  Kindergarten students: 48  Elementary students: 309  High school students: 700  Teachers: 25  Admin: 6</p> <p>(9:00-20:00)  <u>Engineering college</u>  Students: 570  Faculty: 25  Janitor: 6  <u>Architectural college</u>  Students: 153  Faculty: 6  <u>Nursing college</u>  Students: 93  Faculty: 10  Janitor: 1</p> <p><b>Shelter capacity:</b>  2000 pax  (non-school time)  400 pax  (temporary retention on open space)</p>	
<b>Safe places (Gathering points at open space w/o facilities)</b>				
1. GTP1	120.26063	14.85375	<ul style="list-style-type: none"> <li>o La Union Street</li> <li>o Narrow local walk way</li> <li>o Houses on two sides of the walk way</li> </ul> <p><b>Capacity: 200 pax</b></p>	




Facility Type	Coordinates		Description	Photo
	Longitude (E)	Latitude (N)		
2. GTP2	120.26076	14.85431	<ul style="list-style-type: none"> <li>○ La Union Street</li> <li>○ Narrow local walk way</li> </ul> <p><b>Capacity: 200 pax</b></p>	
3. GTP3	120.26404	14.85343	<ul style="list-style-type: none"> <li>○ Lacambra Street</li> <li>○ Connects to sloped walkway</li> <li>○ Near GTP5</li> <li>○ Church with one storey building</li> </ul> <p><b>Capacity: 40 pax</b></p>	
4. GTP4	120.26575	14.85295	<ul style="list-style-type: none"> <li>○ Rosal Street</li> <li>○ Private house with open space</li> <li>○ Connects to stair walkway</li> </ul> <p><b>Capacity: 50 pax</b></p>	


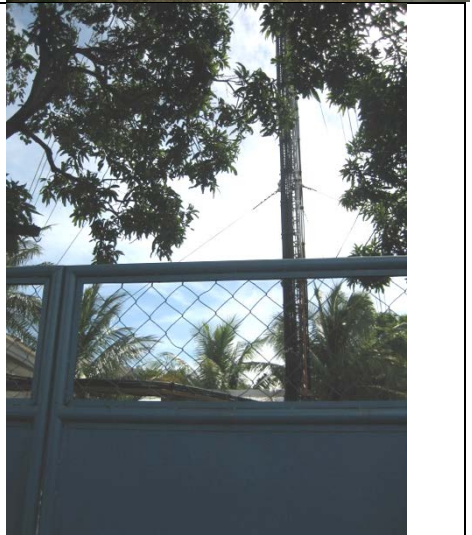

Facility Type	Coordinates		Description	Photo
	Longitude (E)	Latitude (N)		
5. GTP5	120.26387	14.85379	<ul style="list-style-type: none"> <li>○ Lacambra Street</li> <li>○ Two lots of bare land</li> <li>○ Connects to sloped walkway</li> <li>○ Near GTP3</li> </ul> <p><b>Capacity: 100 + 40 pax</b></p>	
6. GTP6	120.26050	14.85855	<ul style="list-style-type: none"> <li>○ Village connects to highway</li> <li>○ Large bare land at the high elevation area</li> <li>○ Link to GTP11, 12, 13, 14 and 15</li> </ul> <p><b>Capacity: 3,000 pax</b></p>	
7. GTP7	120.25774	14.85062	<ul style="list-style-type: none"> <li>○ The Cliff Royal Hotel</li> <li>○ Private land with hotel buildings and rooms</li> <li>○ High elevated area connecting to highway</li> </ul> <p><b>Capacity: 300 pax</b></p>	
8. GTP8	120.25558	14.84786	<ul style="list-style-type: none"> <li>○ Private land lot</li> <li>○ High elevated area connects to Baloy Long Beach road</li> </ul> <p><b>Capacity: 100 pax</b></p>	

Facility Type	Coordinates		Description	Photo
	Longitude (E)	Latitude (N)		
9. GTP9	120.26998	14.8590	<ul style="list-style-type: none"> <li>○ Steep slope area (&gt;20 degree, too steep)</li> <li>○ Too far away from coast</li> </ul> <p><b>Capacity: 80 pax</b></p>	
10. GTP10	120.27284	14.85317	<ul style="list-style-type: none"> <li>○ Pangasinan street</li> <li>○ Bare land on the foothill</li> <li>○ Senior resident revealed the memory of tsunami event during 1950-1960 in Barrio Barretto</li> </ul> <p><b>Capacity: 100 pax</b></p>	
11. GTP11	120.25766	14.85208	<ul style="list-style-type: none"> <li>○ Nueva Ecija street</li> <li>○ Narrow walkway connecting the residential area to high ground</li> <li>○ High ground connected to GTP6</li> <li>○ Pararell route to GTP11-15</li> </ul> <p><b>Capacity: 100 pax</b></p>	
12. GTP12	120.25840	14.85370	<ul style="list-style-type: none"> <li>○ Nueva Ecija street</li> <li>○ Narrow walk way connecting the residential area to high ground</li> <li>○ High ground connected to GTP6</li> <li>○ Pararell route to GTP11-15</li> </ul> <p><b>Capacity: 100 pax</b></p>	

Facility Type	Coordinates		Description	Photo
	Longitude (E)	Latitude (N)		
13. GTP13	120.25866	14.85399	<ul style="list-style-type: none"> <li>○ Nueva Ecija street</li> <li>○ Narrow walk way connecting the residential area to high ground</li> <li>○ High ground connected to GTP6</li> <li>○ Pararell route to GTP11-15</li> </ul> <p><b>Capacity: 100 pax</b></p>	
14. GTP14	120.25881	14.85426	<ul style="list-style-type: none"> <li>○ Nueva Ecija street</li> <li>○ Narrow walk way connecting the residential area to high ground</li> <li>○ High ground connected to GTP6</li> <li>○ Pararell route to GTP11-15</li> </ul> <p><b>Capacity: 100 pax</b></p>	
15. GTP15	120.259211	14.85455	<ul style="list-style-type: none"> <li>○ Neuva Ecija street</li> <li>○ Narrow walk way connecting the residential area to high ground</li> <li>○ High ground connected to GTP6</li> <li>○ Pararell route to GTP11-15</li> </ul> <p><b>Capacity: 100 pax</b></p>	
16. GTP16	120.26883	14.84546	<ul style="list-style-type: none"> <li>○ Highway located on the high elevated area</li> <li>○ Temporary retention area</li> </ul> <p><b>Capacity: 500 pax</b></p>	

Facility Type	Coordinates		Description	Photo
	Longitude (E)	Latitude (N)		
<b>Local government offices</b>				
1. Barangay office	120.26326	14.85153	<p>Includes:</p> <ul style="list-style-type: none"> <li>○ Barangay office building</li> <li>○ Barangay health center</li> <li>○ BPSO rescue office</li> </ul> <p><u>Garage space with</u>            Ambulance: 1            Van: 2            Loader: 1            Truck: 1            Fire rescue truck: 1 (under repair)</p> <p><i>Tsunami prone</i></p>	 
2. Jail	120.26612	14.84986		
3. Police station	120.26579	14.84914		
4. Church	120.27059	14.85257		
<b>Siren</b>				
1. PHIVOLCS tsunami siren 1	120.26554	14.84904	<p>Driftwood Beach</p> <p>Effective siren distance is about 50 m</p>	

Facility Type	Coordinates		Description	Photo
	Longitude (E)	Latitude (N)		
2. PHIVOLCS tsunami siren 2	120.25554	14.84888	Baloy Long Beach Road  Effective siren distance is about 50 m	
<b>Critical supplies</b>				
1. Heavy equipment	120.25762	14.85139	Big Iron Trading & Development Inc. (Private company)  Tel/Fax: +63 47 223 1756 Local cell: +63 908 861 6550 (can also contact the owner at Palm Beach Resort)	
2. Hospital	120.26935	14.84742	Our Lady of Lourdes International Medical Center  General Service: Beds: 99 Doctors: 60 (30 doctors/day) Staff: 145  ER Service: Beds: 6 Doctors: 2 Nurses: 2	

Facility Type	Coordinates		Description	Photo
	Longitude (E)	Latitude (N)		
3. Power supply	120.27085	14.83670	Olongapo Power Substation (Under National Grid Corporation of the Philippines)	
4. Cellular tower	120.26437	14.85111	SMART cellular network tower  <i>Located at the low elevation area</i>	
<b>Potential Vertical Evacuation Buildings (VEB): Baloy Long Beach Area</b>				
1. VEB1	120.25002	14.85065	Apartment <ul style="list-style-type: none"> <li>○ Well engineered RC</li> <li>○ 2-storeys</li> <li>○ Open space on top</li> </ul> <i>Capacity: 50 pax</i>	

Facility Type	Coordinates		Description	Photo
	Longitude (E)	Latitude (N)		
2. VEB2	120.25005	14.85110	<ul style="list-style-type: none"> <li>○ Well engineered RC</li> <li>○ 3-storeys</li> <li>○ Open space on top</li> </ul> <p><b>Capacity: 50 pax</b></p>	
3. VEB3	120.25011	14.84972	<p>Private hotel (Under construction)</p> <ul style="list-style-type: none"> <li>○ Well engineered RC</li> <li>○ 3-storeys</li> <li>○ Open space on top</li> </ul> <p><b>Capacity: 50 pax</b></p>	
4. VEB4	120.25114	14.84944	<p>Private hotel</p> <ul style="list-style-type: none"> <li>○ Well engineered RC</li> <li>○ 3-storeys</li> <li>○ Function hall at 3<sup>rd</sup> Fl.</li> <li>○ Stair is outside the building</li> </ul> <p><b>Capacity: 50 pax</b></p>	

Facility Type	Coordinates		Description	Photo
	Longitude (E)	Latitude (N)		
5. VEB5	120.25192	14.84925	Private house (for rent: may be closed during emergency) <ul style="list-style-type: none"> <li>○ Well engineered RC</li> <li>○ 3-storeys</li> <li>○ Open space on 3<sup>rd</sup> Fl.</li> </ul> <p><b>Capacity: 20 pax</b></p>	
6. VEB6	120.25199	14.84925	Private hotel <ul style="list-style-type: none"> <li>○ Well engineered RC</li> <li>○ 3-storeys</li> <li>○ Open space on 3<sup>rd</sup> Fl.</li> </ul> <p><b>Capacity: 20 pax</b></p>	
7. VEB7	120.25256	14.84904	Private house- 3 adjacent buildings <ul style="list-style-type: none"> <li>○ Well engineered RC</li> <li>○ 2-storeys</li> <li>○ Open space on top</li> </ul> <p><b>Capacity: 45 pax</b> (15 pax/house)</p>	

Facility Type	Coordinates		Description	Photo
	Longitude (E)	Latitude (N)		
8. VEB8	120.25294	14.84895	Private hotel <ul style="list-style-type: none"> <li>o Well engineered RC</li> <li>o 3-storeys</li> <li>o Open space on 3<sup>rd</sup> Fl.</li> <li>o Stair is outside the building</li> </ul> <p><i>Capacity: 30 pax</i></p>	
9. VEB9	120.25460	14.84887	Wild Orchid Beach Resort <ul style="list-style-type: none"> <li>o 48 rooms</li> <li>o Well engineered RC</li> <li>o 5 storeys</li> <li>o 83 staffs/3shifts</li> </ul> <p>Free space is not available for public but can accommodate the guests during emergency</p>	
10.VEB10	120.254653	14.84848	Private apartment <ul style="list-style-type: none"> <li>o Well engineered RC</li> <li>o 2-storeys</li> <li>o Open space on top</li> </ul> <p><i>Capacity: 20 pax</i></p>	

Facility Type	Coordinates		Description	Photo
	Longitude (E)	Latitude (N)		
11.VEB11	120.254703	14.84858	Private apartment <ul style="list-style-type: none"> <li>○ Well engineered RC</li> <li>○ 2-storeys</li> <li>○ Open space on top</li> </ul> <p><b>Capacity: 20 pax</b></p>	
12. VEB12	120.25574	14.84911	Sheavens Hotel <ul style="list-style-type: none"> <li>○ 50 rooms (block 9 rooms, available 41 rooms)</li> <li>○ Well engineered RC</li> <li>○ 4 storeys</li> <li>○ Open space at 4<sup>th</sup> Fl. (100 pax)</li> <li>○ 60 staffs/3 shifts</li> </ul> <p>Free space is not available for public but can accommodate guests during emergency</p>	

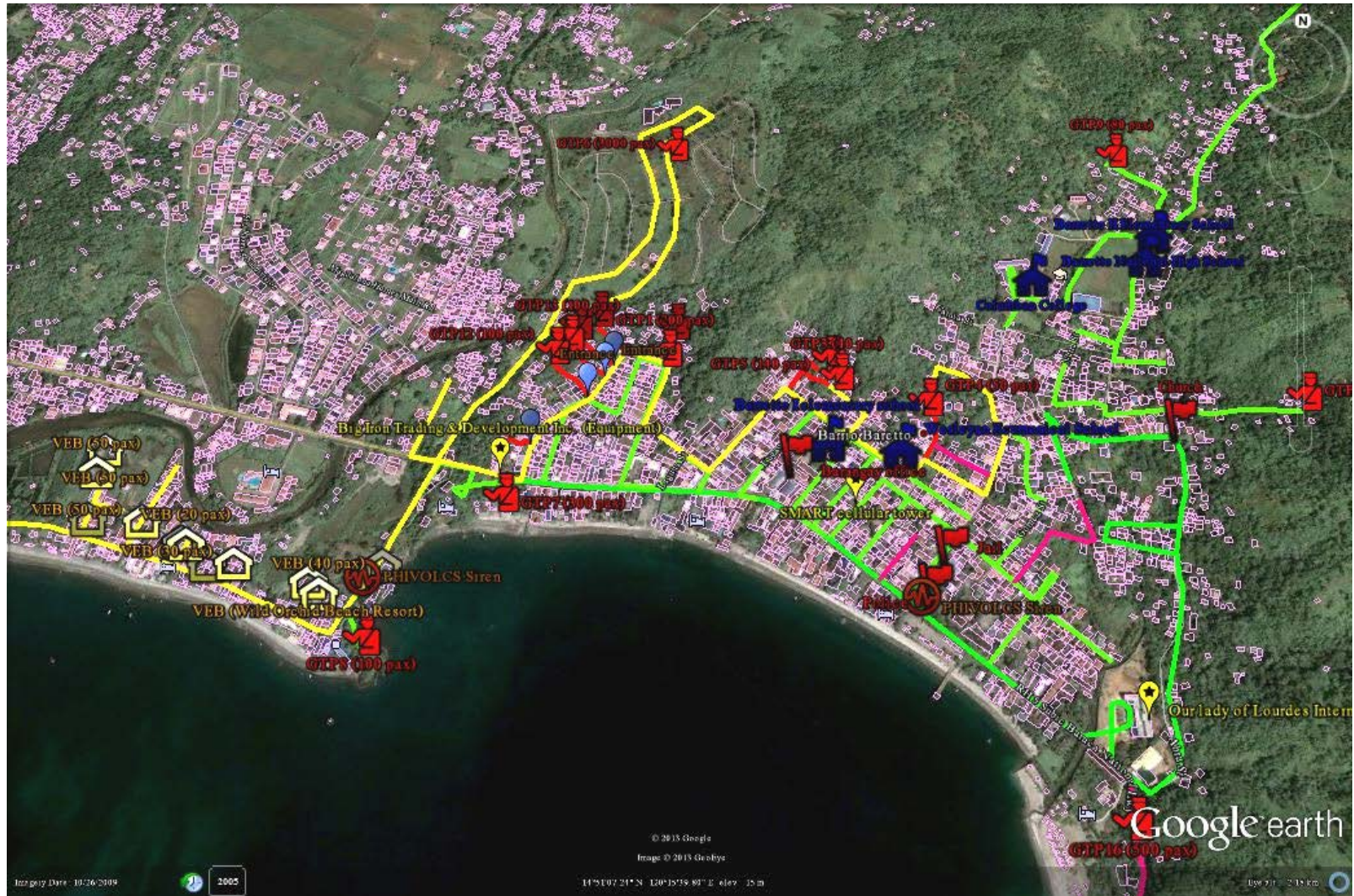


Figure 6.30 Location of critical facilities

## 6.2.4 Problems Encountered and Recommendations

### Demography Data

In this project, the evacuation process considered is by walking only; use of vehicle is not recommended to avoid traffic congestion during an event. Age and gender affects evacuation speed. The elderly has the slowest speed at about 0.75 m/s (Sugimoto et al, 2003). Demography data is important in determining the number of people by age and gender. However, demography data collected from the City Planning and Development Office is not clear, as shown in Table 6.8. The data should be clarified before using for analysis.

Table 6.8 Demography data by age and gender

CBMS StatSim Pro 5.0

Province:

ZAMBALES, III - CENTRAL LUZON

CBMS Core Indicators, Barangay

City/Municipality:

OLONGAPO CITY

The 13+1 dimensions of poverty

Barangay:

Barreto

Indicator	Households		Population					
	Magnitude	Proportion	Magnitude			Proportion		
			Total	Male	Female	Total	Male	Female
<b>DEMOGRAPHY</b>								
Population	3924		14284	7075	7205	100	49.5	50.4
Average household size	4							
Children under 1 year old	303	7.7	309	165	144	2.2	2.3	2
Children under 5 years old	1131	28.8	1495	798	697	10.5	11.3	9.7
Children 0-5 years old	1273	32.4	1792	947	845	12.5	13.4	11.7
Children 6-11 years old	1300	33.1	1890	989	901	13.2	14	12.5
Children 6-12 years old	1430	36.4	2203	1157	1046	15.4	16.4	14.5
Members 12-15 years old	949	24.2	1243	660	583	8.7	9.3	8.1
Members 13-16 years old	935	23.8	1226	647	579	8.6	9.1	8
Members 6-15 years old	1742	44.4	3133	1649	1484	21.9	23.3	20.6
Members 6-16 years old	1839	46.9	3429	1804	1625	24	25.5	22.6
Members 10 years old and above	3920	99.9	11258	5492	5765	78.8	77.6	80
Members of the labor force	3348	85.3	5009	3044	1964	35.1	43	27.3

### Vertical Evacuation Areas

Baloy Long Beach area is located in a low-lying area along the coast. The nearest gathering point for tsunami evacuation is at GTP8, located about 1 km away from the Matain riverside. People from the farthest point (western part near the Matain River) may have to walk for 15-20 minutes to reach the safe place at GTP8, which can accommodate only 100 people. Therefore, potential vertical evacuation buildings were surveyed, as listed in Table 6.7. Most buildings along Baloy Long Beach, however, are private buildings, located within 200m from the shore and, hence, could be severely hit by a tsunami. In case these buildings will be identified as vertical evacuation areas, local authorities need to prove the buildings' stability and communicate to the building owners on the need to provide building access during an event.

## REFERENCES

- Acharya, B., 2000. Accuracy Assessment of DTM Data: A Cost Effective Approach for Large Scale Digital Mapping Project. *IAPRS*, Vol. XXXIII, Amsterdam, 2000. Retrieved from <http://www.earthmapping.com/pdf/papers/Accuracy-Assessment-of-DTM-Data.pdf>
- Amante, C. & B. W. Eakins, 2009. ETOPO1 1 Arc-Minute Global Relief Model: Procedures, Data Sources and Analysis. *NOAA Technical Memorandum NESDIS NGDC-24*, 19 pp, March 2009.
- Asian Disaster Preparedness Center (ADPC), 2007. *Evacuation routes tools ArcGIS toolbox- User's manual*. Italian Ministry for the Environment Land and Sea. Department of Environmental Research and Development, 88 pp.
- Axes, F., et al., 2004. *SPOT 5 Builds a Global Multi-Purpose 3D Database: Reference3D*. Retrieved from <http://www.aars-acrs.org/acrs/proceeding/ACRS2004/Papers/3DG04-7.htm>
- Bureau of Meteorology, Australian Government (BMAG). *Tsunami Facts and Information*. Retrieved from <http://www.bom.gov.au/tsunami/info/index.shtml>
- Burrough, P.A. & McDonnell, R.A., 1998. *Principles of Geographical Information Systems*. Oxford University Press, Oxford. 333pp.
- Department of Disaster Prevention and Mitigation (DDPM), 2005. *Master Plan for Tsunami Evacuation*, 72 pp.
- Dost, R.J.J. & Mannaerts, C.M.M., 2004. *Generation of Lake Bathymetry Using Sonar, Satellite Imagery and GIS*. International Institute for Geo-Information Science and Earth Observation (ITC). Netherlands. Retrieved from [http://www.itc.nl/library/Papers\\_2004/n\\_p\\_conf/dost\\_bat.pdf](http://www.itc.nl/library/Papers_2004/n_p_conf/dost_bat.pdf)
- Doytsher, Y., 2009. *Producing Seamless Multi-Source Quality-Dependent Digital Terrain Models*. Retrieved from [http://www.fig.net/pub/vietnam/papers/ts02e/ts02e\\_doytsher\\_dalyot\\_3590.pdf](http://www.fig.net/pub/vietnam/papers/ts02e/ts02e_doytsher_dalyot_3590.pdf)
- NOAA, 2009. *Field Procedures Manual*. Office of Coast Survey, National Oceanic and Atmospheric Administration. Retrieved from [http://www.nauticalcharts.noaa.gov/hsd/docs/Field\\_Procedures\\_Manual\\_April\\_2009.pdf](http://www.nauticalcharts.noaa.gov/hsd/docs/Field_Procedures_Manual_April_2009.pdf)
- Foytong, P. and Ruangrassamee, A., 2007. *Fragility curves of reinforced concrete buildings damaged by a tsunami for tsunami risk analysis*. The Twentieth KKCNN Symposium on Civil Engineering, Jeju, Korea, 4–5 October 2007, S8-47, 2007.
- Garcin M., Desprates J.F., Fontaine M., Pedreros R., Attanayake N., Fernando S., Srirwardana C.H.E.R., De Silva U. and Poisson B., 2008. Integrated approach for coastal hazards and risks in Sri Lanka, *Nat.Hazards Earth Syst.Sci.*, Vol.8, pp.577-586.
- Hatanaka, K., Toda, M. & Wada, M., 2007. Data Analysis of a Low-Cost Bathymetry System Using Fishing Echo Sounders. *IEEE Xplore*.
- Heyman, W.D., Echochard, J.B. & Biasi, F.B., 2007. Low-Cost Bathymetric Mapping for Tropical Marine Conservation-A Focus on Reef Fish Spawning Aggregation Sites. *Marine Geodesy*, 30:1, 37-50. Available at <http://dx.doi.org/10.1080/01490410701295996>.
- International Oceanographic Commission (IOC), 2001. Improved Global Bathymetry. *Final Report of SCOR Working Group 107. Technical Series 63*. Retrieved from [http://www.scor-int.org/Working\\_Groups/WG107Report.pdf](http://www.scor-int.org/Working_Groups/WG107Report.pdf)

- International Hydrographic Organization (IHO), 2005. *Manual on Hydrography*. International Hydrographic Bureau. Monaco. Retrieved from <http://www.syqwestinc.com/downloads/m-13-contents-chapter1.pdf>
- International Hydrographic Organization (IHO), 2008. *IHO Standards for Hydrographic Surveys*. Fifth Edition. Special Publication N44. International Hydrographic Bureau. Retrieved from [http://www.iho.shom.fr/publicat/free/files/S-44\\_5E.pdf](http://www.iho.shom.fr/publicat/free/files/S-44_5E.pdf)
- International Oceanographic Commission (IOC), 2001. Improved Global Bathymetry. *Final Report of SCOR Working Group 107*. Technical Series 63. Retrieved from [http://www.scor-int.org/Working\\_Groups/WG107Report.pdf](http://www.scor-int.org/Working_Groups/WG107Report.pdf)
- IUGG/IOC TIME Project, 1997. Numerical method of tsunami Simulation with the leap-frog scheme. *Intergovernmental Oceanographic Commission Manuals and Guides*, Vol. 35.
- Japan Aerospace Exploration Agency (JAXA), 2009. ASTER GDEM Readme File – ASTER GDEM Version-1. Retrieved from <http://www.gdem.aster.ersdac.or.jp/> ASTER\_GDEM\_Validation\_Summary\_Report
- Johnson, S., 2000. *The Engineering Handbook “Elevation”*. Retrieved from [ftp://ftp.seu.edu.cn/Pub2/EBooks/Books\\_from\\_EngnetBase/pdf/8576/Section23/Ch144.PDF](ftp://ftp.seu.edu.cn/Pub2/EBooks/Books_from_EngnetBase/pdf/8576/Section23/Ch144.PDF)
- Kechine, M., 2003. *Network Differential GPS: Kinematic Positioning with NASA’s Internet-based Global Differential GPS*.
- Layug, J.E., 2010. *Development of a low-cost bathymetric mapping system for tsunami inundation modeling*. ME thesis Asian Institute of Technology, Thailand, Print.
- Magron, Franck, 2007. Shallow Water Bathymetry. *SPC Fisheries Newsletter #120*.
- Naparat, P., 2011. *Development of methodology to generate topographic DEM for tsunami simulation model INSPIRE*. ME thesis Asian Institute of Technology, Thailand. Print.
- NOAA, 2009. *NOS Hydrographic Surveys Specifications and Deliverables*. U.S. Department of Commerce. National Oceanic and Atmospheric Administration. Retrieved from <http://www.nauticalcharts.noaa.gov/hsd/docs/Specs2009.pdf>
- New York State Department of Transportation, 2009. *Land Survey Standards and Procedures Manual*. Retrieved from <https://www.nysdot.gov/divisios/engineering/design/design-services/land-survey/repository/LSSPM09.pdf>
- Research, Development and Technology Turner-Fairbank Highway Research Center, 1999. *Portable Instrumentation for Real-Time Measurement of Scour at Bridges*. Pub. No. FHWA-RD-99-085. Retrieved from <http://water.usgs.gov/osw/techniques/bs/Fhwa-rd-99-085.pdf>
- Promdumrong, N., 2011. *Developing Methodology for Generating Building Database in Low Cost Condition*. ME thesis Asian Institute of Technology, Thailand. Print.
- Ruangrassamee, A., Yanagisawa, H., Foytong, P., Lukkunaprasit, P., Koshimura, S. and Imamura, F., 2006. Investigation of tsunami induced damage and fragility of building in Thailand after the December 2004 Indian Ocean Tsunami, *Earthquake Spectra*, Vol.22, pp.377-401.
- Satellite Imaging Corp., 2004. *SPOT DEM Product Description Version 1.1*, Retrieved from [www.satimagingcorp.com/.../SPOT\\_DEM\\_Product\\_Description\\_v1-1.pdf](http://www.satimagingcorp.com/.../SPOT_DEM_Product_Description_v1-1.pdf)

*Single Beam Acoustic Depth Measurement Techniques*. EM-1110-2-10003. (2002, January). Retrieved from <http://gisceu.net/PDF/U150.pdf>

Srivihok P., Honda K., Ruangrassamee A., Muangsin V., Naparat P., Foytong P., Promdumrong N., Aphimaeteethomrong P., Intavee A., Layug J.E., and Kosin T., 2012. Development of an online tool for tsunami inundation simulation and tsunami loss estimation, *Continental Shelf Research Journal*, In Presss. (<http://dx.doi.org/10.1016/j.csr.2012.08.021>)

Stumpf, R.P., Hordelred, K., 2003. Determination of Water Depth with High Resolution Satellite Imagery over Variable Bottom Type. *Limnol. Oceanogr.*, 48(1, part 2), pp. 547-556.

Sugimoto, T., Murakami, H., Kozuki, Y. and Nishikawa, K., 2003. A human damage prediction method for tsunami disaster incorporating evacuation activities, *Natural hazard* 29, pp. 585-600.

The US Army Corps of Engineers (USACE), 2002. *Hydrographic Surveying, Engineering and Design, Engineer Manual*, Washington DC.

Umbach, M. J., 1976. *Hydrographic Manual*. Fourth Edition. U.S. Department of Commerce, National Oceanic and Atmospheric Administration and National Ocean. Rookville, Maryland. Retrieved from [http://www.nauticalcharts.noaa.gov/hsd/docs/Hydro\\_Man\\_Ed\\_4\\_Umbach\\_1976\\_81.pdf](http://www.nauticalcharts.noaa.gov/hsd/docs/Hydro_Man_Ed_4_Umbach_1976_81.pdf)

Wilson, G. & Richards, J., 2006. Procedural Documentation and Accuracy Assessment of Bathymetric Maps and Area/Capacity Tables for Small Reservoirs. *Scientific Investigations Report 2006-5208*. U.S. Department of the Interior and U.S. Geological Survey. Denver, Colorado. Retrieved from <http://pubs.usgs.gov/sir/2006/5208/pdf/SIR-06-5208.pdf>

Valencia, N., Gardi, A., Gauraz, A., Leone, F. and Guillande, R., 2011. New tsunami damage functions developed in the framework of SCHEMA project: application to European-Mediterranean coasts, *Natural Hazards and Earth System Science*, Vol.11, pp.2835-2846.

**ANNEX 1**  
**PARTICIPANT and CONTACT LIST**

Office	Contact Details	Participant Name , Designation, Email
<b>Participants</b>		
<b>Bathymetric Survey</b>		
National Mapping and Resource Information Authority	Hydrography Department Binondo, Manila Tel. No. (632) 241-3494 to 98	Ens. Janato Donida <a href="mailto:jun_excalibur@yahoo.com.ph">jun_excalibur@yahoo.com.ph</a>  Ens. Danilo R. Arguelles <a href="mailto:daniilo_spectre@yahoo.com">daniilo_spectre@yahoo.com</a>  Ens. Aaron Andro Ching <a href="mailto:aaron.andro.ching@gmail.com">aaron.andro.ching@gmail.com</a>  Mr. Rodolfo T. Carmen  Mr. Reymarick O. Verzosa  Mr. Michael O. Mesina
Philippine Institute of Volcanology and Seismology	PHIVOLCS Bldg C.P. Garcia Ave., U.P. Campus Diliman, Quezon City Philippines Tel: +632-426-1468 to 79 Fax: +632-929-8366, 927-4524	Mr. Danikko John V. Rivera Science Research Specialist Geology Geophysics R&D <a href="mailto:danikkorivera@gmail.com">danikkorivera@gmail.com</a>
<b>Topographic Survey</b>		
National Mapping and Resource Information Authority	Remote Sensing and Resource Data Analysis Department Lawton Avenue, Fort Andres Bonifacio 1638 Taguig City, Philippines Tel: +63-2-810-4831; +63-2-810-5471	Mr. Saldivar Asprit <a href="mailto:cj.soliven@yahoo.com">cj.soliven@yahoo.com</a>  Mr. Renato P. Esperanza <a href="mailto:rene_esperanza@yahoo.com">rene_esperanza@yahoo.com</a>  Mr. Joseph M. Delovino  Mr. Marlo M. Baetiong
Philippine Institute of Volcanology and Seismology	PHIVOLCS Bldg C.P. Garcia Ave., U.P. Campus Diliman, Quezon City Philippines Tel: +632-426-1468 to 79 Fax: +632-929-8366, 927-4524	Mr. Ericson B. Bariso Science Research Specialist Geology Geophysics R&D <a href="mailto:ericson.bariso@gmail.com">ericson.bariso@gmail.com</a>
<b>Exposure Survey</b>		
Philippine Institute of Volcanology and Seismology	PHIVOLCS Bldg C.P. Garcia Ave., U.P. Campus Diliman, Quezon City Philippines Tel: +632-426-1468 to 79 Fax: +632-929-8366, 927-4524	Mr. Danikko John V. Rivera Science Research Specialist Geology Geophysics R&D <a href="mailto:danikkorivera@gmail.com">danikkorivera@gmail.com</a>  Mr. Ericson B. Bariso
National Mapping and Resource Information Authority	Hydrography Department Binondo, Manila Tel. No. (632) 241-3494 to 98	Ens. Aaron Andro Ching <a href="mailto:aaron.andro.ching@gmail.com">aaron.andro.ching@gmail.com</a>
Olongapo City Disaster Risk Reduction and Management Office		Mr. Irvin C. Paras, RSO Research and Planning Division Chief <a href="mailto:irvinparas@yahoo.com">irvinparas@yahoo.com</a>

Barangay Barretto, Olongapo City		Mr. Joel E. Banez Executive Officer, B.P.S.O and Rescue Mobile: 091192682083
<b>Key Contacts</b>		
Philippine Institute of Volcanology and Seismology	PHIVOLCS Bldg C.P. Garcia Ave., U.P. Campus Diliman, Quezon City Philippines  Tel: +632-426-1468 to 79 Fax: +632-929-8366, 927-4524	Dr. Renato Solidum Director <a href="mailto:renato_solidum@yahoo.com">renato_solidum@yahoo.com</a>  Dr. Bartolome C. Bautista Deputy Director <a href="mailto:bart_bautista@yahoo.com">bart_bautista@yahoo.com</a>  Dr. Arturo S. Daag Chief Geology and Geophysics Research and Development Division <a href="mailto:asdaag@yahoo.com">asdaag@yahoo.com</a>  Ms. Mylene M. Villegas Chief Geological Disaster Awareness and Preparedness Division <a href="mailto:Mylene_villegas@yahoo.com">Mylene_villegas@yahoo.com</a>  Ms. Joan L.Cruz-Salcedo Science Research Specialist Seismological Observation and Earthquake Prediction Division <a href="mailto:salcedojoan@yahoo.com">salcedojoan@yahoo.com</a>
National Mapping and Resource Information Authority	NAMRIA Main Office Lawton Avenue, Fort Andres Bonifacio 1638 Taguig City, Philippines Tel: +63-2-810-4831; +63-2-810-5471	Ms. Linda SD. Papa Deputy Administrator for Information and Media Department <a href="mailto:lsdpapa@namria.gov.ph">lsdpapa@namria.gov.ph</a>  Mr. Jose C. Cabanayan Deputy Administrator for Surveys <a href="mailto:joecab@namria.gov.ph">joecab@namria.gov.ph</a>  Dr. Rijaldia N. Santos Acting Director Remote Sensing and Resource Data Analysis Department <a href="mailto:daynsantos@yahoo.com">daynsantos@yahoo.com</a>  Mr. Ruel DM. Belen OIC-Director Mapping and Geodesy Department <a href="mailto:Rbellen2001@yahoo.com">Rbellen2001@yahoo.com</a>  Ms. Ofelia T. Castro Assistant Director  Mr. Ronaldo C. Gatchalian Head of Geodesy and Geophysics Division <a href="mailto:ronaldogatchalian@yahoo.com">ronaldogatchalian@yahoo.com</a>  Mr. Nicandro P. Parayno Head of Photogrammetry division

		<p>Mr. Jesus L. Gerardo OIC-Assistant Director Remote Sensing and Resource Data Analysis Department</p> <p>Mr. Rolando A. Dela Cruz OIC-Chief Physicography and Aquatics Division</p>
	<p>Hydrography Department Binondo Branch Tel. No. (632) 241-3494 to 98</p>	<p>Commo. Romeo I. Ho Director <a href="mailto:cdr_romy@yahoo.com.ph">cdr_romy@yahoo.com.ph</a></p> <p>Cap. Virgilio P. Antonio Assistant Director</p> <p>Cdr. Jacinto M. Cablayan OIC-Asst Dir for operations <a href="mailto:sonny1731@yahoo.com">sonny1731@yahoo.com</a></p> <p>Cdr. Ildefonso S. Pascual Jr. CHSD <a href="mailto:ispjr@yahoo.com">ispjr@yahoo.com</a></p> <p>Cdr. Herbert L. Catapang CNCD <a href="mailto:h_catapang@yahoo.com">h_catapang@yahoo.com</a></p> <p>Cdr. Sheilon T. Cadaoas SOL <a href="mailto:sheilonc@yahoo.com">sheilonc@yahoo.com</a></p> <p>Cdr. Rosalina C. Delos Reyes COS <a href="mailto:noly_reyes@yahoo.com">noly_reyes@yahoo.com</a></p> <p>Engr. Raul S. Capistrano COD <a href="mailto:raul_capistrano@yahoo.com">raul_capistrano@yahoo.com</a></p> <p>Mr. Norelius Baloran Chief, Oceanographic Survey Section Oceanography Division <a href="mailto:norelius06@gmail.com">norelius06@gmail.com</a></p> <p>Gelma G. Gascon <a href="mailto:gggelma@yahoo.com">gggelma@yahoo.com</a></p> <p>Ens. Glenn G. Jandayan <a href="mailto:glennjandayan@ymail.com">glennjandayan@ymail.com</a></p> <p>Ens. Rodel G. Guarte <a href="mailto:rodel_guarte@yahoo.com">rodel_guarte@yahoo.com</a></p> <p>Ens. Maylord M. De Chavez <a href="mailto:mmdechavez_upd@ymail.com">mmdechavez_upd@ymail.com</a></p> <p>P/Ens. May Anne L. Javier <a href="mailto:mayannejavier@gmail.com">mayannejavier@gmail.com</a></p> <p>P/Ens Stephanie P. Marquez <a href="mailto:engr.spmarquez@yahoo.com.ph">engr.spmarquez@yahoo.com.ph</a></p>

Olongapo City Disaster Risk Reduction and Management Office		Mr. Angie Layug DRRMO Chief of Olongapo City
Barangay Barretto, Olongapo City		Hon. Carlito A. Baloy ABC President/HOBEA president Mobile: 09295922250  Kgwd. George Hoya JR. Barangay Counselor Mobile: 09993145584
RIMES	1 <sup>st</sup> F. Outreach Bldg., AIT campus 58 Moo 9 Paholyothin Rd Klong Nueng, Klong Luang Pathumthani 12120 Thailand Tel: +662-516-5900 to 01 Fax: +662-516-5902	Dr. Patchanok Srivihok Coastal Hydrodynamics Scientist <a href="mailto:patchanok@rimes.int">patchanok@rimes.int</a>  Ms. J Elaine J Layug Bathymetric Survey and GIS Specialist <a href="mailto:j.elaine@rimes.int">j.elaine@rimes.int</a>  Mr. Panithan Srinuandee Topographic Survey Specialist (Consultant) <a href="mailto:parmarmarm@hotmail.com">parmarmarm@hotmail.com</a>  Ms. Ruby Rose Policarpio Institutional Development Specialist <a href="mailto:ruby@rimes.int">ruby@rimes.int</a>



Figure 1 Survey team from NAMRIA, PHIVOLCS, OCDRRMO, Barangay Barretto and RIMES

## ANNEX 2 TOPOGRAPHIC SURVEY DATA

### 2.1 Results after GPS Data Post-Processing for GCP1 to GCP4

#### Project Summary

Project name: rimes.ttp

Surveyor:

Comment:

Linear unit: Meters

Projection:

Geoid:

Adjustment Summary

Adjustment type: Plane + Height, Minimal constraint

Confidence level: 95 %

Number of adjusted points: 5

Number of plane control points: 1

Number of used GPS vectors: 4

A posteriori plane UWE: 1 , Bounds: ( 1 , 1 )

Number of height control points: 1

A posteriori height UWE: 1 , Bounds: ( 1 , 1 )

Used GPS Observations					
Name	dN (m)	dE (m)	dHt (m)	Horz RMS (m)	Vert RMS (m)
BASE-GCP1	4300.14	-3223.8	0.025	0.006	0.021
BASE-GCP2	1724.7	-2152.1	0.961	0.003	0.006
BASE-GCP3	3722.84	318.923	9.003	0.013	0.024
BASE-GCP4	1867.15	44.093	2.867	0.003	0.005

GPS Observation Residuals					
Name	dN (m)	dE (m)	dHt (m)	Horz RMS (m)	Vert RMS (m)
BASE-GCP1	4300.14	-3223.8	0.025	0.006	0.021
BASE-GCP2	1724.7	-2152.1	0.961	0.003	0.006
BASE-GCP3	3722.84	318.923	9.003	0.013	0.024
BASE-GCP4	1867.15	44.093	2.867	0.003	0.005

Control Points				
Name	Latitude	Longitude	Ell.Height (m)	Code
BASE	14°51'06.21142"N	120°15'17.36192"E	49.684	

Adjusted Points				
Name	Latitude	Longitude	Ell.Height (m)	Code
GCP1	14°53'26.11150"N	120°13'29.50733"E	51.982	
GCP2	14°52'02.32234"N	120°14'05.37048"E	51.243	
GCP3	14°53'07.33555"N	120°15'28.03136"E	59.788	
GCP4	14°52'06.96004"N	120°15'18.83691"E	52.826	

## 2.2 Results after GPS Data Post-Processing for CHK1 to CHK4

### Project Summary

Project name: rimes.ttp

Surveyor:

Comment:

Linear unit: Meters

Projection:

Geoid:

Adjustment Summary

Adjustment type: Plane + Height, Minimal constraint

Confidence level: 95 %

Number of adjusted points: 5

Number of plane control points: 1

Number of used GPS vectors: 4

A posteriori plane UWE: 1 , Bounds: ( 1 , 1 )

Number of height control points: 1

A posteriori height UWE: 1 , Bounds: ( 1 , 1 )

Used GPS Observations					
Name	dN (m)	dE (m)	dHt (m)	Horz RMS (m)	Vert RMS (m)
BASE-chk1	-513.1	1439.68	0.418	0.001	0.003
BASE-chk2	-54.867	785.725	0.737	0.002	0.004
BASE-chk3	104.947	1344.07	-0.021	0.005	0.01
BASE-chk4	64.53	-1300.6	-0.097	0.004	0.006

GPS Observation Residuals					
Name	dN (m)	dE (m)	dHt (m)	Horz RMS (m)	Vert RMS (m)
BASE-chk1	-513.1	1439.68	0.418	0.001	0.003
BASE-chk2	-54.867	785.725	0.737	0.002	0.004
BASE-chk3	104.947	1344.07	-0.021	0.005	0.01
BASE-chk4	64.53	-1300.6	-0.097	0.004	0.006

Control Points				
Name	Latitude	Longitude	Ell.Height (m)	Code
BASE	14°51'06.21142"N	120°15'17.36192"E	49.684	

Adjusted Points				
Name	Latitude	Longitude	Ell.Height (m)	Code
chk1	14°50'49.51606"N	120°16'05.51735"E	50.285	
chk2	14°51'04.42586"N	120°15'43.64391"E	50.469	
chk3	14°51'09.62472"N	120°16'02.32050"E	49.805	
chk4	14°51'08.30980"N	120°14'33.85879"E	49.72	

### 2.3 Results after GPS Data Post-Processing for CHK5 and GCP6 to GCP8

#### Project Summary

Project name: rimes.ttp

Surveyor:

Comment:

Linear unit: Meters

Projection:

Geoid:

Adjustment Summary

Adjustment type: Plane + Height, Minimal constraint

Confidence level: 95 %

Number of adjusted points: 5

Number of plane control points: 1

Number of used GPS vectors: 4

A posteriori plane UWE: 1 , Bounds: ( 1 , 1 )

Number of height control points: 1

A posteriori height UWE: 1 , Bounds: ( 1 , 1 )

Used GPS Observations					
Name	dN (m)	dE (m)	dHt (m)	Horz RMS (m)	Vert RMS (m)
BASE-GCP7	-1540.1	2962.3	-0.814	0.007	0.015
BASE-CHK5	-2812	1654.65	1.365	0.008	0.013
BASE-GCP6	583.907	3355.19	49.661	0.013	0.021
BASE-GCP8	-3884.2	2833.97	-3.381	0.012	0.016

GPS Observation Residuals					
Name	dN (m)	dE (m)	dHt (m)	Horz RMS (m)	Vert RMS (m)
BASE-GCP7	-1540.1	2962.3	-0.814	0.007	0.015
BASE-CHK5	-2812	1654.65	1.365	0.008	0.013
BASE-GCP6	583.907	3355.19	49.661	0.013	0.021
BASE-GCP8	-3884.2	2833.97	-3.381	0.012	0.016

Control Points				
Name	Latitude	Longitude	Ell.Height (m)	Code
BASE	14°51'06.21142"N	120°15'17.36192"E	49.684	







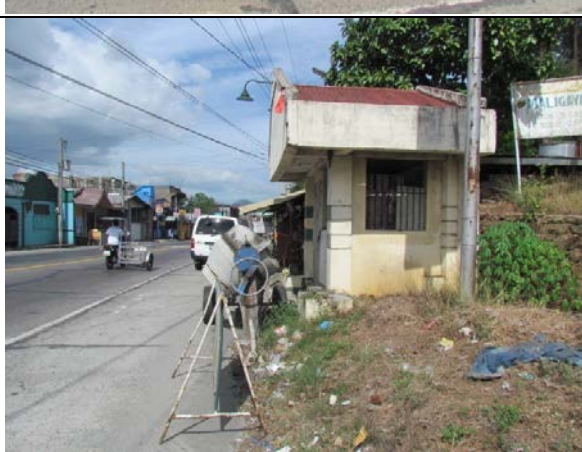
Adjusted Points				
Name	Latitude	Longitude	Ell.Height (m)	Code
GCP7	14°50'16.09694"N	120°16'56.44288"E	49.745	
CHK5	14°49'34.72099"N	120°16'12.70254"E	51.887	
GCP6	14°51'25.20140"N	120°17'09.59310"E	100.254	
GCP8	14°48'59.83146"N	120°16'52.14127"E	48.123	

## 2.4 Description for GCP and CHK Related to this Field Work

<b>GCP 01</b>	Lat: 14°53'26.11150"N
CRS: WGS84	Lon: 120°13'29.50733"E
Date of Survey: 22/01/2013	h: 51.982 m
	
	
	

<b>GCP 02</b>	Lat: 14°52'02.32234"N
CRS: WGS84	Lon: 120°14'05.37048"E
Date of Survey: 22/01/2013	h: 51.243 m
	
	
	
	

<b>GCP 03</b>	Lat: 14°53'07.33555"N
CRS: WGS84	Lon: 120°15'28.03136"E
Date of Survey: 22/01/2013	h: 59.788 m
	
	
	
	

<b>GCP 04</b>	Lat: 14°52'06.96004"N
CRS: WGS84	Lon: 120°15'18.83691"E
Date of Survey: 22/01/2013	h: 52.826
	
	
	
	



<b>GCP 05</b>	Lat: 14°51'06.21142"N
CRS: WGS84	Lon: 120°15'17.36192"E
Date of Survey: 22/01/2013	h: 49.684



<b>GCP 06</b>	Lat: 14°51'25.20140"N
CRS: WGS84	Lon: 120°17'09.59310"E
Date of Survey: 22/01/2013	h: 100.254



<b>GCP 07</b>	Lat: 14°50'16.09694"N
CRS: WGS84	Lon: 120°16'56.44288"E
Date of Survey: 22/01/2013	h: 49.745



<b>GCP 08/2</b>	Lat: 14°48'59.83146"N
CRS: WGS84	Lon: 120°16'52.14127"E
Date of Survey: 22/01/2013	h: 48.123



<b>CHK1</b>	Lat: 14°50'49.51606"N
CRS: WGS84	Lon: 120°16'05.51735"E
Date of Survey: 22/01/2013	h: 50.285
	
	

<b>CHK2</b>	Lat: 14°51'04.42586"N
CRS: WGS84	Lon: 120°15'43.64391"E
Date of Survey: 22/01/2013	h: 50.469
	



<b>CHK3</b>	Lat: 14°51'09.62472"N
CRS: WGS84	Lon: 120°16'02.32050"E
Date of Survey: 22/01/2013	h: 49.805





<b>CHK4</b>	Lat: 14°51'08.30980"N
CRS: WGS84	Lon: 120°14'33.85879"E
Date of Survey: 22/01/2013	h: 49.720





<b>CHK5</b>	Lat: 14°49'34.72099"N
CRS: WGS84	Lon: 120°16'12.70254"E
Date of Survey: 22/01/2013	h: 51.887





For more information, contact RIMES at:

RIMES Program Unit  
2<sup>nd</sup> Fl. Outreach Bldg.  
Asian Institute of Technology Campus  
P.O. Box 4, Klong Luang, Pathumthani, 12120 Thailand  
Phone: 662-516-5900 to 01; Fax: 662-516-5902  
Website: <http://www.rimes.int/>  
E-mail: [rimes@rimes.int](mailto:rimes@rimes.int)